The Official Journal of the Chinese Stomatological Association (CSA)

Chinese Journal of Dental Research

CJDR

VOLUME 25 NUMBER 1 2022

Chinese Journal of Dental Research

The Official Journal of the Chinese Stomatological Association (CSA)

Chinese Journal of Dental Research

The Official Journal of the Chinese Stomatological Association (CSA)

Review

Article

Case report

Chinese Journal of Dental Research

CN 10-1194/R • ISSN 1462-6446 • eISSN 1867-5646 • Quarterly

The Official Journal of the Chinese Stomatological Association
Co-sponsor: Peking University School of Stomatology, Quintessenz Verlag

Publication Department

Production Manager: Megan Platt (London, UK)
Managing Editor: Xiao Xia ZHANG (Beijing, P.R. China)

Address: 4F, Tower C, Jia 18#, Zhongguancun South Avenue, HaiDian District, 100081, Beijing, P.R. China.
Tel: 86 10 82195785, **Fax:** 86 10 62173402
Email: editor@cjdrcsa.com

Manuscript submission: Information can be found on the Guidelines for Authors page in this issue. To submit your outstanding research results more quickly, please visit: http://mc03.manuscriptcentral.com/cjdr

Administrated by: China Association for Science and Technology
Sponsored by: Chinese Stomatological Association and Popular Science Press
Published by: Popular Science Press
Printed by: Beijing ARTRON Colour Printing Co Ltd
Subscription (domestically) by Post Office

Chinese Journal of Dental Research is indexed in MEDLINE.

For more information and to download the free full text of the issue, please visit
www.quint.link/cjdr
http://www.cjdrcsa.com

Acknowledgements

We would like to express our gratitude to the peer reviewers for their great support to the journal in 2021.

Abi Rached-Junior, Fuad Jacob (Brazil)
Agudelo-Suárez, Andrés (Colombia)
Ahmed, Sarfraz (Pakistan)
Al-Moraissi, Essam (Yemen)
Antunes, Jose Leopoldo Ferreira (Brazil)
Ardeshirylajimi, Abdolreza (Iran)
Atarbashi-Moghadam, Fazele (Iran)
Azañedo, Diego (Peru)
Baghaei, Kaveh (Iran)
Bauer, Jose (Brazil)
Bayindir, Funda (Turkey)
Beldüz Kara, Nihal (Turkey)
Bhawal, Ujjal (Japan)
Buyuk, Suleyman (Turkey)
Chen, Bin (China)
Chen, Fa Ming (China)
Chen, Su (China)
Chen, Zhi (China)
Chrcanovic, Bruno R (Sweden)
Chu, Chun Hung (Hong Kong, China)
Coban, Gokhan (Turkey)
Corchuelo, Jairo (Colombia)
Cristiane, Koga-Ito (Brazil)
Cynthia, Evangeline (India)
Dai, Ning (China)
Dhirawat, Jotikasthira (Thailand)
Erdemir, Uğur (Turkey)
Erdogan, Ozgur (Turkey)
Estrela, Carlos (Brazil)
Fan, Yuan (China)
Fan, Zhi Peng (China)
Feng, Hai Lan (China)
Figueiredo, Rui (Spain)
Fu, Kai Yuan (China)
Ge, Wen Shu (China)
Ghahraman, Leila (Iran)
Ghelichi-Ghojogh, Muosa (Iran)
Graf, Daniel (Canada)
Gu, Xin Hua (China)
Gu, Yan (China)
Gunpinar, Sadiye (Turkey)
Güzel, Rezan (Turkey)
Hajeer, Mohammad Y (Syria)
Hari, Petsos (Germany)
He, Chuang Long (China)
Hou, Ben Xiang (China)
Huang, Cui (China)
Huang, Ding Ming (China)
Huang, Xiao Feng China
Jia, Ling Fei (China)
Jiang, Jiu Hui (China)
Jiang, Qian Zhou (China)
Jiang, Shao Yun (China)
Jin, Li Jian (Hong Kong, China)
Kallarakkal, Thomas (Malaysia)
Khurana, Prakhar (India)
Köseoğlu, Serhat (Turkey)
Koşumcu, Sevim (Turkey)
Kowash, Mawlood
(United Arab Emirates)
Kum, Kee-Yeon (South Korea)
Kurt, Ayça (Turkey)
León, Jorge Esquiche (Brazil)
León-Manco, Roberto (Peru)
Li, Gang (China)
Li, Hong Bo (China)
Li, Mei (New Zealand)
Liang, Yu Hong (China)
Lin, Huan Cai (China)
Liu, Da Wei (China)
Liu, Deng Gao (China)
Liu, Jian Zhang (China)
Liu, Ou Sheng (China)
Liu, Xiao Hua (United States)
Liu, Xue Nan (China)
Lorenzo, Susana (Brazil)
Lu, Rui fang (China)
Mai, Sui (China)
Menini, Maria (Italy)
Mohtasham, Nooshin (Iran)
Nokhbatolfoghahaei, Hanieh (Iran)
Ozturk, Taner (Turkey)
Paksoy, Tugce (Turkey)
Pan, Shao Xia (China)
Pan, Ya Ping (China)
Pan, Yong Chu (China)
Panda, Saurav (India)
Patil, Nikita (India)
Peng, Xian (China)
Pimkhaokham, Atiphan (Thailand)
Rajabi, Abdolhalim (Iran)
Rengifo-Reina, Herney A (Colombia)
Rezaei Rad, Maryam (Iran)
Rirattanapong, Praphasri (Thailand)
Rong, Qi Guo (China)
Rossi-Fedele, Giampiero (Australia)
Schuch, Helena Silveira (Brazil)
Sharma, Divyas (India)
Shokri, Abbas (Iran)
Souza, Erick Miranda (Brazil)
Sriram, Srikanthan (India)
Sun, Hong Chen (China)
Sun, Zhi Peng (China)
Tahmaseb, Ali (Netherlands)
Tavakoly , Belin (Iran)
Tuner, Jan (Sweden)
Umemura, Naoki (Japan)
Üstün, Kemal (Turkey)
Wang, Chun Xiao (China)
Wang, Xiao Yan (China)
Wang, Yi Xiang (China)
Wax, MK (United States)
Yan, Fu Hua (China)
Yang, Kai (China)
Yang, Rui Li (China)
Yildirim, Handan (Turkey)
Yiu, Cynthia Kar Yung
(Hong Kong, China)
Zeng, Dong Lin (China)
Zhang, Cheng Fei (Hong Kong, China)
Zhang, Lei (China)
Zheng, Shu Guo (China)
Zhou, Yong Sheng (China)
Zhou, Zhi Bo (China)

Editorial Office
Chinese Journal of Dental Research

UNDERSTANDING THE LANGUAGE OF CELLS

NEW

Reinhard Gruber | Bernd Stadlinger | Hendrik Terheyden (Eds.)

CELL-TO-CELL COMMUNICATION

CELL-ATLAS – VISUAL BIOLOGY IN ORAL MEDICINE

Volume 7

Hardcover, 244 pages, 298 illus.
ISBN 978-1-78698-107-3, €86

The deepest understanding of the cells of the oral system will be found in decoding their communication and seeing how it is regulated. Once we have understood their language, clinicians might be able to talk to cells and control their action.

This book by 47 world-renowned experts – for each chapter at least one clinician and one basic scientist – highlights a reliable and actual state of research regarding this topic that quickly moves forward. Beyond the classic cell types addressed in the first part of the book and visualized by colored scanning electron microscopic (SEM) images, organ systems or model systems of cell-to-cell communication of a more generic type are presented in four additional chapters in the second part.

This book – accompanied by an augmented reality (AR) app that allows you to experience the process of bone resorption virtually – should help to open the vision of how we can regenerate tissues and heal diseases by controlling the language of the cells, and shows us the direction in which research and therapy will go in the future.

OUTLINE

Supported by EMS SDA SWISS DENTAL ACADEMY

www.quint.link/VisualBiology
books@quintessenz.de
+49 30 76180-667
QUINTESSENCE PUBLISHING

Editorial

4 February 2022, the "start of spring" day, the first of the 24 solar terms of the year and also part of the Chinese New Year festival, marked the opening of the XXIV Winter Olympic Games (Beijing 2022). Beijing is now the first city to have hosted both the Summer and Winter Olympics and Paralympics. These events are great opportunities for athletes and sports fans from all over the world to meet. We hope the pandemic will end soon, that the world will return to normal, and that we will work "together for a shared future".

For our journal, with great support and cooperation from Berlin, London and Beijing, we have continued to work smoothly over the past year. We have welcomed 14 new members, who are renowned international scholars, to our editorial board. We would like to thank them for their support and contribution!

In this issue, I would like to recommend several articles. The first of these is "Emerging role of high glucose levels in cancer progression and therapy" contributed by Dr Cai et al, members of Prof Tie Jun Li's team from Peking University School of Stomatology. The article offers a comprehensive review of this broad topic. Extensive research has indicated that high glucose plays an important role in the development and progression of cancer. As a novel finding in cancer progression and therapy, high glucose needs to be studied further, and I think this article may offer a new perspective for readers who work in cancer research.

There are also two other reviews. The first of these is "Exploration of genetic variants of non-syndromic cleft lip with or without palate and underlying mechanisms" by Prof Lin Wang's team at the Affiliated Hospital of Stomatology, Nanjing Medical University. They performed functional studies on related loci and genes by using molecular biology, cell biology, animal models and other methods, which provide a basis for the construction of the NSCL/P genetic map in the Chinese population and help to implement individualised prophylaxis and treatment. The second is contributed by Prof Tian's group at the West China Hospital of Stomatology, Sichuan University, entitled "Microspheres and their potential in endodontic regeneration application", which summarises the properties and characteristics of microsphere scaffold used in tissue engineering, placing emphasis on their advantages and applications in endodontic regeneration.

The systematic review on "Accuracy of mandibular reconstruction with a vascularised Iliac flap using 3D templates" and systematic review and meta-analysis "Relationship between presence of third molars and prevalence of periodontal pathology of adjacent second molars", from Shanghai Ninth People's Hospital, Shanghai Jiao Tong University School of Medicine, College of Stomatology, and School of Stomatology, Fourth Military Medical University, respectively, are sure to be helpful to clinicians in their practice. There is also a research article on "Near infrared laser photobiomodulation of periodontal ligament stem cells" from the School of Dentistry, Hamadan University of Medical Sciences, Iran, and a case report on "Management of separated instruments extruded into the maxillary sinus and soft tissue" from the School of Stomatology, Capital Medical University, China that are worthy of your attention.

I wish you a very happy, healthy and successful new year!

Prof Guang-yan Yu
Editor-in-chief

MASTER THE BASICS

NEW

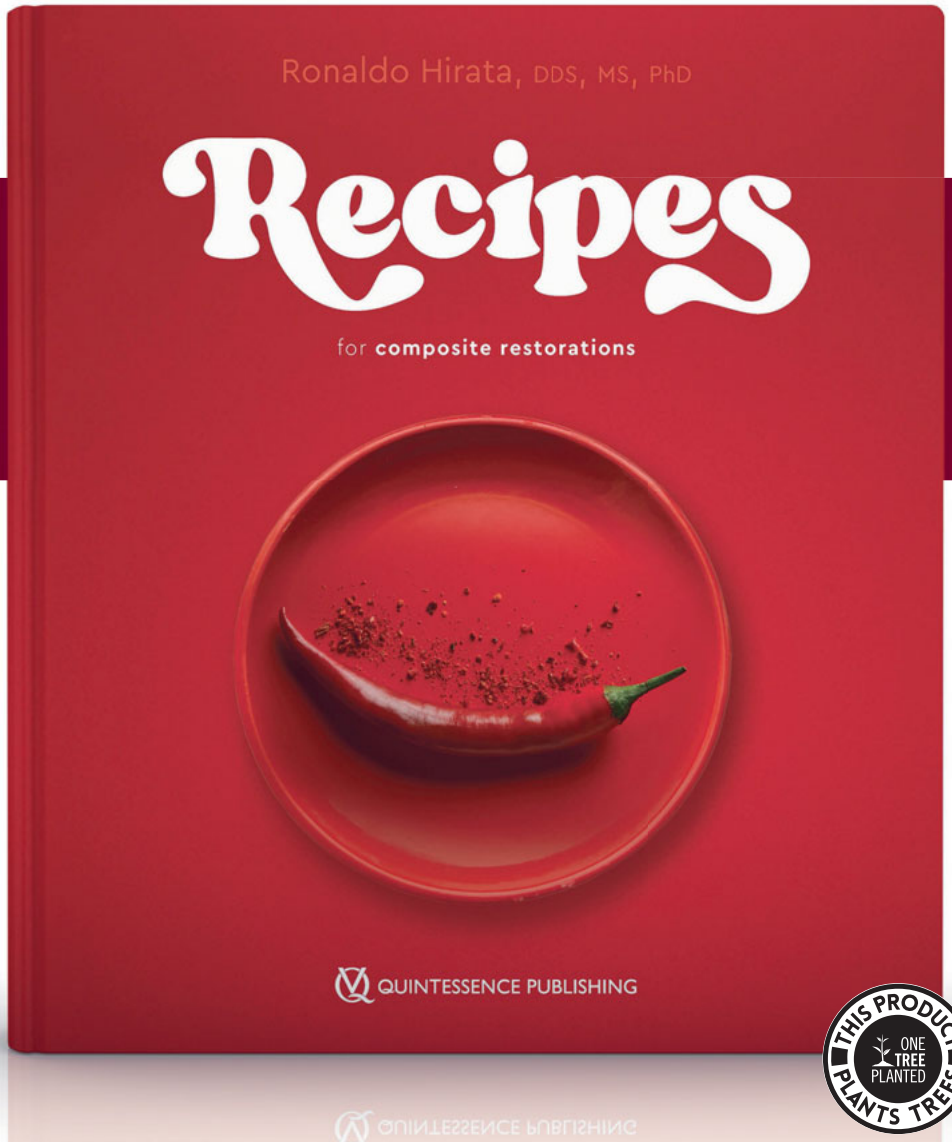

Ronaldo Hirata

Recipes for Composite Restorations

456 pages, 1,076 illus.
ISBN 978-1-64724-067-7
€258

Although many dental manuals have been called "cookbooks," none has ever embraced the style so fully as this new book. In its pages, the practitioner is fully reimagined as a master chef, and 26 esthetic restorative protocols are presented as gourmet recipes, ready to be learned and savored. The purpose of this book is to encourage true mastery of the fundamentals while avoiding the most common pitfalls. Dr Hirata demonstrates how to make the most of composite materials by focusing on the details and techniques that can really improve the final results. In restorative dentistry, the key is to use the right materials with the best technique. However, that is not enough. Any chef knows that once you have learned the fundamentals, your best work must also reflect your personal character, and the same goes for the work of restorative dentists. By focusing on the skillful use of the right ingredients and tools, this tour de force will teach you how to take the heat and take your restorative protocols to the next level. Keep it simple. Master the basics.

www.quint.link/recipes
books@quintessenz.de
+49 (0)30 761 80 667
QUINTESSENCE PUBLISHING

Emerging Role of High Glucose Levels in Cancer Progression and Therapy

Xin Jia CAI[1,2], Jian Yun ZHANG[1,2], Ao Bo ZHANG[1,2], Xuan ZHOU[1,2], He Yu ZHANG[2,3], Tie Jun LI[1,2]

Extensive research has indicated that high glucose levels play an important role in cancer. A high glycaemic index, glycaemic load diet, high sugar intake, high blood glucose and diabetes mellitus all increase the risk of cancer. Various signals are involved in high glucose–induced tumorigenesis, cancer proliferation, apoptosis, invasion and multidrug resistance. Reactive oxygen species might be important targets in cancer progression that are induced by high glucose levels. Drugs such as metformin and resveratrol may inhibit high glucose–induced cancer. As the impact of high glucose levels on cancer progression and therapy is a novel finding, further research is required.

Key words: *cancer, high glucose, progression, therapy, tumorigenesis*
Chin J Dent Res 2022;25(1):11–20; doi: 10.3290/j.cjdr.b2752695

Many studies have shown that high glucose (HG) is closely related to tumorigenesis and cancer progression. HG is linked to abnormal glucose metabolism[1,2]. The study of abnormal glucose metabolism is not only shedding light on carcinogenesis, but is also revealing new principles of the biochemistry of aberrant cancer cell proliferation, apoptosis and invasion, as well as multidrug resistance.

Foods that contain carbohydrates, which are digested, absorbed and metabolised quickly, are considered high glycaemic index (GI) foods (GI ≥ 70 on the glucose scale). The glycaemic load (GL) is the product of the GI and the total available carbohydrate content in a given amount of food (GL = GI × available carbohydrate/given amount of food)[3]. High GI and GL diets are associated with cancers of the upper aerodigestive tract and digestive system[1,2]. Table 1[4-37] lists specific risk factors and cancer types. High GI diets are associated with increased risk of oesophageal adenocarcinoma, oesophageal squamous cell carcinoma, colorectal cancer, colon cancer, pancreatic cancer, renal cell carcinoma, prostate cancer and bladder cancer[5,6,16,18-20,30]. High GL diets increase the risk of oesophageal squamous cell carcinoma and mammary carcinomas, and gastric, colorectal, rectal, colon, pancreatic, endometrial, ovarian and bladder cancers[6,7,16,19,20,33,35,36]. Makarem et al[38] found that high sugar intake increases the risk of cancer by 60% to 95%, and high consumption of sugary beverages increases the risk by 23% to 200%. Dietary sugar is positively associated with hepatocellular car-

1 Department of Oral Pathology, Peking University School and Hospital of Stomatology, National Centre of Stomatology & National Clinical Research Centre for Oral Diseases, Beijing, P.R. China.
2 Research Unit of Precision Pathologic Diagnosis in Tumours of the Oral and Maxillofacial Regions, Chinese Academy of Medical Sciences (2019RU034), Beijing, P.R. China.
3 Central Laboratory, Peking University School and Hospital of Stomatology, Beijing, P.R. China.

Corresponding authors: Prof Tie Jun LI, Department of Oral Pathology, Peking University School and Hospital of Stomatology, Beijing 100081, P.R. China. Tel/Fax: 86-10-82195203. Email: litiejun22@vip.sina.com; and Dr He Yu ZHANG, Central Laboratory, Peking University School and Hospital of Stomatology, Beijing 100081, P.R. China. Tel/Fax: 86-10-82195770. Email: zhangheyu1983@sina.cn

This work was supported by research grants from the National Nature Science Foundation of China (81671006 and 81300894) and CAMS Innovation Fund for Medical Sciences (2019-I2M-5-038).

Table 1 Clinical evidence of high glucose involved in tumorigenesis and progression[4-37].

Cancer type	Risk factors	Study
Thyroid cancer	High level of fasting plasma glucose, diabetes mellitus	Zhan et al[4]
Oesophageal carcinoma	Intake of sucrose, sweetened desserts/beverages, high GI diet, high GL diet, high level of fasting plasma glucose, diabetes mellitus	Zhan et al[4], Li et al[5], Eslamian et al[6]
Breast cancer	High GL diet, high fat/high sugar diet, high level of fasting plasma glucose, diabetes mellitus, high blood random glucose	Zhan et al[4], Thompson et al[7], Lambertz et al[8], Sieri et al[9], Raza et al[10], Contiero et al[11]
Lung cancer	High level of fasting plasma glucose, diabetes mellitus	Zhan et al[4], Luo et al[12]
Liver cancer	High sugar diet, high level of fasting plasma glucose, diabetes mellitus	Zhan et al[4], Fedirko et al[13], Healy et al[14]
Biliary tract cancers, gallbladder cancer	High consumption of sweetened beverages	Larsson et al[15]
Gastric cancer	High carbohydrate intake, high GL diet, high fasting plasma glucose	Ye et al[16], Ikeda and Kiyohara[17]
Colorectal cancer	High GI diet, high carbohydrate intake, high sugar, high level of fasting plasma glucose, diabetes mellitus	Sieri et al[18,19], Hu et al[20], Galeone et al[21], Cui et al[22], Vulcan et al[23], Jung et al[24], Shin et al[25]
Pancreatic cancer	High GI diet, high level of fasting plasma glucose, diabetes mellitus, high random plasma glucose	Zhan et al[4], Hu et al[20], Rossi et al[26], Nagai et al[27], Pang et al[28], Er et al[29]
Renal carcinoma	High GI diet	Zhu et al[30], Otunctemur et al[31]
Prostate cancer	High GI diet, high GL diet, high serum glucose	Hu et al[20], Arthur et al[32]
Bladder cancer	High GI diet, high GL diet, high consumption of refined carbohydrate foods, high level of fasting plasma glucose, diabetes mellitus	Zhan et al[4], Sieri et al[19], Augustin et al[33]
Cervical cancer	High level of fasting plasma glucose, diabetes mellitus, high nonfasting plasma glucose	Zhan et al[4], Lee et al[34]
Endometrial cancer	High GL diet	Nagle et al[35]
Ovarian cancer	High GL diet	Nagle et al[36]
Primary central nervous system lymphoma	High mean fasting plasma glucose (≥126 mg/dL)	Debata et al[37]
Leukemia	High level of fasting plasma glucose, diabetes mellitus	Zhan et al[4]
Lymphoma	High level of fasting plasma glucose, diabetes mellitus	Zhan et al[4]

cinoma[13]. Larsson et al[15] found that high consumption of sweetened beverages was associated with increased risk of biliary tract cancers, particularly gallbladder cancer. Galeone et al[21] determined that added sugars were associated with increased risk of colon cancer. A high sugar diet increased the risk of mammary cancer in developing mouse pups and incidence of liver tumours in mice[8,14]. High blood glucose increased the risk of leukaemia, lymphoma and lung, breast, thyroid, gastric, pancreatic, colorectal, colon, rectal, prostate, bladder and cervical cancers[4,9,17,22-25,32,34,37]. High blood glucose is associated with cancer stage, aggressiveness, mortality, recurrence and poor survival[10-12,27,32,34,37,39]. Diabetes mellitus (DM) increased the risk of developing oesophageal, thyroid, liver, pancreatic, colorectal, cervical and renal cancer and increased cancer aggressiveness[4,28,29,31].

HG and tumorigenesis

Table 2[40-104] and Fig 1 show the involvement of HG in tumorigenesis and the progression of different cancers through various molecules. HG induced O-GlcNAcylation, expression and transcriptional activity of Yes-associated protein (YAP) led to YAP-dependent tumorigenic phenotypes which contributed to liver tumorigenesis. YAP was found to promote glucose uptake, the synthesis of metabolites involved in the hexosamine biosynthesis pathway (HBP) and cellular O-GlcNAcylation, establishing a positive feedback loop[58]. Qiao et al[59] found that HG induced advanced glycosylation end product–specific receptor (AGER) activating HBP, leading to enhanced O-GlcNAcylation of target proteins, increasing the activity and stability of c-Jun via O-GlcNAcylation of this protein at Ser73 to promote

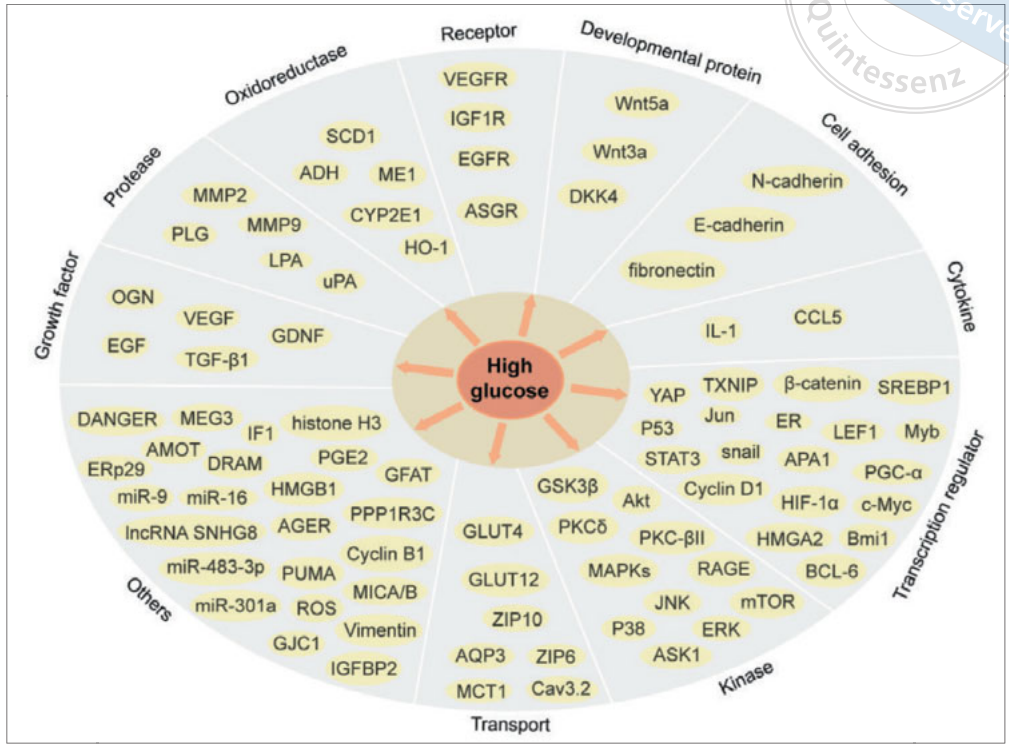

Fig 1 HG involved in tumorigenesis and progression through transcription regulators, kinase, growth factors, proteases, oxidoreductases, receptors, developmental protein, cytokines and other molecules.

tumorigenesis. The c-Jun enhanced AGER transcription thus established a positive feedback loop[59]. HG-induced thioredoxin-interacting protein (TXNIP) expression is involved in oxidative stress via p38 mitogen-activated protein kinases (MAPKs) and extracellular signal-regulated kinase (ERK) pathways, which promoted cancer development[78]. Ito et al found that HG led to cancer by increasing osteopontin (OPN) expression and oxidative stress, accelerating cell proliferation[79]. HG promoted the acquisition of mesenchymal and cancer stem cell (CSC) properties by activating transforming growth factor β1 (TGF-β) signalling and facilitated tumorigenesis[80]. Zhang et al[105] found that HG increased mutagenesis in lymphoblastoid cells via reactive oxygen species (ROS) and null or mutant p53. Overexpression of chemotactic cytokine ligand 5 (CCL5) accelerated diffuse large B cell lymphoma formation in HG[106]. HG maintained hepatic homeostasis by regulating the asialoglycoprotein receptor[107]. Langen et al[41] found that HG decreased the dose absorption ratio (DAR) of 2-18F-fluorodeoxyglucose (FDG) uptake in bronchial carcinoma.

HG and cancer cell proliferation

HG reduces Wnt antagonist Dickkopf 4 (DKK4) protein and promotes cancer cell proliferation by activating the wnt/β-catenin signal via wnt3a-ligand-mediated translocation of β-catenin into the nucleus[60,98]. HG increases ROS levels, which stimulates proliferation by inactivating the c-Jun-NH2-terminal kinase (JNK) pathway[81]. Rezende et al[92] found that HG increased cell proliferation by reducing AMPK activation and affecting oxidative stress. HG promotes cell proliferation by upregulating sterol regulatory element binding protein 1 (SREBP1); SREBP1 also mediates autophagy via negative feedback[82]. Han et al[83] found that HG promoted proliferation via the induction of epidermal growth factor (EGF) expression and transactivation of EGF receptor (EGFR). Zhang et al[42] found that HG stimulated proliferation via phosphoenolpyruvate (PEP)-induced poHis58-FAK signalling. HG stimulates proliferative capacity by elevating O-GlcNAcylation and the expression of zinc finger protein 410 (APA1) and gap junction protein gamma 1 (GJC1)[108]. Upregulation of glial cell line–derived neurotrophic factor (GDNF) and RET ligand–receptor interaction could play a role in the proliferation promoted by HG[84]. Gupta et al[109] found that HG induced proliferation via crosstalk between glycogen synthase kinase 3β (GSK-3β) activation, histone H3 phosphorylation and DNA methylation. Decreases in protein kinase C (PKC)-βII mRNA and protein levels could account for HG-stimulated proliferation[110]. Li et al[93] found that HG induced miR-301a expression, suppressed expression of p21 and smad4 and promoted G1/S

Table 2 Molecular mechanisms of HG involved in tumorigenesis and progression[40-104].

Cancer type	Molecular mechanisms	Study
Nasopharyngeal carcinoma	Snail protein	Zheng et al[40]
Bronchial carcinoma	Dose absorption ratio of FDG uptake	Langen et al[41]
Esophageal carcinoma	poHis58-FAK signalling	Zhang et al[42]
Breast cancer	EMT, ROS, proinflammatory and pro-oxidant environment characterised by the COX-2/PGE2 axis, Zn^{2+} transportation, NF-κB pathway; abrogate the effect of metformin, decrease cellular sensitivity to 4-MU	Zhu et al[43], Viedma-Rodríguez et al[44], Matsui et al[45], Flores-López et al[46], Kallens et al[47], Takatani-Nakase[48], Nasir Kansestani et al[49], Varghese et al[50], Wang et al[51], Pandey et al[52]
Gastric cancer	Multiplicative interaction; attenuate effect of 5-FU	Lin et al[53], Zhao et al[54]
Lung cancer	p53 pathway, RAGE-NOX-4 pathway, ERK/DAPK signal	Wang et al[55], Liao et al[56], Kuron et al[57]
Liver cancer	O-GlcNAcylation, HBP, canonical Wnt signalling pathway, oxidative stress, endoplasmic reticulum stress, EMT, YAP, mitochondrial biogenesis, mitochondrial networking, ATP synthase dimer stability, AMPK/mTOR pathway, STAT3 and AKT signalling pathways, NF-κB/GLUT1 signal	Zhang et al[58], Qiao et al[59], Chauhan et al[60], Chandrasekaran et al[61,62], Jiang et al[63], Li et al[64], Liu et al[65], Domenis et al[66], Lv et al[67], Li et al[68], Liu et al[69]
Cholangiocarcinoma	STAT3, O-GlcNAcylation	Saengboonmee et al[70], Phoomak et al[71]
Colorectal cancer	PTEN/Akt signal, EMT, MMP-9 signalling pathway, attenuate effect of 5-FU, modify adriamycin-induced cancer cell death, bromopyruvate resistance	Ran et al[72], Chen et al[73], Lin et al[74], Ma et al[75], Ganefi et al[76], Ideno et al[77]
Pancreatic cancer	Oxidative stress, p38 MAPK and ERK signalling pathways, mesenchymal and CSC-properties, JNK pathway, autophagy, EMT, increase LDHA activity and HK2, PFKP expression, AMPK signalling pathway, PI3K/AKT/GSK-3β signalling pathway, EGF/EGFR signalling pathway	Li et al[78], Ito et al[79], Rahn et al[80], Luo et al[81], Zhou et al[82], Han et al[83], Liu et al[84], Li et al[85,86], Cheng et al[87], Duan et al[88], Cao et al[89], Han et al[90], Li et al[91]
Prostate cancer	Oxidative stress, G1/S cell cycle transition, upregulate aerobic glycolysis, N-linked glycosylation, reduce docetaxel-induced cell apoptosis, reduce expression of IGFBP2	Rezende et al[92], Li et al[93], Huang et al[94], Fukami et al[95], Biernacka et al[96,97]
Bladder cancer	Wnt/β-catenin signalling pathway	Gao et al[98]
Endometrial cancer	EMT, overexpression of β-catenin, inhibit STAT3 expression	Gu et al[99], Han et al[100], Zhou et al[101], Wallbillich et al[102]
B-cell lymphoma	EMT, Wnt/β-catenin signalling pathway, abrogate etoposide chemotherapy effect	Wang et al[103], Shao et al[104]

cell cycle transition and cell proliferation. HG induces proliferation via STAT3 activation by increasing nuclear STAT3, p-STAT3, cyclin D1, vimentin and MMP270. Reema et al[111] found that HG promoted cell proliferation and clonogenicity by activating pro-oncogenic signalling. HG enhances the growth of cancer cell colonies by activating Akt[112].

HG and cancer cell apoposis

HG induces cell apoptosis through increased oxidative stress by increasing the intracellular ROS level, lipid peroxidation, protein carbonyl and 3-nitrotyrosine (3-NT) adduct formation and HG-mediated induction of alcohol dehydrogenase (ADH) and cytochrome P4502E1 (CYP2E1)[61,62]. HG triggers endoplasmic reticulum (ER) and oxidative stress, and integrates the signalling cascades into apoptosis signal-regulating kinase 1 (ASK1) and causes phosphorylation and activation of p38 and JNK MAPK signals, eventually leading to cell apoptosis[63]. It was also argued that HG enhances proliferation and inhibits apoptosis by JNK-mediated downregulation of the p53 pathway and increases p38 MAPK phosphorylation[55,113]. Zhu et al[43] found that HG enhanced cell proliferation, migration and invasion and suppressed apoptosis by increasing protein kinase C delta (PKCδ)-phosphorylation and proteasome activity.

HG and cancer cell invasion and metastasis

HG induces migration and invasion by monounsaturated fatty acids (MUFAs), suppressing PTEN/Akt signalling and regulating the epithelial–mesenchymal transition (EMT) mediated by stearoyl-CoA desaturase 1 (SCD1)[72]. HG upregulates high mobility group AT-hook 2 (HMGA2) and high mobility group box 1 (HMGB1) to induce EMT via the Wnt/β-catenin signalling pathway and production of hydrogen peroxide[85,103,114]. HG induces the binding of plasminogen to the cell surface and promotes the activation of plasminogen and

EMT[44]. HG activates the insulin-like growth factor 1 receptor (IGF1R)/Src axis and upregulates the expression of EMT, ERK, cyclin B1 and N-cadherin signalling pathways by mediating the downregulation of miR-9 expression[73]. HG increases the expression of glucose transport protein 4 (GLUT4) and glucose transporter 12 (GLUT12) and promotes EMT by upregulating vascular endothelial growth factor (VEGF)/VEGF receptor (VEGFR) and oestrogen receptors (ERs). GLUT4 also supplies more energy for the growth of cancer cells by increasing glucose intake[45,99]. Lin et al[74] found that HG promoted the migration and invasion of cancer cells via the signal transducer and activator of transcription 3 (STAT3)-induced matrix metalloproteinase-9 (MMP-9) signalling pathway. HG increases expression of MMP-9 and MMP-2, downregulates E-cadherin expression, upregulates snail and induces higher malic enzyme 1 (ME1) activity[40,100,115]. Li et al[86] found that HG increased the production of ROS in a concentration-dependent manner. HG induces superoxide dismutase-dependent production of hydrogen peroxide, increases the expression of urokinase plasminogen activator (uPA), vimentin and fibronectin mediated by ROS and upregulates haem oxygenase-1 (HO-1) expression via ROS or the TGF-β1/PI3K/Akt signalling pathway[46,86,116]. HG modulates O-GlcNAcylation through the expression of glucosamine-fructose-6-phosphate amidotransferase (GFAT) and vimentin[71]. HG induces the establishment of a proinflammatory, pro-oxidant environment characterised by the cyclooxygenase-2 (COX-2)/PGE2 axis. Stromal-derived PGE2, acting as a stimulator of interleukin-1 (IL-1) epithelial expression, promotes the acquisition of motile properties by epithelial cells and the maintenance of COX-2/PGE2-dependent inflammation[47]. Cheng et al[87] found that the accumulation of hypoxia-inducible factor-1α (HIF-1α) induced by HG increased lactate dehydrogenase A (LDHA) activity and hexokinase 2 (HK2) and phosphofructokinase platelet type (PFKP) expression. Tomoka et al[48] found that HG induced Zn^{2+} transport via zinc transporters ZIP6 and ZIP10. Zhou et al[117] found that HG promoted cell migration via aquaporin 3 (AQP3).

HG and angiogenesis

Liao et al[56] found that HG increased the protein expression of receptor for advanced glycation end products (RAGE) and nicotinamide adenine dinucleotide phosphate oxidase-4 (NOX4) and affected angiogenesis and tumour metabolism via the RAGE-NOX-4 pathway. HG increased proliferation and angiogenesis and decreased apoptosis due to activation of the NF-κB pathway by increasing ROS[49]. Huang et al[94] found that HG led to lysophosphatidic acid (LPA) synthesis and upregulated aerobic glycolysis and VEGF-C production.

HG and cancer prognosis

Li et al[64] found the effect of maternally expressed gene 3 (MEG3) binding to miR-483-3p as molecular miRNA sponge. Overexpression of miR-483-3p suppressed ERp29 expression. HG negatively regulates the expression of endoplasmic reticulum protein 29 (ERp29) by inhibiting MEG3. ERp29 regulates the biological functions of carcinoma cells through EMT, which leads to a poor prognosis for hepatocellular carcinoma patients with HG64. In gastric cancer, a poor prognosis was associated with the multiplicative interaction of HG and long non-coding RNA (lncRNA) SNHG853. Yang et al[118] found that HG affected the outcome of colorectal cancer patients by inhibiting miR-16 expression and the expression of its downstream genes Myb and VEGFR2.

HG and abnormal molecular expression in cancer cells

Liu et al[65] found that HG enhanced the expression and O-GlcNAcylation of angiomotin (AMOT) and stimulated nuclear accumulation, transcription activity, interactions with transcription factors and transcription of target genes of YAP via AMOT. HG induces overexpression of β-catenin and subsequent transcription of the target genes by upregulating HBP and O-GlcNAcylation[101]. HG promotes the Wnt-stimulated formation of a lymphoid enhancer factor (LEF)-1/β-catenin complex that is associated with acetylase p300 and displaces SIRT1 deacetylase, leading to increased β-catenin acetylation, its nuclear accumulation and transcription activation119. HG increases expression of inhibitor factor 1 (IF1), decreases the level of transcriptional coactivator PGC-α and reduces mitochondrial biogenesis and ATP synthase dimer stability[66]. Duan et al[88] found that HG inhibits the expression of MHC class I chain-related protein A/B (MICA/B), promotes the expression of Bmi1 and weakens the cytotoxicity of natural killer cells in pancreatic cancer, contributing to immune escape by inhibiting the AMPK signalling pathway and activating the AMPK-Bmi1-GATA2-MICA/B axis. Fukami et al[95] found that HG induced N-linked glycosylation-mediated functional upregulation and overexpression of Cav3.2. Lee et al[120] determined that HG increased transcriptional activity and repressed the methylation of protein phosphatase 1 regulatory subunit 3C (PPP1R3C), and Briata et al[121] found that HG reduced c-myc expression.

HG and cancer chemoresistance or radioresistance

HG attenuated 5-fluorouracil (5-FU)–induced tumour growth inhibition by decreasing cell death and increasing DNA replication[54,75]. HG reduced the effect of metformin on cancer cell proliferation, cell death and cell cycle arrest and lost efficacy in inhibiting the mTOR pathway[50,111]. HG inhibited drug-induced p53 Ser46 phosphorylation, and mutual unbalance between p53-dependent apoptosis and damage-regulated autophagy modulator (DRAM) modified adriamycin (ADR)-induced cell death[76,122]. Kwon et al[57] found that HG-induced overexpressed inositol 1,4,5-trisphosphate receptor interacting protein (DANGER) bound to the death domain (DD) of death-associated protein kinase (DAPK) and inhibited ERK/DAPK-induced death, which accounted for radioresistance. HG suppressed bromopyruvate uptake and bromopyruvate-induced cell death by downregulating bromopyruvate carrier monocarboxylate transporter 1 (MCT1)[77]. HG-induced BCL-6 overexpression abrogated the effect of etoposide chemotherapy-induced cell death[104]. Wang et al[51] found that HG decreased carcinoma cellular sensitivity to 4-methylumbelliferone (4-MU)-inhibited cell proliferation. Biernacka et al[96] found that HG reduced docetaxel-induced cell apoptosis by upregulating insulin-like growth factor binding proteins 2 (IGFBP2). Liu et al[123] found that HG upregulated side population (SP, a key factor contributing to drug resistance) cells mediated by the Akt pathway. Nishiwada et al[124] found that 1% concentration sevoflurane in HG enhanced cell proliferation.

HG and cancer therapy

HG could reduce the sensitivity of cancer cells to docetaxel through a reduction in the expression of IGFBP2; however, metformin inhibits cell proliferation, reduces cell survival, promotes apoptosis of carcinoma cell induced by HG through activation of the AMPK/mTOR pathway, inhibits STAT3 and its target proteins stimulated by HG and negates the HG-mediated reduction in sensitivity to docetaxel[67,97,102]. Resveratrol played an important role in suppressing HG-driven ROS-induced cancer progression by inhibiting the ERK, p38 MAPK, STAT3, and AKT signalling pathways[68,89]. Indomethacin inhibited HG-induced proliferation and invasion by upregulating E-cadherin and activating the PI3K/AKT/GSK-3β signalling pathway[90]. Curcumin suppressed HG-driven EGF-induced invasion and migration by inhibiting the EGF/EGFR signalling pathway and its downstream signalling molecules, including ERK and Akt[91]. Aspirin inhibited cell proliferation by modulating abnormal glucose metabolism via NF-κB (or NF-κB/HIF1α)/GLUT1 signalling[69]. HG increased the cytotoxicity induced by carboplatin and 5-FU and decreased their IC50 because of the synergistic effect of the HG-mediated reduction in P-glycoprotein (P-gp) levels as well as increased drug accumulation, which enhanced ROS levels[52].

Conclusion

In summary, HG induced by various signals increases the risk of cancer. Studies of the role played by HG in cancer progression and therapy have revealed new connections between nutrient utilisation and the tumorigenic state. As interest in cancer and glucose metabolism grows, combining therapies of HG inhibitors with other modalities may be effective.

Conflicts of interest

The authors declare no conflicts of interest related to this study.

Author contribution

Drs Xin Jia CAI, Jian Yun ZHANG, Ao Bo ZHANG and Xuan ZHOU analysed the data and drafted the manuscript; Drs Tie Jun LI, He Yu ZHANG, Jian Yun ZHANG and Xin Jia CAI designed the research; Drs Tie Jun LI, He Yu ZHANG and Jian Yun ZHANG obtained copies of studies and revised the manuscript. All authors read and approved the submitted version.

(Received Sep 09, 2021; accepted Nov 24, 2021)

References

1. Cai X, Li X, Tang M, et al. Dietary carbohydrate intake, glycaemic index, glycaemic load and digestive system cancers: An updated dose-response meta-analysis. Br J Nutr 2019;121:1081–1096.
2. Augustin LS, Gallus S, Franceschi S, et al. Glycemic index and load and risk of upper aero-digestive tract neoplasms (Italy). Cancer Causes Control 2003;14:657–662.
3. Augustin LS, Kendall CW, Jenkins DJ, et al. Glycemic index, glycemic load and glycemic response: An International Scientific Consensus Summit from the International Carbohydrate Quality Consortium (ICQC). Nutr Metab Cardiovasc Dis 2015;25:795–815.
4. Zhan YS, Feng L, Tang SH, et al. Glucose metabolism disorders in cancer patients in a Chinese population. Med Oncol 2010;27:177–184.

5. Li N, Petrick JL, Steck SE, et al. A pooled analysis of dietary sugar/carbohydrate intake and esophageal and gastric cardia adenocarcinoma incidence and survival in the USA. Int J Epidemiol 2017;46:1836–1846.
6. Eslamian G, Jessri M, Hajizadeh B, Ibiebele TI, Rashidkhani B. Higher glycemic index and glycemic load diet is associated with increased risk of esophageal squamous cell carcinoma: A case-control study. Nutr Res 2013;33:719–725.
7. Thompson HJ, Neuhouser ML, Lampe JW, et al. Effect of low or high glycemic load diets on experimentally induced mammary carcinogenesis in rats. Mol Nutr Food Res 2016;60:1416–1426.
8. Lambertz IU, Luo L, Berton TR, et al. Early exposure to a high fat/high sugar diet increases the mammary stem cell compartment and mammary tumor risk in female mice. Cancer Prev Res (Phila) 2017;10:553–562.
9. Sieri S, Muti P, Claudia A, et al. Prospective study on the role of glucose metabolism in breast cancer occurrence. Int J Cancer 2012;130:921–929.
10. Raza U, Asif MR, Rehman AB, Sheikh A. Hyperlipidemia and hyper glycaemia in breast cancer patients is related to disease stage. Pak J Med Sci 2018;34:209–214.
11. Contiero P, Berrino F, Tagliabue G, et al. Fasting blood glucose and long-term prognosis of non-metastatic breast cancer: A cohort study. Breast Cancer Res Treat 2013;138:951–959.
12. Luo J, Chen YJ, Chang LJ. Fasting blood glucose level and prognosis in non-small cell lung cancer (NSCLC) patients. Lung Cancer 2012;76:242–247.
13. Fedirko V, Lukanova A, Bamia C, et al. Glycemic index, glycemic load, dietary carbohydrate, and dietary fiber intake and risk of liver and biliary tract cancers in Western Europeans. Ann Oncol 2013;24:543–553.
14. Healy ME, Lahiri S, Hargett SR, et al. Dietary sugar intake increases liver tumor incidence in female mice. Sci Rep 2016;6:22292.
15. Larsson SC, Giovannucci EL, Wolk A. Sweetened beverage consumption and risk of biliary tract and gallbladder cancer in a prospective study. J Natl Cancer Inst 2016;108:djw125.
16. Ye Y, Wu Y, Xu J, Ding K, Shan X, Xia D. Association between dietary carbohydrate intake, glycemic index and glycemic load, and risk of gastric cancer. Eur J Nutr 2017;56:1169–1177.
17. Ikeda F, Kiyohara Y. Helicobacter pylori infection and hyperglycemia/diabetes are associated with an increased risk of gastric cancer iIn Japanese]. Gan To Kagaku Ryoho 2015;42:529–533.
18. Sieri S, Krogh V, Agnoli C, et al. Dietary glycemic index and glycemic load and risk of colorectal cancer: Results from the EPIC-Italy study. Int J Cancer 2015;136:2923–2931.
19. Sieri S, Agnoli C, Pala V, et al. Dietary glycemic index, glycemic load, and cancer risk: Results from the EPIC-Italy study. Sci Rep 2017;7:9757.
20. Hu J, La Vecchia C, Augustin LS, et al. Glycemic index, glycemic load and cancer risk. Ann Oncol 2013;24:245–251.
21. Galeone C, Pelucchi C, La Vecchia C. Added sugar, glycemic index and load in colon cancer risk. Curr Opin Clin Nutr Metab Care 2012;15:368–373.
22. Cui G, Zhang T, Ren F, et al. High blood glucose levels correlate with tumor malignancy in colorectal cancer patients. Med Sci Monit 2015;21:3825–3833.
23. Vulcan A, Manjer J, Ohlsson B. High blood glucose levels are associated with higher risk of colon cancer in men: A cohort study. BMC Cancer 2017;17:842.
24. Jung KJ, Kim MT, Jee SH. Impaired fasting glucose, single-nucleotide polymorphisms, and risk for colorectal cancer in Koreans. Epidemiol Health 2016;38:e2016002.
25. Shin HY, Jung KJ, Linton JA, Jee SH. Association between fasting serum glucose levels and incidence of colorectal cancer in Korean men: The Korean Cancer Prevention Study-II. Metabolism 2014;63:1250–1256.
26. Rossi M, Lipworth L, Polesel J, et al. Dietary glycemic index and glycemic load and risk of pancreatic cancer: A case-control study. Ann Epidemiol 2010;20:460–465.
27. Nagai M, Murakami Y, Tamakoshi A, et al. Fasting but not casual blood glucose is associated with pancreatic cancer mortality in Japanese: EPOCH-JAPAN. Cancer Causes Control 2017;28:625–633.
28. Pang Y, Kartsonaki C, Guo Y, et al. Diabetes, plasma glucose and incidence of pancreatic cancer: A prospective study of 0.5 million Chinese adults and a meta-analysis of 22 cohort studies. Int J Cancer 2017;140:1781–1788.
29. Er KC, Hsu CY, Lee YK, Huang MY, Su YC. Effect of glycemic control on the risk of pancreatic cancer: A nationwide cohort study. Medicine (Baltimore) 2016;95:e3921 [erratum 2016;95:e5074].
30. Zhu J, Tu H, Matin SF, Tannir NM, Wood CG, Wu X. Glycemic index, glycemic load and carbohydrate intake in association with risk of renal cell carcinoma. Carcinogenesis 2017;38:1129–1135.
31. Otunctemur A, Ozbek E, Sahin S, et al. Diabetes mellitus as a risk factor for high grade renal cell carcinoma. Asian Pac J Cancer Prev 2014;15:3993–3996.
32. Arthur R, Møller H, Garmo H, et al. Association between baseline serum glucose, triglycerides and total cholesterol, and prostate cancer risk categories. Cancer Med 2016;5:1307–1318.
33. Augustin LS, Taborelli M, Montella M, et al. Associations of dietary carbohydrates, glycaemic index and glycaemic load with risk of bladder cancer: A case-control study. Br J Nutr 2017;118:722–729.
34. Lee YY, Choi CH, Kim CJ, et al. Glucose as a prognostic factor in non-diabetic women with locally advanced cervical cancer (IIB-IVA). Gynecol Oncol 2010;116:459–463.
35. Nagle CM, Olsen CM, Ibiebele TI, et al. Glycemic index, glycemic load and endometrial cancer risk: Results from the Australian National Endometrial Cancer study and an updated systematic review and meta-analysis. Eur J Nutr 2013;52:705–715.
36. Nagle CM, Kolahdooz F, Ibiebele TI, et al. Carbohydrate intake, glycemic load, glycemic index, and risk of ovarian cancer. Ann Oncol 2011;22:1332–1338.
37. Debata A, Yoshida K, Ujifuku K, et al. Hyperglycemia is associated with poor survival in primary central nervous system lymphoma patients. Tumori 2017;103:272–278.
38. Makarem N, Bandera EV, Nicholson JM, Parekh N. Consumption of sugars, sugary foods, and sugary beverages in relation to cancer risk: A systematic review of longitudinal studies. Annu Rev Nutr 2018;38:17–39.
39. Parekh N, Lin Y, Hayes RB, Albu JB, Lu-Yao GL. Longitudinal associations of blood markers of insulin and glucose metabolism and cancer mortality in the third National Health and Nutrition Examination Survey. Cancer Causes Control 2010;21:631–642.
40. Zheng FJ, Ye HB, Wu MS, Lian YF, Qian CN, Zeng YX. Repressing malic enzyme 1 redirects glucose metabolism, unbalances the redox state, and attenuates migratory and invasive abilities in nasopharyngeal carcinoma cell lines. Chin J Cancer 2012;31:519–531.
41. Langen KJ, Braun U, Rota Kops E, et al. The influence of plasma glucose levels on fluorine-18-fluorodeoxyglucose uptake in bronchial carcinomas. J Nucl Med 1993;34:355–359.
42. Zhang J, Gelman IH, Katsuta E, et al. Glucose drives growth factor-independent esophageal cancer proliferation via phosphohistidine-focal adhesion kinase signaling. Cell Mol Gastroenterol Hepatol 2019;8:37–60.
43. Zhu S, Yao F, Li WH, et al. PKC?-dependent activation of the ubiquitin proteasome system is responsible for high glucose-induced human breast cancer MCF-7 cell proliferation, migration and invasion. Asian Pac J Cancer Prev 2013;14:5687–5692.

44. Viedma-Rodríguez R, Martínez-Hernández MG, Flores-López LA, Baiza-Gutman LA. Epsilon-aminocaproic acid prevents high glucose and insulin induced-invasiveness in MDA-MB-231 breast cancer cells, modulating the plasminogen activator system. Mol Cell Biochem 2018;437:65–80.
45. Matsui C, Takatani-Nakase T, Maeda S, Nakase I, Takahashi K. Potential roles of GLUT12 for glucose sensing and cellular migration in MCF-7 human breast cancer cells under high glucose conditions. Anticancer Res 2017;37:6715–6722.
46. Flores-López LA, Martínez-Hernández MG, Viedma-Rodríguez R, Díaz-Flores M, Baiza-Gutman LA. High glucose and insulin enhance uPA expression, ROS formation and invasiveness in breast cancer-derived cells. Cell Oncol (Dordr) 2016;39:365–378.
47. Kallens V, Tobar N, Molina J, et al. Glucose promotes a pro-oxidant and pro-inflammatory stromal microenvironment which favors motile properties in breast tumor cells. J Cell Biochem 2017;118:994–1002.
48. Takatani-Nakase T. Migration behavior of breast cancer cells in the environment of high glucose level and the role of zinc and its transporter [in Japanese]. Yakugaku Zasshi 2013;133:1195–1199.
49. Nasir Kansestani A, Mansouri K, Hemmati S, Zare ME, Moatafaei A. High glucose-reduced apoptosis in human breast cancer cells is mediated by activation of NF-κB. Iran J Allergy Asthma Immunol 2019;18:153–162.
50. Varghese S, Samuel SM, Varghese E, Kubatka P, Büsselberg D. High glucose represses the anti-proliferative and pro-apoptotic effect of metformin in triple negative breast cancer cells. Biomolecules 2019;9:16.
51. Wang R, Zhou W, Wang J, et al. Role of hyaluronan and glucose on 4-methylumbelliferone-inhibited cell proliferation in breast carcinoma cells. Anticancer Res 2015;35:4799–4805.
52. Pandey V, Chaube B, Bhat MK. Hyperglycemia regulates MDR-1, drug accumulation and ROS levels causing increased toxicity of carboplatin and 5-fluorouracil in MCF-7 cells. J Cell Biochem 2011;112:2942–2952.
53. Lin Y, Hu D, Zhou Q, Lin X, Lin J, Peng F. The fasting blood glucose and long non-coding RNA SNHG8 predict poor prognosis in patients with gastric carcinoma after radical gastrectomy. Aging (Albany NY) 2018;10:2646–2656 [erratum 2018;10:4294].
54. Zhao W, Chen R, Zhao M, Li L, Fan L, Che XM. High glucose promotes gastric cancer chemoresistance in vivo and in vitro. Mol Med Rep 2015;12:843–850.
55. Wang L, Zhong N, Liu S, Zhu X, Liu Y. High glucose stimulates proliferation and inhibits apoptosis of non-small-cell lung cancer cells by JNK-mediated downregulation of p53 pathway. Acta Biochim Biophys Sin (Shanghai) 2017;49:286–288.
56. Liao YF, Yin S, Chen ZQ, Li F, Zhao B. High glucose promotes tumor cell proliferation and migration in lung adenocarcinoma via the RAGE-NOXs pathway. Mol Med Rep 2018;17:8536–8541.
57. Kwon T, Youn H, Son B, et al. DANGER is involved in high glucose-induced radioresistance through inhibiting DAPK-mediated anoikis in non-small cell lung cancer. Oncotarget 2016;7:7193–7206.
58. Zhang X, Qiao Y, Wu Q, et al. The essential role of YAP O-GlcNAcylation in high-glucose-stimulated liver tumorigenesis. Nat Commun 2017;8:15280.
59. Qiao Y, Zhang X, Zhang Y, et al. High glucose stimulates tumorigenesis in hepatocellular carcinoma cells through AGER-dependent O-GlcNAcylation of c-Jun. Diabetes 2016;65:619–632.
60. Chouhan S, Singh S, Athavale D, et al. Glucose induced activation of canonical Wnt signaling pathway in hepatocellular carcinoma is regulated by DKK4. Sci Rep 2016;6:27558.
61. Chandrasekaran K, Swaminathan K, Chatterjee S, Dey A. Apoptosis in HepG2 cells exposed to high glucose. Toxicol In Vitro 2010;24:387–396.
62. Chandrasekaran K, Swaminathan K, Kumar SM, Clemens DL, Dey A. Increased oxidative stress and toxicity in ADH and CYP2E1 overexpressing human hepatoma VL-17A cells exposed to high glucose. Integr Biol (Camb) 2012;4:550–563.
63. Jiang Q, Yuan Y, Zhou J, et al. Apoptotic events induced by high glucose in human hepatoma HepG2 cells involve endoplasmic reticulum stress and MAPK's activation. Mol Cell Biochem 2015;399:113–122.
64. Li X, Cheng T, He Y, et al. High glucose regulates ERp29 in hepatocellular carcinoma by LncRNA MEG3-miRNA 483-3p pathway. Life Sci 2019;232:116602.
65. Liu Y, Lu Z, Shi Y, Sun F. AMOT is required for YAP function in high glucose induced liver malignancy. Biochem Biophys Res Commun 2018;495:1555–1561.
66. Domenis R, Bisetto E, Rossi D, Comelli M, Mavelli I. Glucose-modulated mitochondria adaptation in tumor cells: A focus on ATP synthase and inhibitor factor 1. Int J Mol Sci 2012;13:1933–1950.
67. Lv Y, Tian N, Wang J, Yang M, Kong L. Metabolic switching in the hypoglycemic and antitumor effects of metformin on high glucose induced HepG2 cells. J Pharm Biomed Anal 2018;156:153–162.
68. Li Y, Zhu W, Li J, Liu M, Wei M. Resveratrol suppresses the STAT3 signaling pathway and inhibits proliferation of high glucose-exposed HepG2 cells partly through SIRT1. Oncol Rep 2013;30:2820–2828.
69. Liu YX, Feng JY, Sun MM, et al. Aspirin inhibits the proliferation of hepatoma cells through controlling GLUT1-mediated glucose metabolism. Acta Pharmacol Sin 2019;40:122–132.
70. Saengboonmee C, Seubwai W, Pairojkul C, Wongkham S. High glucose enhances progression of cholangiocarcinoma cells via STAT3 activation. Sci Rep 2016;6:18995.
71. Phoomak C, Vaeteewoottacharn K, Silsirivanit A, et al. High glucose levels boost the aggressiveness of highly metastatic cholangiocarcinoma cells via O-GlcNAcylation. Sci Rep 2017;7:43842.
72. Ran H, Zhu Y, Deng R, et al. Stearoyl-CoA desaturase-1 promotes colorectal cancer metastasis in response to glucose by suppressing PTEN. J Exp Clin Cancer Res 2018;37:54.
73. Chen YC, Ou MC, Fang CW, Lee TH, Tzeng SL. High glucose concentrations negatively regulate the IGF1R/Src/ERK axis through the microRNA-9 in colorectal cancer. Cells 2019;8:326.
74. Lin CY, Lee CH, Huang CC, Lee ST, Guo HR, Su SB. Impact of high glucose on metastasis of colon cancer cells. World J Gastroenterol 2015;21:2047–2057.
75. Ma YS, Yang IP, Tsai HL, Huang CW, Juo SH, Wang JY. High glucose modulates antiproliferative effect and cytotoxicity of 5-fluorouracil in human colon cancer cells. DNA Cell Biol 2014;33:64–72.
76. Garufi A, Pistritto G, Baldari S, Toietta G, Cirone M, D'Orazi G. p53-dependent PUMA to DRAM antagonistic interplay as a key molecular switch in cell-fate decision in normal/high glucose conditions. J Exp Clin Cancer Res 2017;36:126.
77. Ideno M, Sasaki S, Kobayashi M, Futagi Y, Narumi K, Iseki K. Influence of high glucose state on bromopyruvate-induced cytotoxicity by human colon cancer cell lines. Drug Metab Pharmacokinet 2016;31:67–72.
78. Li W, Wu Z, Ma Q, et al. Hyperglycemia regulates TXNIP/TRX/ROS axis via p38 MAPK and ERK pathways in pancreatic cancer. Curr Cancer Drug Targets 2014;14:348–356.
79. Ito M, Makino N, Matsuda A, et al. High glucose accelerates cell proliferation and increases the secretion and mRNA expression of osteopontin in human pancreatic duct epithelial cells. Int J Mol Sci 2017;18:807.
80. Rahn S, Zimmermann V, Viol F, et al. Diabetes as risk factor for pancreatic cancer: Hyperglycemia promotes epithelial-mesenchymal-transition and stem cell properties in pancreatic ductal epithelial cells. Cancer Lett 2018;415:129–150.
81. Luo J, Xiang Y, Xu X, et al. High glucose-induced ROS production stimulates proliferation of pancreatic cancer via inactivating the JNK pathway. Oxid Med Cell Longev 2018;2018:6917206.

82. Zhou C, Qian W, Li J, et al. High glucose microenvironment accelerates tumor growth via SREBP1-autophagy axis in pancreatic cancer. J Exp Clin Cancer Res 2019;38:302.
83. Han L, Ma Q, Li J, et al. High glucose promotes pancreatic cancer cell proliferation via the induction of EGF expression and transactivation of EGFR. PLoS One 2011;6:e27074.
84. Liu H, Ma Q, Li J. High glucose promotes cell proliferation and enhances GDNF and RET expression in pancreatic cancer cells. Mol Cell Biochem 2011;347:95–101.
85. Li W, Zhang L, Chen X, Jiang Z, Zong L, Ma Q. Hyperglycemia promotes the epithelial-mesenchymal transition of pancreatic cancer via hydrogen peroxide. Oxid Med Cell Longev 2016;2016:5190314.
86. Li W, Ma Q, Li J, et al. Hyperglycemia enhances the invasive and migratory activity of pancreatic cancer cells via hydrogen peroxide. Oncol Rep 2011;25:1279–1287.
87. Cheng L, Qin T, Ma J, et al. Hypoxia-inducible factor-1α mediates hyperglycemia-induced pancreatic cancer glycolysis. Anticancer Agents Med Chem 2019;19:1503–1512.
88. Duan Q, Li H, Gao C, et al. High glucose promotes pancreatic cancer cells to escape from immune surveillance via AMPK-Bmi1-GATA2-MICA/B pathway. J Exp Clin Cancer Res 2019;38:192.
89. Cao L, Chen X, Xiao X, Ma Q, Li W. Resveratrol inhibits hyperglycemia-driven ROS-induced invasion and migration of pancreatic cancer cells via suppression of the ERK and p38 MAPK signaling pathways. Int J Oncol 2016;49:735–743.
90. Han L, Peng B, Ma Q, et al. Indometacin ameliorates high glucose-induced proliferation and invasion via modulation of e-cadherin in pancreatic cancer cells. Curr Med Chem 2013;20:4142–4152.
91. Li W, Wang Z, Xiao X, et al. Curcumin attenuates hyperglycemia-driven EGF-induced invasive and migratory abilities of pancreatic cancer via suppression of the ERK and AKT pathways. Oncol Rep 2019;41:650–658.
92. Rezende LP, Galheigo MRU, Landim BC, et al. Effect of glucose and palmitate environment on proliferation and migration of PC3-prostate cancer cells. Cell Biol Int 2019;43:373–383.
93. Li X, Li J, Cai Y, et al. Hyperglycaemia-induced miR-301a promotes cell proliferation by repressing p21 and Smad4 in prostate cancer. Cancer Lett 2018;418:211–220.
94. Huang YL, Lin YC, Lin CC, Chen WM, Chen BPC, Lee H. High glucose induces VEGF-C expression via the LPA1/3-Akt-ROS-LEDGF signaling axis in human prostate cancer PC-3 cells. Cell Physiol Biochem 2018;50:597–611.
95. Fukami K, Asano E, Ueda M, Sekiguchi F, Yoshida S, Kawabata A. High glucose induces N-linked glycosylation-mediated functional upregulation and overexpression of Cav3.2 T-type calcium channels in neuroendocrine-like differentiated human prostate cancer cells. J Pharmacol Sci 2017;133:57–60.
96. Biernacka KM, Uzoh CC, Zeng L, et al. Hyperglycaemia-induced chemoresistance of prostate cancer cells due to IGFBP2. Endocr Relat Cancer 2013;20:741–751.
97. Biernacka KM, Persad RA, Bahl A, Gillatt D, Holly JM, Perks CM. Hyperglycaemia-induced resistance to Docetaxel is negated by metformin: A role for IGFBP-2. Endocr Relat Cancer 2017;24:17–30.
98. Gao L, Xu FM, Shi WJ, et al. High-glucose promotes proliferation of human bladder cancer T24 cells by activating Wnt/β-catenin signaling pathway. Eur Rev Med Pharmacol Sci 2018;22:8151–8160.
99. Gu CJ, Xie F, Zhang B, et al. High glucose promotes epithelial-mesenchymal transition of uterus endometrial cancer cells by increasing ER/GLUT4-mediated VEGF secretion. Cell Physiol Biochem 2018;50:706–720.
100. Han J, Zhang L, Guo H, et al. Glucose promotes cell proliferation, glucose uptake and invasion in endometrial cancer cells via AMPK/mTOR/S6 and MAPK signaling. Gynecol Oncol 2015;138:668–675.
101. Zhou F, Huo J, Liu Y, et al. Elevated glucose levels impair the WNT/β-catenin pathway via the activation of the hexosamine biosynthesis pathway in endometrial cancer. J Steroid Biochem Mol Biol 2016;159:19–25.
102. Wallbillich JJ, Josyula S, Saini U, et al. High glucose-mediated STAT3 activation in endometrial cancer is inhibited by metformin: Therapeutic implications for endometrial cancer. PLoS One 2017;12:e0170318.
103. Wang Y, Tan J, Wu H, Yi C. High glucose promotes epithelial-mesenchymal transition, migration and invasion in A20 murine di□use large B-cell lymphoma cells through increased expression of high mobility group AT-hook 2 (HMGA2). Med Sci Monit 2019;25:3860–3868.
104. Shao Y, Ling CC, Liu XQ. High concentrations of glucose suppress etoposide-induced cell death of B-cell lymphoma through BCL-6. Biochem Biophys Res Commun 2014;450:227–233.
105. Zhang Y, Zhou J, Wang T, Cai L. High level glucose increases mutagenesis in human lymphoblastoid cells. Int J Biol Sci 2007;3:375–379.
106. Zhang J, Luo J, Liu F, et al. Diabetes mellitus potentiates diffuse large B-cell lymphoma via high levels of CCL5. Mol Med Rep 2014;10:1231–1236.
107. Weiss P, Ashwell G, Morell AG, Stockert RJ. Modulation of the asialoglycoprotein receptor in human hepatoma cells: Effect of glucose. Hepatology 1994;19:432–439.
108. Chen Y, Liu R, Chu Z, et al. High glucose stimulates proliferative capacity of liver cancer cells possibly via O-GlcNAcylation-dependent transcriptional regulation of GJC1. J Cell Physiol 2018;234:606–618.
109. Gupta C, Kaur J, Tikoo K. Regulation of MDA-MB-231 cell proliferation by GSK-3β involves epigenetic modifications under high glucose conditions. Exp Cell Res 2014;324:75–83.
110. Yamamoto M, Patel NA, Taggart J, Sridhar R, Cooper DR. A shift from normal to high glucose levels stimulates cell proliferation in drug sensitive MCF-7 human breast cancer cells but not in multidrug resistant MCF-7/ADR cells which overproduce PKC-betaII. Int J Cancer 1999;83:98–106.
111. Wahdan-Alaswad R, Fan Z, Edgerton SM, et al. Glucose promotes breast cancer aggression and reduces metformin efficacy. Cell Cycle 2013;12:3759–3769.
112. Matsui C, Takatani-Nakase T, Maeda S, Takahashi K. High-glucose conditions promote anchorage-independent colony growth in human breast cancer MCF-7 cells. Biol Pharm Bull 2018;41:1379–1383.
113. Wang L, Bai YY, Yang Y, et al. Diabetes mellitus stimulates pancreatic cancer growth and epithelial-mesenchymal transition-mediated metastasis via a p38 MAPK pathway. Oncotarget 2016;7:38539–38550.
114. Ohmori H, Luo Y, Fujii K, et al. Dietary linoleic acid and glucose enhances azoxymethane-induced colon cancer and metastases via the expression of high-mobility group box 1. Pathobiology 2010;77:210–217.
115. Li JT, Zhang HW, Guo XH, et al. Effects of high glucose on in vitro invasiveness of human breast cancer cell line MDA-MB-435 [in Chinese]. Zhonghua Yi Xue Za Zhi 2013;93:89–92.
116. Kang X, Kong F, Wu X, et al. High glucose promotes tumor invasion and increases metastasis-associated protein expression in human lung epithelial cells by upregulating heme oxygenase-1 via reactive oxygen species or the TGF-β1/PI3K/Akt signaling pathway. Cell Physiol Biochem 2015;35:1008–1022.
117. Zhou Y, Wang Y, Wang S, Shen L. Hyperglycemia promotes human gastric carcinoma progression via aquaporin 3. Dig Dis Sci 2015;60:2338–2345.
118. Yang IP, Tsai HL, Huang CW, et al. High blood sugar levels significantly impact the prognosis of colorectal cancer patients through down-regulation of microRNA-16 by targeting Myb and VEGFR2. Oncotarget 2016;7:18837–18850.

119. Chocarro-Calvo A, García-Martínez JM, Ardila-González S, De la Vieja A, García-Jiménez C. Glucose-induced β-catenin acetylation enhances Wnt signaling in cancer. Mol Cell 2013;49:474–486.
120. Lee SK, Moon JW, Lee YW, et al. The effect of high glucose levels on the hypermethylation of protein phosphatase 1 regulatory subunit 3C (PPP1R3C) gene in colorectal cancer. J Genet 2015;94:75–85.
121. Briata P, Laurino C, Gherzi R. c-myc gene expression in human cells is controlled by glucose. Biochem Biophys Res Commun 1989;165:1123–1129.
122. Garufi A, D'Orazi G. High glucose dephosphorylates serine 46 and inhibits p53 apoptotic activity. J Exp Clin Cancer Res 2014;33:79.
123. Liu PP, Liao J, Tang ZJ, et al. Metabolic regulation of cancer cell side population by glucose through activation of the Akt pathway. Cell Death Differ 2014;21:124–135.
124. Nishiwada T, Kawaraguchi Y, Uemura K, Sugimoto H, Kawaguchi M. Effect of sevoflurane on human hepatocellular carcinoma HepG2 cells under conditions of high glucose and insulin. J Anesth 2015;29:805–808.

Exploration of Genetic Variants of Non-syndromic Cleft Lip with or without Palate and Underlying Mechanisms

Yong Chu PAN[1,2,3#], Lan MA[1,4#], Shu LOU[1,2], Gui Rong ZHU[1,2], Xin YU[1,2], Lin WANG[1,2,3]

Non-syndromic cleft lip with/without cleft palate (NSCL/P) is one of the most common birth defects in humans with an overall prevalence of one per 1000 live births. Due to genetic and environmental influences, the fusion of the lips or palate may be interrupted at any stage and cause a cleft. Over decades, dozens of susceptible genes and loci have been identified using multiple genetic approaches. Our group has collected samples of NSCL/P patients since 2008 and established the biobank. We discovered numerous susceptible loci related to the occurrence of NSCL/P in the Chinese population, such as 16p13.3, 1q32.2, 10q25.3 and 17p13.1. In addition, we performed functional studies on related loci and genes by using molecular biology, cell biology, animal models and other methods to provide a basis for the construction of the NSCL/P genetic map in the Chinese population and help to implement individualised prophylaxis and treatment. Future efforts will focus on identifying functional variants, investigating pathways and other interactions, and including phenotypic and ethnic diversity in research.

Key words: *cleft lip, cleft palate, craniofacial abnormalities, genetics*
Chin J Dent Res 2022;25(1):21–27; doi: 10.3290/j.cjdr.b2752691

Non-syndromic cleft lip with or without cleft palate (NSCL/P) is a common human birth defect characterised by craniofacial abnormality due to incomplete separation between the nasal and oral cavities[1]. Its prevalence ranges from 1/700 to 1/1000, depending on ethnicity and geographical area[2,3]. Common risk factors for NSCL/P include genetic risk factors, environmental exposure and their interaction[4-7]. As only a few people exposed to the same risk factors suffer from NSCL/P, genetic susceptibility is considered to play a crucial role.

Most genomic variation can be attributed to single nucleotide polymorphisms (SNPs), which are useful markers for genetic association studies of disease susceptibility or adverse drug reactions[8]. To date, various genetic approaches have been applied to identify genetic factors that put individuals at risk of NSCL/P. Initially, candidate gene association studies were performed to test genetic variants in genes relevant to NSCL/P9. Later, the associations of SNPs in the pathway with the risk of NSCL/P were investigated using a candidate pathway association study approach[10]. Genome-wide association studies (GWASs) have since successfully identified numerous loci associated with NSCL/P[11]. A possible polygenic threshold model of inheritance is supported by the identification of common genetic risk variants for NSCL/P from GWASs and SNP heritability estimates of around 30%[12]. All these studies have facilitated understanding of the pathogenic mechanisms of NSCL/P and improved clinical management of patients.

1 Jiangsu Key Laboratory of Oral Diseases, Nanjing Medical University, Nanjing, P.R. China.
2 Department of Orthodontics, Affiliated Hospital of Stomatology, Nanjing Medical University, Nanjing, P.R. China.
3 State Key Laboratory of Reproductive Medicine, Nanjing Medical University, Nanjing, P.R. China.
4 Department of Environmental Genomics, School of Public Health, Nanjing Medical University, Nanjing, P.R. China.

# These authors contributed equally to this work.

Corresponding author: Dr Lin WANG, Department of Orthodontics, Affiliated Hospital of Stomatology, Nanjing Medical University, Nanjing, P.R. China. Tel: 86-25-69593165; Fax: 86-25-69593186. Email: lw603@njmu.edu.cn

The present review summarises the approaches to, advances in and future prospects for genetic variant discovery and functional interpretation. We then complement our description with examples from susceptibility loci identified in our study where the use of these approaches has advanced our biological understanding of NSCL/P. In addition, we assess the extensive genetic, molecular and cell biological evidence that have implications for studies on NSCL/P.

Candidate gene association studies in NSCL/P

Candidate gene association studies have proven to be an effective approach in genetic association studies based on case-control populations to identify risk variants involved in specific diseases, which have the advantages of being cheap and easy to implement quickly[13]. These studies on NSCL/P always begin with selection of a putative candidate gene, which could play a critical role in the development of cleft lip and palate under investigation[14]. To date, there is a large amount of literature and experimental and sequencing data that can be used to can be used to identify candidate genes for NSCL/P. For example, p63 as a Wnt signalling target was found to be involved in midfacial development in mice[15]. FOXE1 mutations were detected to be associated with Bamforth-Lazarus syndrome, characterised by thyroid dysgenesis and cleft lip[16]. To explore the functional significance and potential association trait of the candidate genes of NSCL/P further, selection of a putative candidate gene was followed by evaluating and screening polymorphisms, usually the representative SNPs called tagging SNPs[17] or/and functional SNPs, which affect gene transcription. Finally, the selected SNPs were genotyped in the experimental population, including cases and controls, to make an association analysis between SNPs and the risk of NSCL/P.

Thus far, candidate gene association studies have successfully identified a group of specific variants and genes that may lead to the development of NSCL/P[18-21]. In recent years, our group has also carried out candidate gene association studies to identify additional SNPs that pose risks and evaluated their potential as biomarkers in the future.

IRF6

The first genetic variant associated with NSCL/P was either valine or isoleucine at amino acid position 274 (V274I) located in IRF69. IRF6 has been reported to be involved in Van der Woude syndrome, accompanied by the occurrence of CLP or deformity of the lower lip[22]. Zucchero et al[9] carried out transmission-disequilibrium testing (TDT) and case-control analyses in 8003 individuals from 1968 multiethnic families and detected that V274I in IRF6 was the risk genetic variation related to NSCL/P. In 2010, our group also genotyped polymorphisms in IRF6 and evaluated their associations with NSCL/P in a Chinese Han population[23]. We determined that rs2235371 and rs642961, which regulated levels of IRF6 mRNA and protein, significantly affect the susceptibility of NSCL/P.

MSX1

MSX1 is regionally expressed in the early critical stage of craniofacial development and participates in craniofacial and nervous system development as a transcriptional suppressor[24]. In addition, Msx1-deficient transgenic mice have been found to show general craniofacial deformity, including cleft palate, alveolar bone abnormalities and dental dysplasia[25]. Ma et al[26] selected four functional SNPs in MSX1, which were located in 3′UTR, exon and 5′UTR regions, and evaluated their susceptibility to NSCL/P among 602 cases and 605 healthy controls from a Chinese Han population. rs12532 located in 3′UTR of MSX1 was detected to be related to the development of NSCL/P by affecting the binding of miR-3649 to MSX1[26].

MYH9

MYH9 has been reported to play an important role in the development of palatal fusion[27]. MYH9 is a candidate gene and it is therefore worth exploring which SNPs on it are associated with the risk of NSCL/P and how these sites regulate gene expression to cause the disease; thus, we selected independent functional SNPs located in 3′UTR, exon and 5′UTR regions based on the SNP database and HapMap Project database. We made a further biological functional prediction for these sites and four SNPs were included. Through the two-stage population sample verification, including 1275 cases and 1295 controls, followed by a series of functional experiments, rs12107 in the 3’UTR and rs2269529 in the exon region were identified to be related to NSCL/P by upregulating expression of MYH9[28].

Candidate pathway association studies in NSCL/P

The biological processes that occur during the development of human embryos are carried out by several pathways in a tightly regulatory manner. At the phenotypic level, dysregulation of these processes could lead

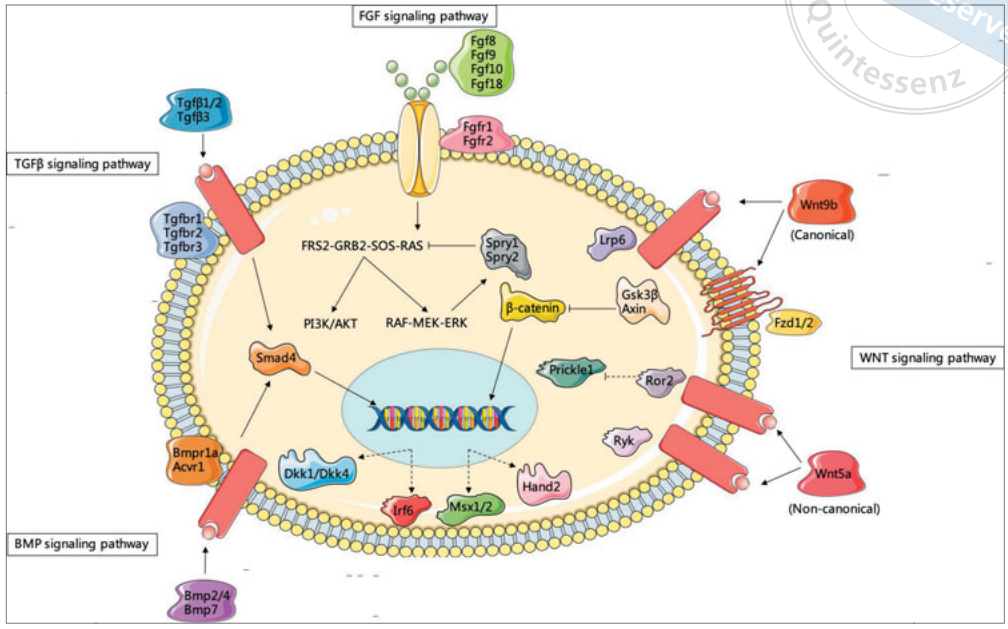

Fig 1 Main molecular pathways involved in NSCL/P. Susceptibility genes in NSCL/P affect different signalling pathways, including WNT, TGFβ, BMP, and FGF signalling pathway.

to malformations during the early embryonic development, such as NSCL/P[6,29]. Diverse signalling cues and attendant proteins work together during closure of the lip and growth of the palatal shelves across embryogenesis, including BMP, FGF, TGFβ and WNT signalling pathways (Fig 1)[10,30-32]. Pathway studies have been based on the association analysis between tag SNPs and the risk of NSCL/P defining SNPs related to NSCL/P on pathway genes.

WNT pathway

Vijayan et al[33] performed an association analysis based on 20 SNPs on WNT pathway genes in 471 individuals with NSCL/P and 504 unrelated control individuals of Caucasian ethnicity, and a significant association was found between GSK3B rs13314595 genotypes and NSCL/P. This study was the first to show the association between GSK3B and NSCL/P and confirmed the role of additional WNT pathway genes as candidates for NSCL/P[33].

Epidermal growth factor receptor (EGFR) pathway

EGFR was reported to regulate cell migration in the embryonic developmental phase[34,35], which was closely related to the development of craniofacial structure[36]. Our group has conducted an in-depth exploration of genetic variation in biological pathways[37]. Li et al[37] selected a superpathway of endocytic trafficking of EGFR and investigated the associations of SNPs in the pathway with the risk of NSCL/P. The study suggested that the genetic variants of SHTN1, AP2B1 and NTRK1 in the investigated superpathway showed statistical evidence for association with the risk of NSCL/P[37].

Autophagy pathway

In addition to selecting pathways that have been reported to be significantly related to lip and palate development, we also selected pathways related to other diseases and that are involved in early embryonic development for in-depth research. As a conserved lysosomal degradation process in eukaryotes, autophagy protects cells from different kinds of stress, such as starvation, hypoxia or exposure to toxic molecules[38]. In the early development stage, autophagy has been shown to be essential in the transition of oocytes to embryos, postpartum survival, development, differentiation and ageing in mouse models[39]. Lou et al[40] conducted a two-stage case-control study with 2027 NSCL/P cases and 1843 controls to explore associations between genetic variants in the autophagy pathway and the risk of NSCL/P, and found that rs2301104 in the autophagy pathway gene HIF1A was associated with susceptibility to NSCL/P. Moreover, the authors explored the functional roles of the SNP and the gene through in vivo and in vitro experiments and found that the risk allele of rs2301104 reduced the enhancer activity and expression of HIF1A, and also that knockdown of HIF1A affected cell functions, which may increase susceptibility to NSCL/P[40].

Table 1 GWASs identified newly discovered SNPs associated with NSCL/P.

PMID	Newly discovered SNPs with $P < 5 \times 10^{-8}$				Population	Study
19270707	rs987525				European	Birnbaum et al[44]
19656524	rs17085106				European	Grant et al[45]
20023658	rs227731	rs7078160			European	Mangold et al[46]
20436469	rs10863790				European	Beaty et al[47]
21618603	rs2294426				European	Beaty et al[48]
22863734	rs560426	rs8001641	rs7632427	rs861020	European	Ludwig et al[49]
	rs13041247	rs742071	rs7590268	rs12543318		
25775280	rs2235371	rs8049367	rs4791774		Chinese	Sun et al[50]
28054174	rs9439714	rs72728734	rs12944377	rs1588366	Asian European Latino or African	Leslie et al[51]
	rs66515264	rs6540559	rs9911652	rs6029258		
	rs3789432	rs12070337	rs55658222	rs75477785		
	rs9439713	rs6072081	rs10886040	rs11841646		
	rs7566780	rs76479869	rs11072494	rs1109430		
	rs17242358	rs1234719				
28087736	rs6740960	rs4901118	rs3746101		European Asian	Ludwig et al[12]
28232668	rs7552	rs2064163	rs12229654	rs11066150	Chinese European Asian	Yu et al[52]
	rs481931	rs6585429	rs2304269	rs957448		
	rs10512248	rs2872615	rs287982	rs9381107		
	rs12681366	rs12229892	rs6495117	rs2283487		
	rs1907989	rs13317	rs908822	rs7871395		
	rs3741442	rs705704	rs9545308	rs7148069		
	rs1243572	rs2289187	rs1838105	rs6129653		
	rs2006771	rs78212183	rs10462065	rs7017252		
30067744	rs255877	rs2522825			European	Howe et al[53]
30277614	rs72804706				African Asian Latin American North American	Carlson et al[54]
30452639	rs80004662	rs113691307			African	Butali et al[55]
31609978	rs12405750	rs17820943	rs730570	rs765366	Chinese	Huang et al[56]
	rs4752028	rs57700751	rs625882	rs116910459		
	rs730643	rs698406	rs1009136	rs3468		
	rs4646211	rs8061677	rs78669990	rs72741048		
	rs72688980	rs6791526				
32373937	rs8071332	rs8076457	rs1215465	rs3138512	European	Dardani et al[57]

GWAS of NSCL/P

GWASs are dedicated to detecting the associations between SNPs and complex traits and diseases in samples among populations[41]. An increasing number of SNPs have been reported to participate in the development of traits and diseases since the first GWAS for age-related macular degeneration (AMD) was published in 2005[42].

To date, the National Human Genome Research Institute (NHGRI) Catalog[43] of published GWASs has identified 15 studies (Table 1)[12,44-57] including 101 newly discovered SNPs relevant to NSCL/P with $P < 5 \times 10^{-8}$. In 2009, Birnbaum et al[44] conducted the first NSCL/P GWAS on a cohort of the European population and provided evidence that 8q24.21 (rs987525), which lay in a gene desert, was a major susceptibility locus for NSCL/P. Several other GWAS around this time also identified important loci[45-49]. In 2015, our group conducted the first NSCL/P GWAS in a Chinese population, followed by two stages of replication. There were 2577 cases and 3193 controls in total. We identified 16p13.3 (rs8049367 between CREBBP and ADCY9) as a new susceptible locus for NSCL/P and confirmed that the reported loci at 1q32.2, 10q25.3, 17p13.1 and 20q12 were effectual[50]. Then, a 2017 GWAS and meta-analysis on the Chinese population linked both previously known and novel SNPs and genes with NSCL/P[52].

As the lip formation processes differ from those for the palate, as do their respective causes and risk factors, Huang et al[56] aimed to dissect the risk factors underlying the pathogenesis of cleft lip only (CLO) and cleft palate only (CPO) using 6986 cases and 10,165 controls. A total of 18 genes/loci were responsible for subtypes, including nine for CPO, seven for CLO and two for both conditions. Interestingly, an opposite effect of the genetic variants was observed in the IRF6 gene for CPO and CLO. The latest GWAS of NSCL/P not only performed a meta-analysis, but also sought to evaluate the causal effects of genetic liability to NSCL/P on educational attainment and intelligence[57].

GWAS offers great advantages in identifying novel variant–trait associations which lead to the discovery of novel biological mechanisms and provide insight into ethnic variation of complex traits[58]; however, GWAS cannot necessarily specify which variant at a locus is the 'causal variant' and identify all genetic determinants of complex traits[59]. Thus, post-GWAS strategies have been proposed to identify the causal variants and understand their biological consequences.

Hah et al[60] conducted a targeted sequencing study of 13 NSCL/P GWAS loci in 1409 trios from European and Asian ancestries and found that rs227727 near the NOG gene disrupted enhancer activity, a mutation in PAX7 disrupted the DNA binding of the encoded TF in vitro and another mutation disrupted the activity of a neural crest enhancer downstream of FGFR2 both in vitro and in vivo. In our study, rs2262251 (G>C) in lncRNA RP11-462G12.2 was in high linkage disequilibrium (LD) with rs8049367, which was identified in our previous GWAS on NSCL/P. Through a series of experiments, we found rs2262251 was involved in the RP11-462G12.2-miR-744-5p-IQSEC2 regulatory axis to affect NSCL/P development[61]. The functional consequences illustrated an SNP in lncRNA leading to NSCL/P and also proved that lncRNA, miRNA and genes constituted a complicated and coordinative regulatory network.

Conclusion and future perspectives

The past decades have seen a series of remarkable discoveries in human genetic variants related to NSCL/P through genes, pathways and GWAS strategies. The future of NSCL/P research is likely to be characterised by three aspects. The first challenge is to understand the functional consequences of these SNPs and to accurately elucidate the biological mechanism in the 'post-GWAS' era[62]. Second, next-generation sequencing (NGS) efforts are necessary to uncover rare variants that play an important role in NSCL/P[41]. Third, the combination of whole-genome surveys of genetic variation and multiomics data will show significant value for making new fundamental discoveries in human genetics[58].

Conflicts of interest

The authors declare no conflicts of interest related to this study.

Author contribution

Prof Yong Chu PAN and Dr Lan MA drafted the manuscript; Dr Shu LOU made the figure; Drs Gui Rong ZHU and Xin YU made the table. Profs Lin WANG and Yong Chu PAN designed the manuscript; Prof Lin WANG critically revised the manuscript. All authors read and approved the final manuscript.

(Received Feb 22, 2021; accepted Apr 26, 2021)

References

1. Carinci F, Scapoli L, Palmieri A, Zollino I, Pezzetti F. Human genetic factors in nonsyndromic cleft lip and palate: An update. Int J Pediatr Otorhinolaryngol 2007;71:1509–1519.
2. Mossey PA, Modell B. Epidemiology of oral clefts 2012: An international perspective. Front Oral Biol 2012;16:1–18.
3. Wang M, Yuan Y, Wang Z, et al. Prevalence of orofacial clefts among live births in China: A systematic review and meta-analysis. Birth Defects Res 2017;109:1011–1019.
4. DeRoo LA, Wilcox AJ, Lie RT, et al. Maternal alcohol binge-drinking in the first trimester and the risk of orofacial clefts in offspring: A large population-based pooling study. Eur J Epidemiol 2016;31:1021–1034.
5. Kummet CM, Moreno LM, Wilcox AJ, et al. Passive smoke exposure as a risk factor for oral clefts-A large international population-based study. Am J Epidemiol 2016;183:834–841.
6. Beaty TH, Marazita ML, Leslie EJ. Genetic factors influencing risk to orofacial clefts: Today's challenges and tomorrow's opportunities. F1000Res 2016;5:2800.
7. Beaty TH, Taub MA, Scott AF, et al. Confirming genes influencing risk to cleft lip with/without cleft palate in a case-parent trio study. Hum Genet 2013;132:771–781.
8. Syvänen AC. Accessing genetic variation: Genotyping single nucleotide polymorphisms. Nat Rev Genet 2001;2:930–942.
9. Zucchero TM, Cooper ME, Maher BS, et al. Interferon regulatory factor 6 (IRF6) gene variants and the risk of isolated cleft lip or palate. N Engl J Med 2004;351:769–780.
10. Reynolds K, Zhang S, Sun B, Garland MA, Ji Y, Zhou CJ. Genetics and signaling mechanisms of orofacial clefts. Birth Defects Res 2020;112:1588–1634.
11. Saleem K, Zaib T, Sun W, Fu S. Assessment of candidate genes and genetic heterogeneity in human non syndromic orofacial clefts specifically non syndromic cleft lip with or without palate. Heliyon 2019;5:e03019.

12. Ludwig KU, Böhmer AC, Bowes J, et al. Imputation of orofacial clefting data identifies novel risk loci and sheds light on the genetic background of cleft lip ± cleft palate and cleft palate only. Hum Mol Genet 2017;26:829–842.
13. Patnala R, Clements J, Batra J. Candidate gene association studies: A comprehensive guide to useful in silico tools. BMC Genet 2013;14:39.
14. Kwon JM, Goate AM. The candidate gene approach. Alcohol Res Health 2000;24:164–168.
15. Ferretti E, Li B, Zewdu R, et al. A conserved Pbx-Wnt-p63-Irf6 regulatory module controls face morphogenesis by promoting epithelial apoptosis. Dev Cell 2011;21:627–641.
16. Carré A, Hamza RT, Kariyawasam D, et al. A novel FOXE1 mutation (R73S) in Bamforth-Lazarus syndrome causing increased thyroidal gene expression. Thyroid 2014;24:649–654.
17. Wang S, He S, Yuan F, Zhu X. Tagging SNP-set selection with maximum information based on linkage disequilibrium structure in genome-wide association studies. Bioinformatics 2017;33: 2078–2081.
18. Lin JY, Chen YJ, Huang YL, et al. Association of bone morphogenetic protein 4 gene polymorphisms with nonsyndromic cleft lip with or without cleft palate in Chinese children. DNA Cell Biol 2008;27: 601–605.
19. Omoumi A, Wang Z, Yeow V, et al. Fetal polymorphisms at the ABCB1-transporter gene locus are associated with susceptibility to non-syndromic oral cleft malformations. Eur J Hum Genet 2013;21:1436–1441.
20. Letra A, Zhao M, Silva RM, Vieira AR, Hecht JT. Functional significance of MMP3 and TIMP2 polymorphisms in cleft lip/palate. J Dent Res 2014;93:651–656.
21. Letra A, Silva RA, Menezes R, et al. MMP gene polymorphisms as contributors for cleft lip/palate: Association with MMP3 but not MMP1. Arch Oral Biol 2007;52:954–960.
22. Kondo S, Schutte BC, Richardson RJ, et al. Mutations in IRF6 cause Van der Woude and popliteal pterygium syndromes. Nat Genet 2002;32:285–289.
23. Pan Y, Ma J, Zhang W, et al. IRF6 polymorphisms are associated with nonsyndromic orofacial clefts in a Chinese Han population. Am J Med Genet A 2010;152A:2505–2511.
24. Alappat S, Zhang ZY, Chen YP. Msx homeobox gene family and craniofacial development. Cell Res 2003;13:429–442.
25. van den Boogaard MJ, Dorland M, Beemer FA, van Amstel HK. MSX1 mutation is associated with orofacial clefting and tooth agenesis in humans. Nat Genet 2000;24:342–343.
26. Ma L, Xu M, Li D, et al. A miRNA-binding-site SNP of MSX1 is associated with NSOC susceptibility. J Dent Res 2014;93:559–564.
27. Marigo V, Nigro A, Pecci A, et al. Correlation between the clinical phenotype of MYH9-related disease and tissue distribution of class II nonmuscle myosin heavy chains. Genomics 2004;83:1125–1133.
28. Wang Y, Li D, Xu Y, et al. Functional effects of SNPs in MYH9 and risks of nonsyndromic orofacial clefts. J Dent Res 2018;97:388–394.
29. Li C, Lan Y, Jiang R. Molecular and cellular mechanisms of palate development. J Dent Res 2017;96:1184–1191.
30. Parada C, Chai Y. Roles of BMP signaling pathway in lip and palate development. Front Oral Biol 2012;16:60–70.
31. Komekado H, Yamamoto H, Chiba T, Kikuchi A. Glycosylation and palmitoylation of Wnt-3a are coupled to produce an active form of Wnt-3a. Genes Cells 2007;12:521–534.
32. Galli LM, Barnes TL, Secrest SS, Kadowaki T, Burrus LW. Porcupine-mediated lipid-modification regulates the activity and distribution of Wnt proteins in the chick neural tube. Development 2007;134:3339–3348.
33. Vijayan V, Ummer R, Weber R, Silva R, Letra A. Association of WNT pathway genes with nonsyndromic cleft lip with or without cleft palate. Cleft Palate Craniofac J 2018;55:335–341.
34. Ciccolini F, Mandl C, Hölzl-Wenig G, Kehlenbach A, Hellwig A. Prospective isolation of late development multipotent precursors whose migration is promoted by EGFR. Dev Biol 2005;284:112–125.
35. Mellott DO, Burke RD. Divergent roles for Eph and ephrin in avian cranial neural crest. BMC Dev Biol 2008;8:56.
36. Chai Y, Jiang X, Ito Y, et al. Fate of the mammalian cranial neural crest during tooth and mandibular morphogenesis. Development 2000;127:1671–1679.
37. Li B, Ma L, Zhang C, et al. Associations of genetic variants in endocytic trafficking of epidermal growth factor receptor super pathway with risk of nonsyndromic cleft lip with or without cleft palate. Mol Genet Genomic Med 2018;6:1157–1167.
38. Huang J, Klionsky DJ. Autophagy and human disease. Cell Cycle 2007;6:1837–1849.
39. Hale AN, Ledbetter DJ, Gawriluk TR, Rucker EB 3rd. Autophagy: Regulation and role in development. Autophagy 2013;9:951–972.
40. Lou S, Ma L, Kan S, et al. Association study of genetic variants in autophagy pathway and risk of non-syndromic cleft lip with or without cleft palate. Front Cell Dev Biol 2020;8:576.
41. Visscher PM, Wray NR, Zhang Q, et al. 10 Years of GWAS discovery: Biology, function, and translation. Am J Hum Genet 2017;101:5–22.
42. Klein RJ, Zeiss C, Chew EY, et al. Complement factor H polymorphism in age-related macular degeneration. Science 2005;308:385–389.
43. Welter D, MacArthur J, Morales J, et al. The NHGRI GWAS Catalog, a curated resource of SNP-trait associations. Nucleic Acids Res 2014;42(Database issue):D1001–D1006.
44. Birnbaum S, Ludwig KU, Reutter H, et al. Key susceptibility locus for nonsyndromic cleft lip with or without cleft palate on chromosome 8q24. Nat Genet 2009;41:473–477.
45. Grant SFA, Wang K, Zhang H, et al. A genome-wide association study identifies a locus for nonsyndromic cleft lip with or without cleft palate on 8q24. J Pediatr 2009;155:909–913.
46. Mangold E, Ludwig KU, Birnbaum S, et al. Genome-wide association study identifies two susceptibility loci for nonsyndromic cleft lip with or without cleft palate. Nat Genet 2010;42:24–26.
47. Beaty TH, Murray JC, Marazita ML, et al. A genome-wide association study of cleft lip with and without cleft palate identifies risk variants near MAFB and ABCA4. Nat Genet 2010;42:525–529.
48. Beaty TH, Ruczinski I, Murray JC, et al. Evidence for gene-environment interaction in a genome wide study of nonsyndromic cleft palate. Genet Epidemiol 2011;35:469–478.
49. Ludwig KU, Mangold E, Herms S, et al. Genome-wide meta-analyses of nonsyndromic cleft lip with or without cleft palate identify six new risk loci. Nat Genet 2012;44:968–971.
50. Sun Y, Huang Y, Yin A, et al. Genome-wide association study identifies a new susceptibility locus for cleft lip with or without a cleft palate. Nat Commun 2015;6:6414.
51. Leslie EJ, Carlson JC, Shaffer JR, et al. Genome-wide meta-analyses of nonsyndromic orofacial clefts identify novel associations between FOXE1 and all orofacial clefts, and TP63 and cleft lip with or without cleft palate. Hum Genet 2017;136:275–286.
52. Yu Y, Zuo X, He M, et al. Genome-wide analyses of non-syndromic cleft lip with palate identify 14 novel loci and genetic heterogeneity. Nat Commun 2017;8:14364.
53. Howe LJ, Lee MK, Sharp GC, et al. Investigating the shared genetics of non-syndromic cleft lip/palate and facial morphology. PLoS Genet 2018;14:e1007501.
54. Carlson JC, Nidey NL, Butali A, et al. Genome-wide interaction studies identify sex-specific risk alleles for nonsyndromic orofacial clefts. Genet Epidemiol 2018;42:664–672.
55. Butali A, Mossey PA, Adeyemo WL, et al. Genomic analyses in African populations identify novel risk loci for cleft palate. Hum Mol Genet 2019;28:1038–1051.
56. Huang L, Jia Z, Shi Y, et al. Genetic factors define CPO and CLO subtypes of nonsyndromicorofacial cleft. PLoS Genet 2019;15:e1008357.

57. Dardani C, Howe LJ, Mukhopadhyay N, et al. Cleft lip/palate and educational attainment: cause, consequence or correlation? A Mendelian randomization study. Int J Epidemiol 2020;49:1282–1293.
58. Tam V, Patel N, Turcotte M, Bossé Y, Paré G, Meyre D. Benefits and limitations of genome-wide association studies. Nat Rev Genet 2019;20:467–484.
59. Gallagher MD, Chen-Plotkin AS. The post-GWAS era: From association to function. Am J Hum Genet 2018;102:717–730.
60. Hah N, Murakami S, Nagari A, Danko CG, Kraus WL. Enhancer transcripts mark active estrogen receptor binding sites. Genome Res 2013;23:1210–1223.
61. Yun L, Ma L, Wang M, et al. Rs2262251 in lncRNA RP11-462G12.2 is associated with nonsyndromic cleft lip with/without cleft palate. Hum Mutat 2019;40:2057–2067.
62. Farashi S, Kryza T, Clements J, Batra J. Post-GWAS in prostate cancer: From genetic association to biological contribution. Nat Rev Cancer 2019;19:46–59.

用科技的光芒照耀每一个梦想

“科普中国”传播科学新知，弘扬科学精神。

中国科学技术协会
China Association for Science and Technology

致敬创新的登攀者
中国科学技术协会第十次全国代表大会

Microspheres and their Potential in Endodontic Regeneration Application

Ting YANG[1,2,3], Li XIE[1,2,3], Rui Tao ZHANG[1,2,3], Wei Dong TIAN[1,2,3]

Microspheres have been widely utilised as versatile carriers in biomedical applications. In recent years, as a new type of injectable scaffold, microspheres have attracted increasing attention in the field of regenerative medicine owing to their various advantages including their small size, large specific surface area and mimicry of the 3D native environment. These characteristics enable them to adopt the narrow and irregular anatomy of the tooth and become an ideal scaffold for endodontic regeneration. Microspheres play an important role in carrying biologics (cells, biomolecules and drugs), which effectively regulate the fate of stem cells and control the release of growth factors and drugs. Cell-laden microspheres, which can be divided into microcarriers and microcapsules, have great application prospects in dental pulp regeneration. This paper summarises the properties and characteristics of microsphere scaffolds used in tissue engineering, placing emphasis on their advantages and applications in endodontic regeneration.

Key words: *dental pulp, endodontic regeneration, microcapsules, microcarriers, microspheres*
Chin J Dent Res 2022;25(1):29–36; doi: 10.3290/j.cjdr.b2752709

Dental pulpitis and periapical periodontitis are common diseases in stomatology. The conventional treatment, root canal therapy, involves removing the infected dental pulp completely, cleaning the root canal and filling it with bioinert materials[1]; however, due to the loss of vitality, the repaired tooth is often prone to postoperative fracture and repeated infection[2]. Endodontic regeneration, based on modern tissue engineering, is expected to become an alternative strategy to restore the structure and function of dental pulp[1]. Among the three essential elements in tissue engineering, namely stem cells, scaffolds and growth factors, scaffolds serve as an artificial extracellular matrix (ECM), which is critical to support the proliferation and differentiation of stem cells[1]. A scaffold can also incorporate biomolecules or drugs and control the release profile, which can further regulate stem cells and their microenvironment.

In general, pulp regeneration scaffolds, like other scaffolds for tissue regeneration, should adhere to the following principles: good biocompatibility, biosafety, biodegradability, mechanical stability, favourable cell microenvironment and appropriate biochemical and biophysical clues. For endodontic regeneration, due to the unique dental anatomy, the selection and design of the scaffold must strive for pertinency and practicability to meet the specific requirements. Regarding the irregular and complex root canal system, the ideal scaffold

1 Engineering Research Centre of Oral Translational Medicine, Ministry of Education, State Key Laboratory of Oral Diseases, National Clinical Research Centre for Oral Diseases, West China Hospital of Stomatology, Sichuan University, Chengdu, Sichuan Province, P.R. China.
2 National Engineering Laboratory for Oral Regenerative Medicine, West China Hospital of Stomatology, Sichuan University, Chengdu, Sichuan Province, P.R. China.
3 Department of Oral and Maxillofacial Surgery, West China Hospital of Stomatology, Sichuan University, Chengdu, Sichuan Province, P.R. China.

Corresponding authors: Dr Li XIE and Dr Wei Dong TIAN, West China Hospital of Stomatology, Sichuan University, #14, 3rd Section, Renmin South Road, Chengdu 610041, P.R. China. Tel/Fax: 86-28-85503499. Email: samuel0121@163.com; drtwd@sina.com

This study was supported by the National Key R&D Programme of China (grant number 2017YFA0104800) and the National Natural Science Foundation of China (grant number 81970968,81600895).

needs to fill the irregular pulp cavity and support cells in differentiating within, whereas the pulp cavity only communicates with the periapical tissue through the apical aperture (~ 1 mm). Thus, the injectable scaffold is considered more appealing for endodontic regeneration and further clinical transformation[3]. At present, the commonly used injectable scaffolds for endodontic engineering are mainly divided into two categories: hydrogel and microspheres[3]. Hydrogel scaffolds for endodontic regeneration have been examined in many published reviews[4,5]. Polymer microspheres, however, are a new type of injectable scaffold and have shown great application prospects after being introduced in the field of pulp regeneration, which has not yet been reviewed. This review therefore aims to summarise the current advances in microsphere scaffolds in research into endodontic regeneration.

Overview of microspheres for tissue engineering

Microsphere technology for animal cell culture was first used in 1967 and has gradually matured and been used widely in many biomedical fields such as cell transplantation, drug delivery and biomolecule production[6]. The present review focuses mainly on cell-based microspheres for endodontic regeneration. Microspheres are generally spherical polymerised networks prepared from biomaterials using physical or chemical methods, with a diameter ranging from 1 to 1000 μm[7] and especially within 500 μm[8]. They include microcarriers, in which cells are directly integrated with microspheres, and microcapsules, in which cells are encapsulated within microspheres[9]. As a microcarrier used for cell culture, a larger specific area can provide more support for cells, which is conducive to adhesion and proliferation; however, due to the limitation of oxygen diffusion, microcapsules used for cell delivery are usually 100~400 μm in diameter. Large microspheres lead to internal cell apoptosis whereas small ones carry fewer cells and are even internalised by cells[10]. Recently, a variety of biomaterials has been developed to fabricate microspheres. The selected materials and their degradation products must be non-toxic and induce limited inflammatory or immune responses after transplantation in vivo. More importantly, the materials must be able to form microspheres quickly and easily, so only polymers with crosslinkable functional groups or partially modified by crosslinkable moieties are suitable choices. The selected materials should be made into microspheres from the precursor solution using the appropriate techniques. Generally, microcarriers are preformed, thus reducing any direct adverse effects on cells during preparation. Common preparation techniques include solvent evaporation (single or double emulsion), emulsion polymerisation, spray drying and phase inversion microencapsulation[11-14]; however, microcapsules are prepared directly from a suspension formed by mixing cross-linkable polymer and cells to microspheres, with cells encapsulated inside the microspheres. Usually, the preparation method needs to be mild, such as electrostatic droplets, microfluidic technique and 3D printing[15-17], to reduce damage to the cells during the preparation process.

Microspheres offer several advantages for stem cells in tissue regeneration: their spherical structure provides cells with a 3D microenvironment simulating natural extracellular matrix, which is more conducive to maintaining their function and phenotype than two-dimensional monolayer culture[18]; their small size and large specific surface area allow rapid diffusion of oxygen, nutrients and metabolites[7,9]; they support cell attachment, proliferation and differentiation in vitro, which further enhance cell viability and tissue regeneration after cell transplantation to the target defect site[3,11]; and microsphere scaffolds could protect the delivered stem cells, reduce shear stress injury during injection and prevent the immune system from being attacked[19]. They have performed excellently in a wide range of tissue engineering and regeneration medicine applications, such as bone and cartilage, vascular and cardiac[9,20]. It is imperative to comprehensively consider the characteristics of the repaired tissue, the inherent bioactivity of the material, the appropriateness of the fabrication technique and the types of delivery cells to overcome the difficulties of regenerating specific tissue[21].

Application of microspheres in endodontic regeneration

Dental pulp is a kind of connective tissue that is rich in blood vessels and nerves, surrounded by hard dentine and connected with periapical tissue through a narrow apical foramen[22]. The lack of effective collateral circulation means that once the dental pulp becomes infected, the necrotic pulp cannot be reversed and must be removed completely. Recently, strategies for pulp regeneration have focused mainly on cell sheets and cell-laden hydrogels, whereas microsphere scaffolds are relatively few. Cell sheets can form an abundant extracellular matrix without the support of scaffolds but are difficult to transport into the narrow root canal system directly[23,24]. Hydrogel is also widely used as a scaffold for endodontic regeneration owing to its injectability and simulation of the extracellular matrix; however,

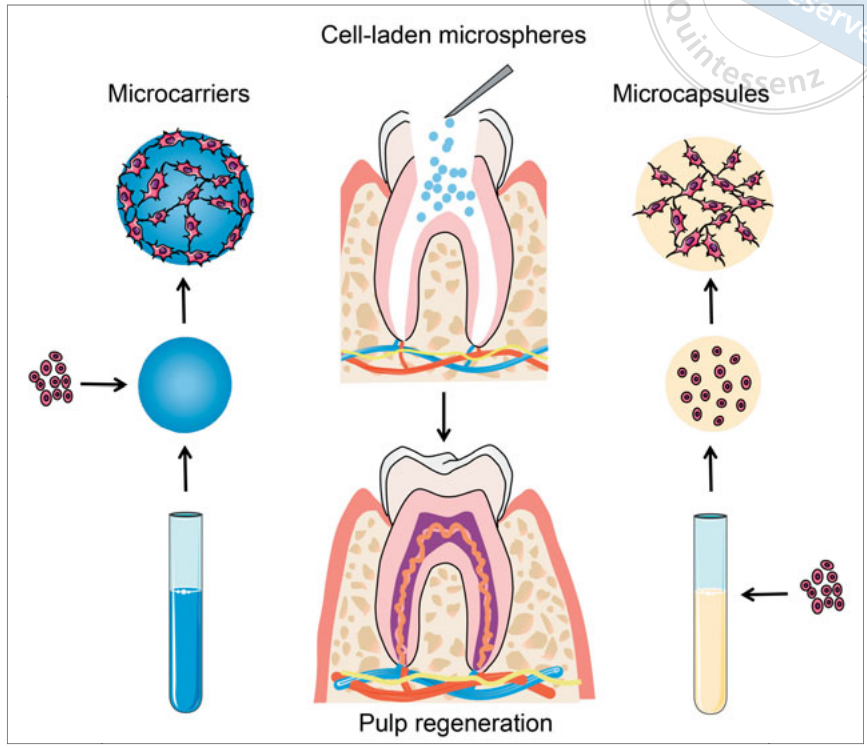

Fig 1 Schematic illustration of microspheres used for pulp regeneration. Microspheres can be classified as microcarriers or microcapsules according to their different cell-laden delivery applications. Microcarriers are usually preformed into large amounts of tiny particles, and then cells are loaded on their surfaces. In contrast, microcapsules are prepared by mixing crosslinkable polymers with cells to encapsulate cells within them.

crosslinked hydrogel bulk restricts the rapid diffusion of oxygen and nutrients. Microsphere scaffolds therefore offer unique advantages in application for endodontic regeneration[25,26]. First, their small size allows them to be injected into narrow and irregular root canals[9]; second, their small volume supports the rapid diffusion of oxygen and nutrients, which is conducive to the survival of transplanted stem cells in the early ischemic environment of the root canal system[7,9]; and third, they allow cells to adhere and proliferate in vitro for a period of time to form microtissues, which can enhance their vitality and function in this bionic 3D microenvironment[3,19,27]. A schematic illustration of cell-laden microspheres applied in endodontic regeneration is presented in Fig 1.

Most microspheres used in endodontic regeneration are loaded with cells for in vitro cell culture and in vivo cell delivery[9], and others have been encapsulated with various effective components for related research application, such as pulp capping, apexification and root canal disinfection.

Application for dentine and pulp tissue engineering

Microspheres can be classified as microcarriers and microcapsules according to their different cell-laden delivery applications[9]. Microcarriers are usually preformed into large amounts of tiny particles, then cells are loaded on their surfaces, whereas microcapsules are prepared by mixing crosslinkable polymers with cells to encapsulate cells within them.

Microcarriers

Conventional polymer microcarriers are solid spheres with a smooth surface where cells can attach and grow. Microcarriers offer cells a microsized 3D platform that is conducive to cell connection and substance exchange compared with the conventional two-dimensional culture. Combined with a bioreactor mimicking biological environments in vitro, microcarriers can accelerate cell proliferation and differentiation[28]. Bhuptani and Patravale[28] used a double emulsion solvent extraction technique to prepare interconnected porous poly(lactic-co-glycolic acid) (PLGA) microspheres with a particle size of 100 to 200 μm and a pore diameter of 10 to 30 μm. They found that porous microspheres provided a favourable microenvironment for human dental pulp stem cells (hDPSCs) to support cell adhesion, proliferation and survival[28]. Zou et al[29] also applied a double emulsion solvent extraction technique to fabricate PLGA microspheres with diameters of around 150 to 400 μm, which supported hDPSCs proliferation and odontogenic differentiation. Due to their hydrophobicity and the lack of cell adhesion moieties of synthetic material, PLGA microspheres were coated with type I collagen to improve their surface bioactivity; this sur-

face modification enhanced cell adhesion, proliferation and odontogenic differentiation[29]. Garzón et al[30] utilised self-assembled technology and the solvent evaporation technique to prepare poly(L-lactic acid)-block-poly(L-lysine) (PLLA) into two kinds of microspheres with different surfaces, fibrous and smooth. Both offered good biocompatibility, biosafety and odontogenic potential and could form bioactive injectable aggregates that promoted dentine regeneration in both in vitro and in vivo models; however, fibrous microspheres presented advantages in supporting cell adhesion and spreading, expressing collagen type I and promoting microsphere degradation, which may be related to the biomimetic structure of collagen fibres[30]. Kuang et al[12] used self-assembly and thermally induced phase separation techniques to prepare PLLA nanofibrous spongy microspheres with a diameter of approximately 30 to 60 μm, biomimetic nanofibrous architecture (160 nm) and an interconnected porous structure (10 to 20 μm) where hDPSCs could adhere to the outer surface and inner pores. In comparison to nanofibrous microspheres and smooth microspheres, nanofibrous spongy microspheres further promoted cell adhesion, proliferation and differentiation, and their degradation was also faster, showing great potential for dentine–pulp complex regeneration[12]. Then, they further induced cell differentiation into blood vessels by 3D hypoxic-primed culture of the cell-laden microspheres and found that expression of vascular endothelial growth factor (VEGF) of hDPSCs could be promoted and pulp-like tissue with rich vasculature could be regenerated in situ after injection into the pulp cavity of rat teeth[12]. Wang et al[31] used thermally-induced phase separation and emulsification methods to fabricate PLLA nanofibrous microspheres carrying human stem cells from the apical papilla (SCAP), and PLGA microspheres with controlled release of bone morphogenetic protein-2 (BMP-2). The addition of BMP-2 enhanced the odontoblast differentiation of human SCAP whether it was cultured in a monolayer or seeded on nanofibrous microspheres in a spinner flask[31]. This demonstrated that sustained release of BMP-2 from PLGA microspheres enhanced the odontogenic differentiation of SCAP to regenerate dental tissue[31]. Li et al[27] designed a hierarchical nanofibrous microsphere in which heparin, binding with vascular endothelial growth factor (VEGF), was conjugated onto a gelatine nanosphere, then fixed in injectable PLLA nanofibrous microspheres. The microspheres controlled the release of growth factors for over 4 weeks to promote the migration of human umbilical vein endothelial cells and simulate the structure of the extracellular matrix to support the proliferation of DPSCs[27]. The potential of these microspheres in dental pulp regeneration has been verified after being applied to full-length root canals with one end sealed in vivo[27]. Manaspon et al[14] used a combination of the water-in-oil emulsion technique and EDC/NHS crosslinking to fabricate fibrinogen and thrombin-crosslinked fibrinogen microspheres, with a mean diameter of 213.9 ± 35.9 μm and 199.9 ± 41.9 μm, respectively. These microspheres did not alter the cell viability of the hDPSCs, but thrombin-crosslinked fibrinogen microspheres had an advantage over the fibrinogen microspheres in promoting cell attachment and spreading[14]; however, their biological effects in promoting odontoblastic/osteogenic differentiation and their potential for pulp regeneration in vivo need to be investigated further.

Most of the abovementioned microcarriers are made from synthetic materials, except fibrinogen microspheres that are natural materials. Natural materials offer good biocompatibility and degradability[4], but their applications are restricted by limited sources, batch variability and potential pathogen transmission[32]. In contrast, synthetic materials possess good plasticity and reduce the risk of carrying pathogens with natural materials. However, most synthetic materials are restricted by limited biological cues and difficulty of degradation, and PLLA and PLGA are no exception. Although they offer good biocompatibility and biodegradability, they still need to improve cell adhesion with surface modification due to the lack of biological cues. In addition, their degradation problem is more obvious due to the closed root canal and insufficient blood supply[30]. It is therefore necessary to adjust the degradation through appropriate material composition and structure design. For example, nanofibrous spongy microspheres degrade faster than nanofibrous microspheres despite having been prepared from PLLA. Synthetic materials often have adjustable physical and chemical properties, but their degradation products need to be evaluated for cytotoxicity.

Microcapsules

In contrast with prefabricated microcarriers where cells are seeded after preparation, microcapsules can wrap cells together during preparation, providing the latter with a 3D environment that resembles natural tissues[20]. Hydrogel is a kind of crosslinked hydrophilic polymer network that has mechanical properties similar to many soft tissues. Due to its rheological property, degradability and simulation of the natural extracellular matrix, it is widely used as a substrate for cell culture, a scaffold for tissue engineering and a carrier for the delivery of biologics[25]. Although injectable hydrogel can be injected

into the defect location in a minimally invasive manner, cell interactions are limited in the process of hydrogel formation. Moreover, microspheres with larger specific surface areas provide more cell anchoring sites than bulk hydrogels. Thus, instead of the conventional form of hydrogel crosslinking into clusters, hydrogel microspheres combine the advantages of hydrogel matrix and microspheres[7] and are easy to transport to small-sized defect locations.

Our team took the lead in introducing hydrogel microspheres into endodontic regeneration. We prepared arginine-glycine-aspartic acid (RGD)-alginate-based hydrogel microcapsules using the electrostatic microdroplet method. These microspheres encapsulate and deliver hDPSCs, load and slowly release VEGF and form more blood vessels and new tissues in in vivo experiments[26]. This multifunctional hydrogel microsphere loaded with cells and biomolecules is an instructive scaffold strategy in vascularised endodontic regeneration. Unfortunately, the alginate material did not support cell spreading even after RGD modification, and some of the material remained undegraded after transplantation in vivo for 1 month. We therefore prepared hydrogel microspheres using photocrosslinked gelatine methacryloyl (GelMA), which offers excellent bioactivity and biodegradability, instead of alginate to improve its performance in cell adhesion and degradation. GelMA microspheres support hDPSC spreading, proliferation and ECM protein secretion and finally form a microtissue. In addition, hDPSC-laden GelMA microspheres can withstand cryopreservation, which supports their future clinical transformation. hDPSC-laden GelMA microspheres showed better degradability and new pulp–dental tissue generation than GelMA hydrogel bulk in vivo, possessing great potential for endodontic regeneration and transformation applications[33].

Hydrogel microcapsules prepared using the electrostatic microdroplet method have normal particle size distribution; other fabrication methods, such as microfluidic and 3D bioprinting technology, could control the particle size more accurately and form monodispersed phase microspheres. Taking the complex structure and function of dental pulp into account, cell-laden microcapsules need to be improved further to achieve functional pulp tissue regeneration. For instance, microspheres carrying oxygen-releasing components could improve the oxygen supply to maintain the survival of cells in the early ischemic environment[34], and the delivery of bioactive factors could endow microspheres with the function of angiogenesis and nerve promotion[26,27]. A summary of microspheres applied in endodontic regeneration can be found in Supplemental Table 1 (provided on request).

Other related applications for endodontic regeneration

Microspheres laden with protein, inorganics and antibiotics are effective methods to deliver these biomolecules to the target location. They can not only prevent the biomolecules from being eliminated directly by the immune response, but also prolong the retention of biomolecules and avoid the toxic impacts and side effects of burst release on the surrounding cells.

Incorporate biomolecules in pulp capping

A variety of microspheres loaded with biomolecules have been used for pulp capping, including natural materials such as fibrinogen and hydroxyapatite, and synthetic materials such as poly(ethylene)glycol and PLGA. These microcarriers are used to bind biomolecules that facilitate odontoblastic/osteogenic differentiation, such as calcium hydroxide (CH), dexamethasone, prostaglandin E and immobilised Jagged1. Due to their small size and sustained release of biomolecules, these microspheres promote odontoblastic/osteogenic differentiation of hDPSCs[14,35-37]. In addition to promoting dentine bridge formation, microspheres for pulp capping can also carry other effective bioactive factors that promote blood vessel formation, control inflammation and perform other functions[38-41].

Release biomolecules for apexification

Sustained release of biomolecules could be achieved through electrostatic adsorption, physical restriction, material degradation and other methods to better promote tissue regeneration. CH is also widely used as an intracanal medicament for apexification. Cerda-Cristerna et al[42] prepared CH-PLGA microspheres using oil-in-water and oil-in-oil/oil-in-water emulsion solvent evaporation techniques with a diameter of approximately 18.63 ± 7.23 μm and 15.25 ± 7.37 μm. Both can release Ca^{2+} in a sustained manner for up to 30 days; this is better than CH paste which releases it completely in 6 days, thus continuously inducing mineral tissue formation and apical closure[42]. Strom et al[43] prepared CH microspheres surrounded with an alginate shell using an emulsion method. These core–shell structure microspheres, ranging from 75 to 150 μm, can release Ca^{2+} and OH^- in a sustained manner in the root canal for up to 6 months, which should reduce the number of visits required for apexification[43].

Deliver drugs for sterilisation

Using microspheres to carry antibiotics or anti-inflammatory drugs can support the sustained release of drugs in root canals, which is conducive to creating a microenvironment required for pulp regeneration in the infected root canals. Dornelles et al[44] and Cuppini et al[45] introduced amoxicillin-loaded microspheres into endodontic sealer, which did not affect the physicochemical properties and biocompatibility and possessed antibacterial activity against endodontic bacteria. Appropriate use of antibiotics in endodontic regeneration requires not only disinfection of root canals, but also reduction of adverse effects on stem cells[2]. Parhizkar et al[46] developed PLGA-coated ceramic microparticles as a drug delivery system for endodontic application in which new triple antibiotics were loaded in the PLGA coating. These drug-loaded microspheres demonstrate bioactivity and biocompatibility and release antibiotics for up to 3 weeks against root canal microorganisms[46].

Summary and prospects

Endodontic regeneration involves not only regeneration of structure, but also restoration of function. Dental pulp is a kind of special connective tissue composed of various cells with special functions such as dentinogenesis, nutrition supply and sensory function. The cell-laden microspheres used in pulp tissue engineering can form pulp-like tissue to a certain extent, with blood vessels and dentine formation, and even achieve full-length regeneration in the root canal; however, their functional restoration remains to be verified further. On the one hand, the new tissue needs to integrate with the host tissue, particularly the early reconstruction of the vascular network to maintain sufficient oxygen and nutrition. This is key to maintaining the long-term survival of stem cells after transplantation, especially in the ischemic microenvironment of the root canal. On the other hand, the sensory function of the new tissue can be restored and the vital pulp can play a defensive and protective role; this needs to be verified through preclinical animal experiments and clinical trials. The microspheres are endowed with the microenvironment induced by angiogenesis and neurogenesis, which is conducive to the realisation of multifunctional microspheres to restore the complex tissue structure and function of dental pulp.

Although the application of microspheres for endodontic regeneration has achieved preliminary results, there are still some limitations based on current research. For example, the degradation of the material should match the rate of tissue regeneration; otherwise, the material residues will occupy part of the space and impede complete regeneration of the pulp. This problem can be avoided by choosing materials with better biodegradability or by changing the concentration, composition and structure of microspheres. In addition, due to the limited volume of the root canal system, the cell density within the microsphere must be considered to provide sufficient stem cells for endodontic regeneration. Microspheres can be cultured in vitro for a period of time before implantation to achieve cell proliferation, and they are not only for cell delivery, but also serve as bioinduced scaffolds for microtissue formation; however, the relationship between culture time and microtissue formation remains to be explored further. Moreover, in the process of promoting clinical transformation, large-scale, repeatable, low-cost and efficient manufacturing technology and safe and effective storage technology still need to be explored.

For endodontic regeneration, the microsphere scaffold should support cell adhesion and proliferation in vitro, protect cells from stress during injection and provide a good microenvironment for cell differentiation in vivo[47]. Through the design of the microsphere scaffold, the biocompatibility and material degradation rate can be adjusted to maximise the function of stem cells and achieve endodontic regeneration. In addition to carrying cells, microspheres could encapsulate other biomolecules such as growth factors and drugs to further extend the functions of microspheres, introducing selective cues that support the desired cellular responses and improving the local microenvironment. In conclusion, microspheres are versatile and practical carriers that display great potential in endodontic regeneration for clinical applications.

Conflicts of interest

The authors declare no conflicts of interest related to this study.

Author contribution

Drs Ting YANG and Li XIE discussed and determined the content and structure of the manuscript; Dr Ting YANG drafted the manuscript; Drs Ting YANG and Rui Tao ZHANG were in charge of the figure, Drs Li XIE and Rui Tao ZHANG revised the manuscript; Dr Wei Dong TIAN was responsible for approval before submitting this article.

(Received Feb 19, 2021; accepted May 24, 2021)

References

1. Gong T, Heng BC, Lo EC, Zhang C. Current advance and future prospects of tissue engineering approach to dentin/pulp regenerative therapy. Stem Cells Int 2016;2016:1–13.
2. Yang J, Yuan G, Chen Z. Pulp regeneration: Current approaches and future challenges. Front Physiol 2016;7:58.
3. Chang B, Ahuja N, Ma C, Liu X. Injectable scaffolds: Preparation and application in dental and craniofacial regeneration. Mater Sci Eng R Rep 2017;111:1–26.
4. Galler KM, D'Souza RN, Hartgerink JD, Schmalz G. Scaffolds for dental pulp tissue engineering. Adv Dent Res 2011;23:333–339.
5. Fukushima KA, Marques MM, Tedesco TK, et al. Screening of hydrogel-based scaffolds for dental pulp regeneration-A systematic review. Arch Oral Biol 2019;98:182–194.
6. van Wezel AL. Growth of cell-strains and primary cells on microcarriers in homogeneous culture. Nature 1967;216:64–65.
7. Brun-Graeppi AK, Richard C, Bessodes M, Scherman D, Merten OW. Cell microcarriers and microcapsules of stimuli-responsive polymers. J Control Release 2011;149:209–224.
8. Zein N, Harmouch E, Lutz JC, et al. Polymer-based instructive scaffolds for endodontic regeneration. Materials (Basel) 2019;12:2347.
9. Leong W, Wang DA. Cell-laden polymeric microspheres for biomedical applications. Trends Biotechnol 2015;33:653–666.
10. Ferreira L, Squier T, Park H, Choe H, Kohane DS, Langer R. Human embryoid bodies containing nano- and microparticulate delivery vehicles. Adv Mater 2008;20:2285–2291.
11. Li B, Wang X, Wang Y, et al. Past, present, and future of microcarrier-based tissue engineering. J Orthop Translat 2015;3:51–57.
12. Kuang R, Zhang Z, Jin X, et al. Nanofibrous spongy microspheres for the delivery of hypoxia-primed human dental pulp stem cells to regenerate vascularized dental pulp. Acta Biomater 2016;33: 225–234.
13. Kuang R, Zhang Z, Jin X, et al. Nanofibrous spongy microspheres enhance odontogenic differentiation of human dental pulp stem cells. Adv Healthc Mater 2015;4:1993–2000.
14. Manaspon C, Boonprakong L, Porntaveetus T, Osathanon T. Preparation and characterization of Jagged1-bound fibrinogen-based microspheres and their cytotoxicity against human dental pulp cells. J Biomater Appl 2020;34:1105–1113.
15. Xie M, Gao Q, Zhao H, et al. Electro-assisted bioprinting of low-concentration GelMA microdroplets. Small 2019;15:e1804216.
16. Zhao X, Liu S, Yildirimer L, et al. Injectable stem cell-laden photocrosslinkable microspheres fabricated using microfluidics for rapid generation of osteogenic tissue constructs. Adv Funct Mater 2016;26:2809–2819.
17. He Q, Liao Y, Zhang J, et al. "All-in-one" gel system for whole procedure of stem-cell amplification and tissue engineering. Small 2020;16:e1906539.
18. Caron MMJ, Emans PJ, Coolsen MME, et al. Redifferentiation of dedifferentiated human articular chondrocytes: Comparison of 2D and 3D cultures. Osteoarthritis Cartilage 2012;20:1170–1178.
19. Wei DX, Dao JW, Chen GQ. A micro-ark for cells: Highly open porous polyhydroxyalkanoate microspheres as injectable scaffolds for tissue regeneration. Adv Mater 2018;30:e1802273.
20. Newsom JP, Payne KA, Krebs MD. Microgels: Modular, tunable constructs for tissue regeneration. Acta Biomater 2019;88:32–41.
21. Ahrens CC, Dong Z, Li W. Engineering cell aggregates through incorporated polymeric microparticles. Acta Biomater 2017;62:64–81.
22. Kaushik SN, Kim B, Walma AM, et al. Biomimetic microenvironments for regenerative endodontics. Biomater Res 2016;20:14.
23. Syed-Picard FN, Ray HL Jr, Kumta PN, Sfeir C. Scaffoldless tissue-engineered dental pulp cell constructs for endodontic therapy. J Dent Res 2014;93:250–255.
24. Itoh Y, Sasaki JI, Hashimoto M, Katata C, Hayashi M, Imazato S. Pulp regeneration by 3-dimensional dental pulp stem cell constructs. J Dent Res 2018;97:1137–1143.
25. Daly AC, Riley L, Segura T, Burdick JA. Hydrogel microparticles for biomedical applications. Nat Rev Mater 2020;5:20–43.
26. Zhang R, Xie L, Wu H, et al. Alginate/laponite hydrogel microspheres co-encapsulating dental pulp stem cells and VEGF for endodontic regeneration. Acta Biomater 2020;113:305–316.
27. Li X, Ma C, Xie X, Sun H, Liu X. Pulp regeneration in a full-length human tooth root using a hierarchical nanofibrous microsphere system. Acta Biomater 2016;35:57–67.
28. Bhuptani RS, Patravale VB. Porous microscaffolds for 3D culture of dental pulp mesenchymal stem cells. Int J Pharm 2016;515:555–564.
29. Zou H, Wang G, Song F, Shi X. Investigation of human dental pulp cells on a potential injectable poly(lactic-co-glycolic acid) microsphere scaffold. J Endod 2017;43:745–750.
30. Garzón I, Martin-Piedra MA, Carriel V, Alaminos M, Liu X, D'Souza RN. Bioactive injectable aggregates with nanofibrous microspheres and human dental pulp stem cells: A translational strategy in dental endodontics. J Tissue Eng Regen Med 2018;12:204–216.
31. Wang W, Dang M, Zhang Z, et al. Dentin regeneration by stem cells of apical papilla on injectable nanofibrous microspheres and stimulated by controlled BMP-2 release. Acta Biomater 2016;36:63–72.
32. Ajay Sharma L, Sharma A, Dias GJ. Advances in regeneration of dental pulp--A literature review. J Investig Clin Dent 2015;6:85–98.
33. Yang T, Zhang Q, Xie L, et al. hDPSC-laden GelMA microspheres fabricated using electrostatic microdroplet method for endodontic regeneration. Mater Sci Eng C Mater Biol Appl 2021;121:111850.
34. Agata H, Kagami H, Watanabe N, Ueda M. Effect of ischemic culture conditions on the survival and differentiation of porcine dental pulp-derived cells. Differentiation 2008;76:981–993.
35. Hunter AR, Kirk EE, Robinson DH, Kardos TB. A slow release calcium delivery system for the study of reparative dentine formation. Endod Dent Traumatol 1998;14:112–118.
36. Zhang M, Ni S, Zhang X, et al. Dexamethasone-loaded hollow hydroxyapatite microsphere promotes odontogenic differentiation of human dental pulp cells in vitro. Odontology 2020;108:222–230.
37. Lorencetti-Silva F, Pereira PAT, Meirelles AFG, Faccioli LH, Paula-Silva FWG. Prostaglandin E2 induces expression of mineralization genes by undifferentiated dental pulp cells. Braz Dent J 2019;30: 201–207.
38. Limjeerajarus CN, Sonntana S, Pajaree L, et al. Prolonged release of iloprost enhances pulpal blood flow and dentin bridge formation in a rat model of mechanical tooth pulp exposure. J Oral Sci 2019;61: 73–81.
39. Li F, Liu X, Zhao S, Wu H, Xu HH. Porous chitosan bilayer membrane containing TGF-β1 loaded microspheres for pulp capping and reparative dentin formation in a dog model. Dent Mater 2014;30: 172–181.
40. Niu X, Liu Z, Hu J, Rambhia KJ, Fan Y, Ma PX. Microspheres assembled from chitosan-graft-poly(lactic acid) micelle-like core-shell nanospheres for distinctly controlled release of hydrophobic and hydrophilic biomolecules. Macromol Biosci 2016;16:1039–1047.
41. Mathieu S, Jeanneau C, Sheibat-Othman N, Kalaji N, Fessi H, About I. Usefulness of controlled release of growth factors in investigating the early events of dentin-pulp regeneration. J Endod 2013;39: 228–235.
42. Cerda-Cristerna BI, Breceda-Leija A, Méndez-González V, et al. Sustained release of calcium hydroxide from poly(DL-lactide-co-glycolide) acid microspheres for apexification. Odontology 2016;104:318–323.
43. Strom TA, Arora A, Osborn B, Karim N, Komabayashi T, Liu X. Endodontic release system for apexification with calcium hydroxide microspheres. J Dent Res 2012;91:1055–1059.

44. Dornelles NB Jr, Collares FM, Genari B, et al. Influence of the addition of microsphere load amoxicillin in the physical, chemical and biological properties of an experimental endodontic sealer. J Dent 2018;68:28–33.
45. Cuppini M, Zatta KC, Mestieri LB, et al. Antimicrobial and anti-inflammatory drug-delivery systems at endodontic reparative material: Synthesis and characterization. Dent Mater 2019;35:457–467.
46. Parhizkar A, Nojehdehian H, Tabatabaei F, Asgary S. An innovative drug delivery system loaded with a modified combination of triple antibiotics for use in endodontic applications. Int J Dent 2020 25;2020:8859566.
47. Caldwell AS, Aguado BA, Anseth KS. Designing microgels for cell culture and controlled assembly of tissue microenvironments. Adv Funct Mater 2020;30:1907670.

Accuracy of Mandibular Reconstruction with a Vascularised Iliac Flap Using 3D Templates: a Systematic Review

Ting Wei LU[1], Wan Tao CHEN[1], Tong JI[1]

Objective: *To conduct a systemic review for guidance regarding the application of templates in mandibular reconstruction with vascularised iliac flaps.*
Methods: *By searching PubMed, EMBASE and the Cochrane Library and collecting relevant literature, information about the types and accuracy of templates was extracted. Data relating to surgical time were also included for further analysis.*
Results: *Eight studies were included. The data analysis showed that the accuracy of operations with templates was higher than that of conventional surgery. The mean deviation was between 0.70 and 3.72 mm. The operational time was shortened to 314.4 minutes and the graft ischemic time was reduced to 15.6 to 26.8 minutes. Application of functional or specifically designed templates can improve the accuracy and shorten surgical time.*
Conclusion: *Templates can increase the accuracy and efficiency of mandibular reconstruction with vascularised iliac flaps, which will benefit patients' prognosis and subsequent functional restoration. Further studies should be conducted into application of templates to improve the accuracy of reconstructions.*

Key words: *mandible reconstruction, template, vascularised iliac flap, virtual surgery*
Chin J Dent Res 2022;25(1):37–43; doi: 10.3290/j.cjdr.b2752689

The mandible accounts for the lower third of the maxillofacial region and plays an important role in maintaining face shape and function. However, factors such as inflammation, trauma and tumours lead to mandibular defects, which not only affect chewing and speaking but also have negative impacts on social life and mental health due to changes in appearance. Mandibular reconstruction is therefore crucial to improving patients' quality of life[1].

Bell[2] stated that the ideal conditions for bone transplantation should include stimulation of bone regeneration and replacement of lost bone tissue with new bone; no antigenic effect; the ability to rapidly regenerate blood vessels and establish blood circulation with the surrounding tissues; and the ability for the grafts to combine with the surrounding mandibular blocks. Autogenous bone transplantation is a suitable choice. Since Taylor et al[3] began to carry out ilium transplantation with deep circumflex iliac vessels in 1979, the combination of a vascularised bone flap and titanium plates in rigid internal fixation has become the gold standard for mandibular reconstruction. Among the different kinds of grafts, the fibula and ilium are widely used in mandibular reconstruction[4]. In most cases, the

1 Department of Oral and Maxillofacial-Head & Neck Oncology, Shanghai Ninth People's Hospital, Shanghai Jiao Tong University School of Medicine; College of Stomatology, Shanghai Jiao Tong University; National Centre for Stomatology; National Clinical Research Centre for Oral Diseases; Shanghai Key Laboratory of Stomatology, Shanghai, P.R. China.

Corresponding author: Dr Tong JI, Department of Oral and Maxillofacial-Head & Neck Oncology, Shanghai Ninth People's Hospital, Shanghai Jiao Tong University School of Medicine, College of Stomatology, #639 Zhizaoju Road, Shanghai 200011, P.R. China. Tel: 86 21 23271699; Fax: 86 21 63135412. Email: jitong70@hotmail.com

This study was supported by the 'Star of Jiaotong University' Major Projects grant (no 20210103) to Wantao Chen and a grant from the Shanghai high level local university innovation team.

fibula is the first choice for repairing the mandible, and is superior to the ilium due to its long pedicle length and adequate skin paddle, which are characteristics that the ilium lacks. In some cases, however, especially for patients who do not need an extra long pedicle or who already have enough soft tissue, the ilium offers irreplaceable advantages. Compared with the fibula, the shape and contour of the iliac bone are more likely to match the curve of the mandible and it is rich in bone mass. It contains a generous cancellous and dense cortex of bone with an abundant blood supply, which is beneficial to dental repair after surgery[5]. Thus, under the premise of meeting the indications, considering the balance of function and aesthetics of the donor and recipient regions, a vascularised iliac flap is a good choice for reconstruction of mandibular defects[6].

From computer-aided navigation technology and surgical templates to recent virtual reality, augmented reality and mixed reality technology, an increasing number of high-tech techniques are being used in mandibular reconstruction[7]. In recent years, virtual surgery and 3D templates have been widely used in clinical practice. Surgeons use virtual surgery technology to design the operation plan and then apply it during surgery through the template. Many studies have reported that templates can improve the accuracy of mandibular reconstruction, but there is a lack of systematic clarification and analysis. As such, we systematically reviewed the research status and accuracy of templates in mandibular reconstruction with vascularised iliac flaps.

Operation process

The preoperative computed tomography (CT) scan of the maxillofacial and bilateral iliac regions is introduced into the 3D reconstruction software in DICOM format to form the 3D reconstruction model. The parts that do not relate to the surgery are removed and the lesion model is established. According to the region where the lesion is located, an osteotomy line is designed to simulate mandibular resection. For the fibula flap, a jig is made for guidance by taking a piece of bone that fits a straight line, which would put the plate in direct opposition to the bony surface. However, the iliac crest used for mandibular reconstruction has various curves in different patients, so it is difficult to use the aforementioned jig. Instead, we use the mirror function to duplicate the opposite mandible, fit the ilium to the defect and then adjust its position according to the occlusal relationship of the healthy side. Templates are designed based on the virtual surgery plan (VSP) and then printed into 3D models. Prior to the operation, the titanium plate is pre-bent according to the reconstruction model of the mandible to fit the morphology of the mandible on the reconstructed side. Thus, surgeons do not need to bend the titanium plate during surgery and only have to make small adjustments, which saves time.

After fully exposing the lesion area during surgery, the mandibular resection template is used to assist in the removal of part of the mandible. The reduction template can then help to restore the original position of the free mandibular blocks on both sides. The artery and vein are separated for vascular anastomosis. At the same time, according to the VSP, the vascular pedicle is separated, and the graft is cut with the help of transplant cutting templates. The size and shape of the graft are adjusted in advance according to the in-situ moulding templates. After the vascular pedicle is cut, it is anastomosed with the maxillofacial vessels. The bones from the donor and recipient areas will then be fixed with titanium plates and nails.

Materials and methods

To perform a systematic literature analysis, we referred to PubMed, EMBASE and the Cochrane Library and searched for keywords including computer-assisted, computerised, 3D, CAD, CAM, virtual, template, plate, guide, mandibular, mandible, ilium and iliac.

Studies were included if they met the following criteria:

- mandibular reconstruction;
- use of the vascularised iliac flap as a source of transplantation;
- use of templates in surgery;
- measurement data in the results.

The exclusion criteria included animal experiments, use of a fibula flap, inability to extract relevant data, and reviews, meetings, case reports, etc.

Results

The search strategy identified 354 articles in total, including 175 in PubMed, 13 in Cochrane Library and 166 in EMBASE. After removal of duplicate references, 248 articles remained. Based on the inclusion and exclusion criteria, a total of 17 articles met the requirements by referring to the title and abstract. After full-text reading, nine articles were excluded, three of which did not mention the measurement of accuracy, five did not use templates, and one used a fibula flap. Finally, eight studies and 149 cases were included for further analysis. The specific literature search process is shown in Fig 1.

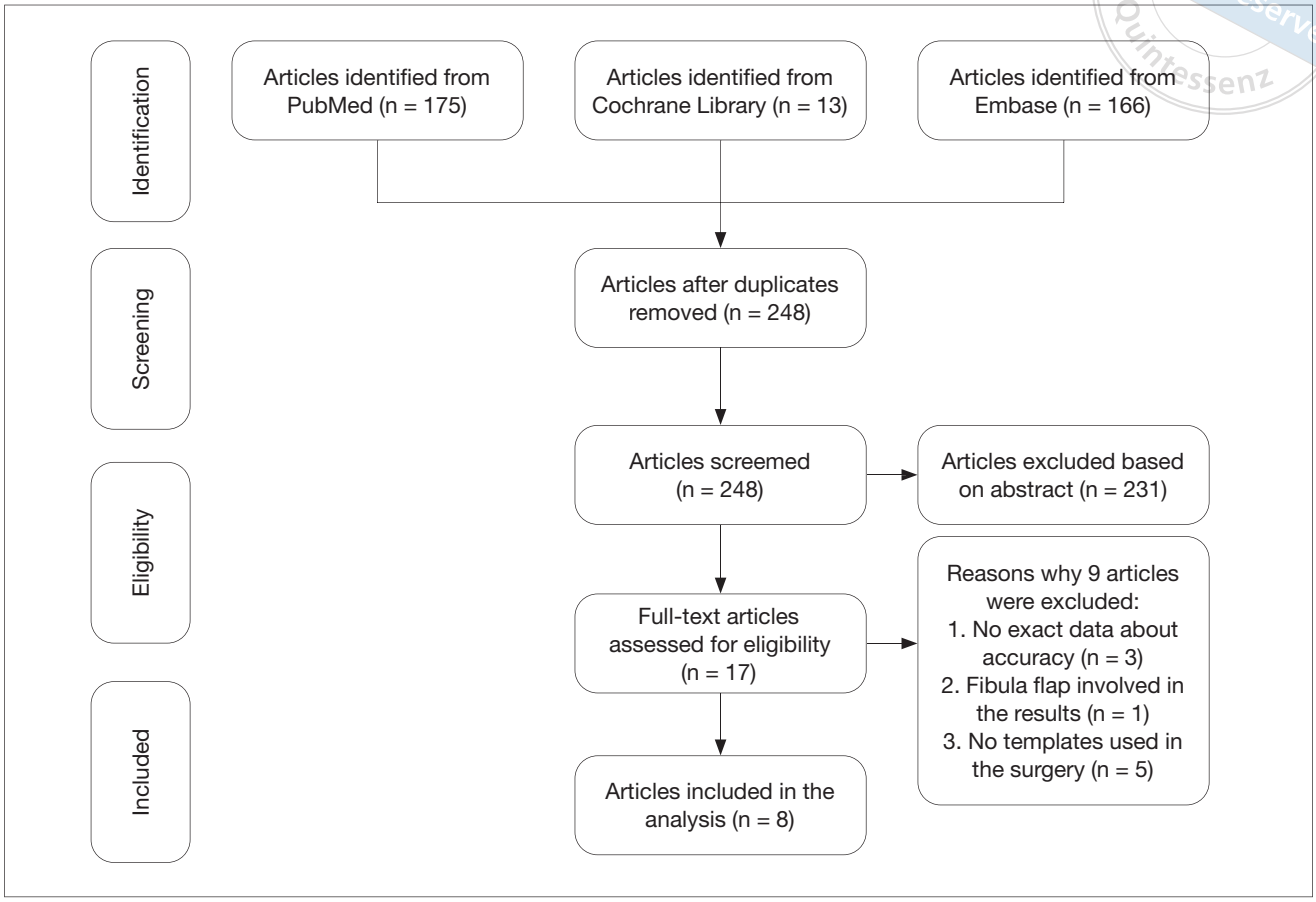

Fig 1 Flow chart for the article selection process.

Five articles designated control groups, and three of these (a randomised prospective clinical study[9] and two retrospective analyses[10,11]) compared the conventional surgical method with template-assisted operation. Three of the eight studies were retrospective analyses of mandibular reconstruction with templates, which were observational studies without a control group[12-14]. One article compared the accuracy of functional templates[15], while another compared simple templates with complex templates[16]. Both were retrospective analyses. Table 1 provides full details of the included studies[9-16].

In the included studies, 55 cases used the traditional operation method; thus, the reconstruction relied only on the experience of doctors without any computer-aided technology. The remaining 94 cases were completed with the aid of templates. According to the classification of mandibular defects set out by Jewer et al[8], there were 123 cases of L-type defects, five cases of H-type defects and one case of LC-type defects, while 20 cases were unclear. All template-assisted operations used the reconstruction model to pre-bend the titanium plate needed in the surgery (Table 1).

SurgiCase CMF (Materialise, Leuven, Belgium), ProPlan CMF (Materialise), 3matic-Software (Materialise), Geomagic Studio (3D Systems, Rock Hill, SC, USA) and Mimics (Materialse) are commonly used software for preoperative template design. The programs used for measuring accuracy in the present study were Geomagic and Mimics (Table 2)[9-16].

For the type of template, a mandibular resection template and a transplant cutting template were used in all eight studies. Five applied a reduction template to restore the relative position of free mandibular blocks at both ends after osteotomy[12-16]. In four articles, an in-situ moulding template was used to adjust the shape of the grafts in the donor area after harvesting the iliac bone and before cutting the vascular pedicle so that it could match with the broken end of the mandible, achieving a good repair effect[10,13,15,16] (Table 2).

Different methods were used to evaluate the accuracy of mandibular reconstruction. In one study, patients were asked to appraise the aesthetic situation of their appearance using a visual analogue scale[9]. Another article compared the displacement of the mandibular mid-

Table 1 Data of the included studies.

Study	Type	Conventional reconstruction (n = 55)	Template-assisted reconstruction (n = 94)	Defect type
Modabber et al[9]	Prospective cohort study	15	5	NR
Ayoub et al[10]	Retrospective cohort study	10	10	20 L
Zhang et al[11]	Retrospective cohort study	30	15	45 L
Shu et al[12]	Retrospective cohort study	NR	8	5 L, 3 H
Li et al[13]	Retrospective cohort study	NR	5	2 L, 2 H, 1 LC
Zheng et al[14]	Retrospective cohort study	NR	4	4 L
Lu et al[15]	Retrospective cohort study	NR	20: 10 with and 10 without in-situ moulding templates	20 L
Zho et al[16]	Retrospective cohort study	NR	27: 13 simple and 14 complicated templates	27 L

H, L and LC refer to the type of mandibular defect according to the classification by Jewer et al[8]; NR, not reported.

Table 2 Data relating to templates used in the surgery.

Study	Mandibular resection template	Transplant cutting template	Reduction template	In-situ moulding template	VSP software	Measurement software
Modabber et al[9]	*	*			SurgiCase CMF	NR
Ayoub et al[10]	*	*		*	ProPlan CMF, 3matic-Software	Geomagic
Zhang et al[11]	*	*			ProPlan CMF	Geomagic
Shu et al[12]	*	*	*		Mimics	NR
Li et al[13]	*	*	*	*	Mimics, Proplan CMF, Geomagic Studio	Mimics
Zheng et al[14]	*	*	*		ProPlan CMF	Geomagic
Lu et al[15]	*	*	*	*	Mimics	Mimics
Zho et al[16]	*	*	*	*	Mimics	NR

*Indicates that a specific type of template was used in the study. NR, not reported.

line, the height of the alveoli and the gap between the grafts and mandibular blocks by measuring the postoperative panoramic radiograph[16]. Five studies imported CT data into Geomagic or Mimics and integrated preoperative design with a postoperative 3D model[10,11,13-15]. The evaluation indices included the position of the osteotomy line and condyle, the curve of the lower edge of the mandible, the volume of the graft and the overall deviation before and after the operation. Two studies imported postoperative data into Mimics, comparing the differences in distance between condyles and mandibular angles and the deviation of the midpoint of the mandible to that of the condylar connection before and after surgery[13,15] (Table 2).

The mean deviation using templates was 0.70 to 3.72 mm before and after the operation, while that for traditional operations was approximately 2.45 to 5.50 mm. Comparatively, the accuracy of reconstruction with templates was higher. Among 64 patients who used reduction templates, the deviation before and after the operation was 0.70 to 2.70 mm. For the 30 cases without reduction templates, the deviation was 1.30 to 3.72 mm. Reduction templates can increase accuracy.

A total of five studies compared the operation time[9,10,13,15,16]. The mean surgical time for the conventional operation method was 525.2 minutes. After using templates, it was reduced to 314.4 minutes. Two studies compared the ischemic time from cutting the vascular pedicle of the graft to vascular anastomosis[9,10]. After using templates, the ischemic time was reduced by 15.6 minutes to 26.8 minutes compared with the conventional operation method. Microspheres can be classified as microcarriers or microcapsules according to their different cell-laden delivery applications[9]. Microcarriers are usually preformed into large amounts of tiny particles, then cells are loaded on their surfaces. On the contrary, microcapsules are prepared by mixing crosslinkable polymers with cells to encapsulate cells within them.

Discussion

For patients with mandibular defects, establishing how to better restore the integrity of their morphology and function is a major challenge. The optimal outcome of mandibular reconstruction is to make the midline axis symmetrical between the affected side and the healthy side[17]. To achieve this, the morphology of the healthy side is used by the mirror function as a reference for the reconstruction of the affected side. The accuracy of mandibular reconstruction refers to the difference between the shape of the mandible after the operation and the preoperative design. The smaller the deviation between the postoperative effect and the preoperative design, the higher the accuracy of mandibular reconstruction will be[18]. The accuracy of mandibular reconstruction could affect patients' appearance and occlusal relationship, as well as the subsequent functional restoration, such as oral dental rehabilitation and the suitable relationship between the temporomandibular joint and disc. Thus, the improvement in accuracy could not only improve the effectiveness of mandibular reconstruction but also benefit functional restoration. Many steps in the process of mandibular reconstruction affect its accuracy, particularly determining the range of osteotomy, adjusting the size and shape of the grafts and splicing and fixing the position of the mandible and grafts. It is difficult to achieve accurate results by relying solely on preoperative CT scans and doctors' experience. The application of computer technology in medical treatment can not only let doctors discuss and determine the surgical plan through virtual surgery but also produce templates through 3D printing technology to transform the VSP into an operation[19].

Fibula flaps are more widely used to reconstruct mandibles, but in some cases, vascularised iliac flaps are a good choice for mandibular reconstruction because of the advantages they offer in terms of shape and characteristics. Studies on the use of templates to repair mandibles with vascularised iliac flaps are currently limited; thus, this review aimed to compare the accuracy of this repair pattern and related evaluation methods. Randomised controlled trials (RCTs) are more scientific and rigorous; however, compared with drug interventions, RCTs are difficult to achieve in surgical interventions, and there are many related interferences. Therefore, no RCTs were included in our retrieval results, most of which are observational retrospective analyses. In addition, there is no uniform standard for evaluation of accuracy, and diverse methods were used in the different articles, so a meta-analysis could not be conducted.

In the eight studies included, three kinds of accuracy evaluation criteria were used: consulting the VAS score awarded by patients, measuring the panoramic radiograph and analysing 3D reconstruction models. The present authors believe that although patient feedback is very important, it is greatly influenced by subjective factors; directly based on the analysis of two-dimensional images, it will be affected by factors such as overlapping and blurring of images. The application of 3D reconstruction software for measurement is more objective and can be comprehensively evaluated in 3D scenarios, so this method of accuracy analysis is more reliable. The measurement indices using 3D reconstruction software can be divided into two categories. The first is importing CT data into Geomagic and comparing the overall or partial differences by fusing the 3D reconstruction models before and after surgery. The second is using Mimics to measure the distance between the points and compare the differences before and after surgery. The most important anatomical landmarks include the condyle, mandibular angle, chin and the curve of the lower edge of the mandible.

The type of mandibular defect also affects the accuracy of mandibular reconstruction. According to the classification set out by Jewer et al[8], four cases of LC-type defects made it difficult to form the chin because they crossed the middle line of the mandible and eight cases of H-type defects were less effective than L-type defects because they did not retain the condyle. Different types of defects are suitable for various reconstruction methods and different numbers of bone blocks. Thus, when evaluating accuracy, the impact of the types of mandibular defects should also be considered fully[16]. Although most of the eight articles included L-type defects, six cases involved chin or condylar defects; however, the accuracy of different types of defects was not discussed separately in the included articles, which could lead to deviation in our analysis.

When examining whether application of templates can improve the accuracy of mandibular reconstruction, studies that created traditional operation groups are more convincing than simple observation studies. Three of the included studies compared the reconstruction effect of the traditional operation method with that of using templates. By importing CT data before and after surgery into the software for 3D reconstruction and measurement, it was determined that the accuracy of template-assisted surgery was significantly higher than that of traditional surgery. Modabber et al[9] and Ayoub et al[10] compared the difference between the number of grafts harvested during the operation and that needed for actual reconstruction. They found that the length of

the grafts was 16.8 and 25.3 mm, respectively, which was longer than actual requirements, while the amount of bone harvested by the templates was basically consistent with the demands. Ghassemi et al[20] pointed out that there is a correlation between the amount of osteotomy in the donor area and postoperative complications. Unnecessary graft harvesting should therefore be minimised during surgery. The precise preoperative design and the assistance of templates can help osteotomy and transplantation processes to become more accurate.

In addition to templates, the use of computer-aided navigation technology in surgery is also common. Zheng et al[21] reported that the minimum deviation before and after surgery was up to 1.8 mm but was still higher than 0.7 mm when using templates. This indicates that preoperative virtual surgery with templates could achieve a better reconstruction effect.

The common templates are mandible resection and transplant cutting templates. These two kinds of osteotomy templates can indicate the osteotomy process in donor and recipient areas. They can not only help to resect the diseased tissues accurately but also reduce the complications caused by excessive osteotomy in the donor areas[22]. After using osteotomy templates, the accuracy of surgery can be improved from a minimum of 5.5 mm to a maximum of 1.3 mm. In addition, many functional templates are used in mandibular reconstruction. Usually, after mandibular osteotomy, the free mandibular blocks at both ends will be pulled by muscles so their relative position will alter, which makes mandibular reconstruction difficult. In one study, surgeons used a titanium plate to play a role in reduction[22]. It is pre-bent according to the reconstruction model to assist with reduction of the mandible, fixing the position of the mandible and graft according to the curve of the titanium plate; however, this method will cause a series of errors due to the displacement and deformation of the titanium plate. A reduction template can guide restoration of the mandible and graft during the operation to improve accuracy.

A total of 64 cases used a reduction template during surgery. The minimum deviation before and after the operation was 0.7 mm. Lu et al[15] compared the operation methods with and without in-situ moulding templates and found that using these templates to adjust the grinding of the graft in the donor area before cutting the vascular pedicle can improve accuracy, reduce graft ischemic time and shorten patients' hospital stay. On the basis of a simple template, Zho et al[16] added a specific design, for example locating holes on the template to accurately guide the repositioning of the titanium plates and bone blocks and to reserve a path for reducing bone loss when sawing. Compared with a simple template, a complex template with a specific design has higher reconstruction accuracy and shorter surgical time. These results suggest that functional templates and modified templates with specific designs can improve the efficiency and accuracy of surgery[23]. Thus, when designing templates, in addition to conventional osteotomy templates, some functional templates and an improved design can be added as required to simplify the operation steps and improve accuracy.

Application of templates simplifies the surgical procedure to a certain extent and reduces surgical time. However, Ayoub et al[10] pointed out that the total surgical time with 3D templates did not change greatly compared with traditional surgery. Although templates can improve efficiency, the process of fixing various templates during surgery increases the surgical time[24]. At the same time, Modabber et al[9], Ayoub et al[10] and Lu et al[18] pointed out that the ischemic time from cutting off the vascular pedicle of grafts to vascular anastomosis was reduced significantly after using in-situ moulding templates[25]. The shorter the ischemic time, the higher the success rate of transplantation[26]. Thus, templates, especially functional templates, play an important role in improving the prognosis of mandibular reconstruction and reducing complications.

However, application of templates causes some problems that may affect the accuracy of mandibular reconstruction. For example, it often takes a long time for the templates designed preoperatively to be delivered from the manufacturer to the hospital, and this will cause some tumours to grow quickly enough to exceed the range of osteotomies designed by the osteotomy template, resulting in the series of templates being unable to be used during surgery. In the process of positioning templates, ensuring their uniqueness is also a challenge that affects accuracy. In addition, the immediate repair effect will change during the process of patients' recovery. The influencing factors include changes in bone, muscle and soft tissue. Thus, personalised template designs should be generated that fully consider patients' actual situation; on the other hand, continuous improvements should be made to the design of templates, that is, making inaccurate template designs delicate, realising that the development and application of functional templates can improve accuracy, simplify operation steps and reduce surgical time.

Conclusion

Compared with conventional surgery, implementing preoperative VSPs with templates to present surgical plans during surgery can improve the accuracy of using

vascularised iliac flaps to repair the mandible and reduce surgical time. In addition, functional templates used to shape grafts before cutting the vascular pedicle could reduce ischemic time and postoperative complications. Many factors can affect the accuracy of the operation, so when designing templates, improvements should be made constantly to improve the prognosis of mandibular reconstruction.

Conflicts of interest

The authors declare no conflicts of interest related to this study.

Author contribution

Dr Ting Wei LU performed the systematic analysis and wrote the article; Drs Tong JI and Wan Tao CHEN revised the manuscript. All authors read and approved the final manuscript.

(Received Mar 22, 2021; accepted Aug 11, 2021)

References

1. Hou G, Wu T, Shang Z, Shao Z. Application of digital surgery and additive manufacturing technology in reconstruction of mandibular defect with vascularized iliac muscle flap [in Chinese]. Zhongguo Shiyan Waike Zazhi 2020;37:635–638.
2. Bell WH. Use of heterogenous bone in oral surgery. J Oral Surg Anesth Hosp Dent Serv 1961;19:459–474.
3. Taylor GI, Townsend P, Corlett R. Superiority of the deep circumflex iliac vessels as the supply for free groin flaps. Clinical work. Plast Reconstr Surg 1979;64:745–759.
4. Lyons AJ, James R, Collyer J. Free vascularised iliac crest graft: An audit of 26 consecutive cases. Br J Oral Maxillofac Surg 2005;43: 210–214.
5. Riediger D. Restoration of masticatory function by microsurgically revascularized iliac crest bone grafts using enosseous implants. Plast Reconstr Surg 1988;81:861–877.
6. Zhang M, Rao P, Xia D, Sun L, Cai X, Xiao J. Functional reconstruction of mandibular segment defects with individual preformed reconstruction plate and computed tomographic angiography-aided iliac crest flap. J Oral Maxillofac Surg 2019;77:1293–1304.
7. Hanken H, Schablowsky C, Smeets R, et al. Virtual planning of complex head and neck reconstruction results in satisfactory match between real outcomes and virtual models. Clin Oral Investig 2015;19:647–656.
8. Jewer DD, Boyd JB, Manktelow RT, et al. Orofacial and mandibular reconstruction with the iliac crest free flap: A review of 60 cases and a new method of classification. Plast Reconstr Surg 1989;84:391–405, discussion 404–405.
9. Modabber A, Gerressen M, Stiller MB, et al. Computer-assisted mandibular reconstruction with vascularized iliac crest bone graft. Aesthetic Plast Surg 2012;36:653–659.
10. Ayoub N, Ghassemi A, Rana M, et al. Evaluation of computer-assisted mandibular reconstruction with vascularized iliac crest bone graft compared to conventional surgery: A randomized prospective clinical trial. Trials 2014;15:114.
11. Zhang W, Yu Y, Wang Y, et al. Improving the accuracy of mandibular reconstruction with vascularized iliac crest flap: Role of computer-assisted techniques. J Craniomaxillofac Surg 2016;44:1819–1827.
12. Shu DL, Liu XZ, Guo B, Ran W, Liao X, Zhang YY. Accuracy of using computer-aided rapid prototyping templates for mandible reconstruction with an iliac crest graft. World J Surg Oncol 2014;12:190.
13. Li Y, Shao Z, Zhu Y, Liu B, Wu T. Virtual surgical planning for successful second-stage mandibular defect reconstruction using vascularized iliac crest bone flap: A valid and reliable method. Ann Plast Surg 2020;84:183–187.
14. Zheng L, Wu W, Shi Y, Zhang J. Mandibular reconstruction with a deep circumflex iliac artery flap using computer-assisted and intraoral anastomosis techniques. J Oral Maxillofac Surg 2019;77:2567–2572.
15. Lu T, Liu Z, Wu T, Shao Z, Sun Y, Sun Z, Liu B. Application of individualized in-situ moulding guide plate in mandibular reconstruction using a vascularized iliac muscle flap [in Chinese]. Kouqaing Yixue Yanjiu 2019;35:766–771.
16. Zho M, Shao Z, Zhu Y, Liu B, Wu T. Comparison of complicated and simple guiding templates in mandibular reconstruction using vascularized iliac crest flap. Biomed Res Int 2019;2019:7496538.
17. Pohlenz P, Blessmann M, Blake F, Li L, Schmelzle R, Heiland M. Outcome and complications of 540 microvascular free flaps: The Hamburg experience. Clin Oral Investig 2007;11:89–92.
18. Roser SM, Ramachandra S, Blair H, et al. The accuracy of virtual surgical planning in free fibula mandibular reconstruction: Comparison of planned and final results. J Oral Maxillofac Surg 2010;68: 2824–2832.
19. Pfaff MJ, Steinbacher DM. Plastic surgery applications using three-dimensional planning and computer-assisted design and manufacturing. Plast Reconstr Surg 2016;137:603e–616e.
20. Ghassemi A, Ghassemi M, Riediger D, Hilgers RD, Gerressen M. Comparison of donor-site engraftment after harvesting vascularized and nonvascularized iliac bone grafts. J Oral Maxillofac Surg 2009;67:1589–1594.
21. Zheng L, Lv X, Zhang J, Liu S, Zhang J, Zhang Y. Translating computer-aided design and surgical planning into successful mandibular reconstruction using a vascularized iliac-crest flap. J Oral Maxillofac Surg 2018;76:886–893.
22. Lu T, Shao Z, Liu B, Wu T. Recent advance in patient-specific 3D printing templates in mandibular reconstruction. J Mech Behav Biomed Mater 2020;106:103725.
23. Picard-Ami LA Jr, Thomson JG, Kerrigan CL. Critical ischemia times and survival patterns of experimental pig flaps. Plast Reconstr Surg 1990;86:739–745.
24. Ramella V, Franchi A, Bottosso S, Tirelli G, Novati FC, Arnež ZM. Triple-cut computer-aided design-computer-aided modeling: More oncologic safety added to precise mandible modeling. J Oral Maxillofac Surg 2017;75:1567.e1-1567.e6.
25. Shen Y, Sun J, Li J, Li MM, Huang W, Ow A. Special considerations in virtual surgical planning for secondary accurate maxillary reconstruction with vascularised fibula osteomyocutaneous flap. J Plast Reconstr Aesthet Surg 2012;65:893–902.
26. Ganry L, Quilichini J, Bandini CM, Leyder P, Hersant B, Meningaud JP. Three-dimensional surgical modelling with an open-source software protocol: Study of precision and reproducibility in mandibular reconstruction with the fibula free flap. Int J Oral Maxillofac Surg 2017;46:946–957.

SEEING INSIDE THE TOOTH

NEW

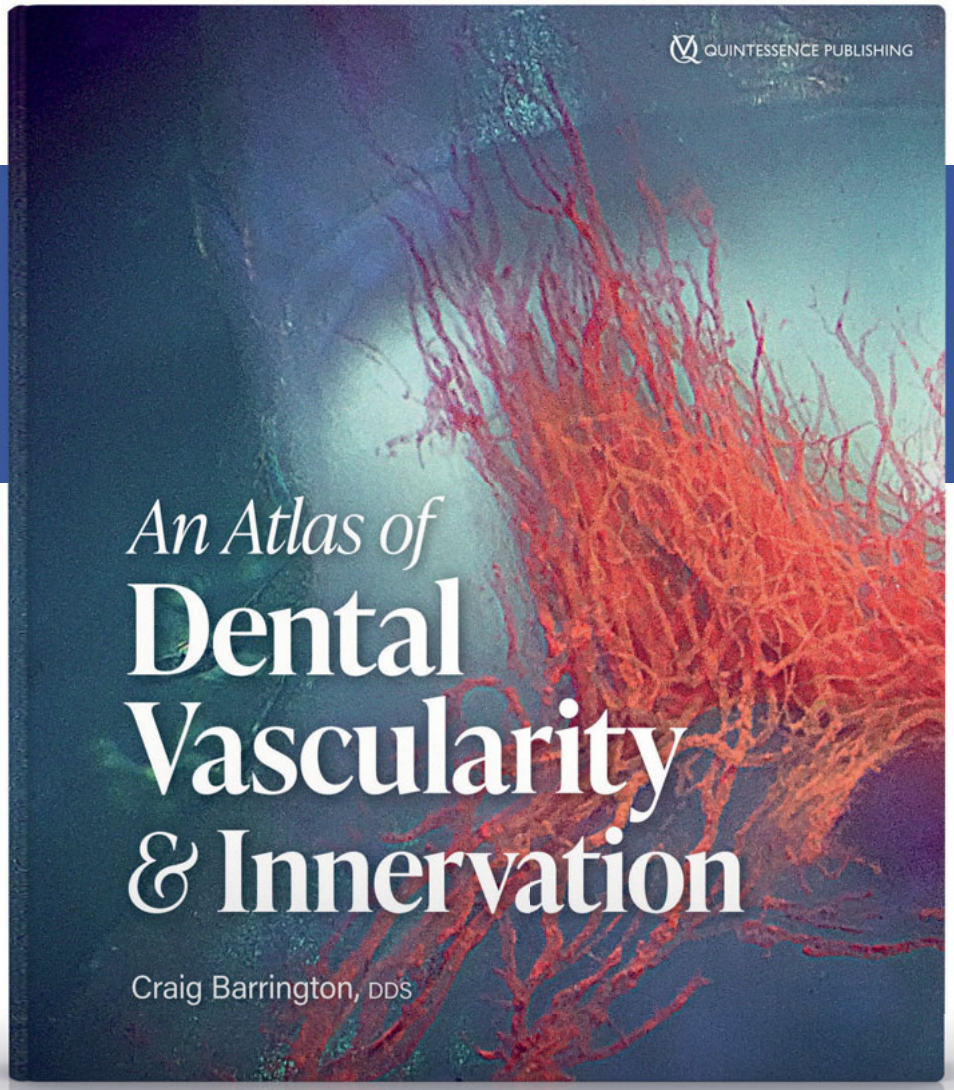

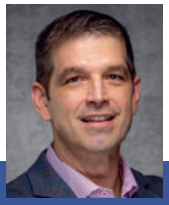

Craig Barrington

An Atlas of Dental Vascularity & Innervation

144 pages, 178 illus.
ISBN 978-1-64724-066-0
€118

Our understanding of internal dental anatomy has remained limited by our inability to see inside a tooth without sectioning it. However, for one dentist working to find a way to see inside a tooth, the answer was diaphanization. This atlas represents the breathtaking results of photographing human teeth that have been made transparent. Dr Barrington has learned as many diaphanization methods as possible to understand how, where, and why transparency can occur in a solid object and translate that to tooth structure. The images in this atlas showcase the internal anatomy of the teeth, with a special emphasis on the innervation and vascular structure and their distribution within the dentin chamber. For each image, the author follows a complex diaphanization method to make an extracted tooth transparent, before photographing the intact internal dental anatomy. Therefore, the images in this book display structures that have rarely been seen so clearly and in three dimensions, including the pulp chamber, apical anatomy, tooth channels as well as pulpal pathology. This atlas pushes our understanding of internal dental anatomy and serves as an inspiration as to what one individual can do to advance knowledge within dentistry.

www.quint.link/diaphanization
books@quintessenz.de
+49 (0)30 761 80 667
QUINTESSENCE PUBLISHING

Relationship between Presence of Third Molars and Prevalence of Periodontal Pathology of Adjacent Second Molars: a Systematic Review and Meta-analysis

Yang YANG[1#], Yi TIAN[1#], Li Juan SUN[1], Hong Lei QU[1], Fa Ming CHEN[1]

Objective: *To estimate the mean prevalence of periodontal pathology of adjacent second molars (A-M2s) to third molars (M3s) and identify related confounding factors.*
Methods: *Studies published before August 2020 were systematically searched in the Cochrane Library, EMBASE and MEDLINE databases. We included cross-sectional studies that evaluated the periodontal pathology of A-M2s based on clinical or radiographic examinations at the molar level. Studies employing similar periodontal parameters were pooled. Clinical attachment loss ≥ 3 mm, alveolar bone loss ≥ 3 mm or ≥ 20% root length were defined as early periodontal defects, and at least one site with probing depth ≥ 5 mm was considered as deep periodontal pockets around A-M2s in the data synthesis.*
Results: *Nine studies (14,749 M3s) were ultimately included in the meta-analysis. On average, 19% of A-M2s showed distal early periodontal defects with the presence of M3s (95% confidence interval [95% CI] 9%–35%). Subgroup analyses suggested the prevalence was 32% (95% CI 16%–54%) in the mandible, and the prevalence was higher with nonimpacted M3s (25%, 95% CI 12%–47%) than with impacted M3s (19%, 95% CI 10%–35%). Additionally, the pooled prevalence for deep periodontal pockets around A-M2s was 52% (95% CI 39%–64%). Subgroup analyses suggested the prevalence was higher in the mandible (62%, 95% CI 45%–76%) than in the maxilla (43%, 95% CI 31%–56%), and for nonimpacted M3s the prevalence reached 50% (95% CI 36%–64%).*
Conclusion: *The presence of M3s, especially mandibular and nonimpacted M3s, negatively affects the periodontal status of A-M2s.*
Key words: *meta-analysis, periodontal pathology, prevalence, second molars, third molars*
Chin J Dent Res 2022;25(1):45–55; doi: 10.3290/j.cjdr.b2752683

1 State Key Laboratory of Military Stomatology, Department of Periodontology, School of Stomatology, National Clinical Research Centre for Oral Diseases, Fourth Military Medical University, Xi'an, P.R. China.
# These authors contributed equally to this work.

Corresponding author: Dr Fa Ming CHEN, Department of Periodontology, School of Stomatology, National Clinical Research Center for Oral Diseases, Fourth Military Medical University, #145 West Changle Road, Xi'an 710032, P.R. China. Tel/Fax: 86-29-84776096. Email: cfmsunhh@fmmu.edu.cn

This study was partially supported by the National Natural Science Foundation of China (Subproject), grant/award number 81991503.

The eruption of third molars (M3s) is restricted by adjacent tissue and limited space, and M3s often indeed fail to fully erupt[1,2]. Their anatomical features frequently lead to food impaction and plaque accumulation in M3 regions[3]. Insufficient plaque control makes M3s and their neighbours, adjacent second molars (A-M2s), vulnerable to periodontal diseases[4]. Studies have found laboratory evidence of increased levels of periodontal pathogens in M3 regions, even with few clinical symptoms of periodontal diseases[5,6]. Periodontal pathogens in M3 regions develop and the periodontal status of A-M2s is affected by age[7]. As early as the 1960s, Ash et

al[8] reported the periodontal risks related to M3s. Since then, there have been a number of studies examining the relationship between the presence of M3s and the periodontal pathology of A-M2s.

Prevalence is one of the most important pieces of data describing the epidemiological characteristics of the periodontal pathology of A-M2s; however, estimates of the prevalence of periodontal pathology of A-M2s at the molar level vary significantly among studies, ranging from 3.1% to 64.5%[9,10]. Diverse periodontal parameters, including probing depth (PD), alveolar bone loss (ABL) and clinical attachment loss (CAL), accompanied by different examined sites (single or multiple sites around A-M2s), have been employed to evaluate the periodontal status of A-M2s[3,11,12], which may partly account for the statistically significant variance in results. Nevertheless, different characteristics of M3s and patients may also contribute to the high degree of heterogeneity in prevalence[13-15]. Impacted M3s (I-M3s) have been reported to be associated with negative periodontal influences on A-M2s[16-18]. Many studies have compared prevalence among impaction types, but diverse results have been recorded for various I-M3 classifications[9,13,14,19]. In addition, studies on periodontal risks associated with nonimpacted M3s (N-M3s) are limited and controversial[11,14,20]. Characterising the confounding factors that cause heterogeneity is important for evaluating the risks of the presence of M3s for individuals.

Estimating the mean prevalence of periodontal pathology of M2s with neighbouring M3s is the first step towards elucidating the relationship between the presence of M3s and the periodontal status of A-M2s, which contributes to M3 clinical decision making. Thus, this systematic review and meta-analysis aimed to synthesise and calculate the mean prevalence of periodontal pathology of A-M2s at the molar level, and to identify the confounding factors that lead to a high degree of variation in prevalence.

Materials and methods

The meta-analysis was performed according to the Preferred Reporting Items for Systematic Reviews and Meta-Analysis (PRISMA) guidelines[20] (Appendix 1, provided on request). The meta-analysis was not registered.

Literature search

The Cochrane Library, EMBASE and MEDLINE databases were searched systematically from inception to August 2020 using specific keywords. The keywords were described by wildcards and MeSH, and the following terms were combined in different databases: "third molar*"; "third-molar*"; "3rd molar*"; "wisdom tooth"; "wisdom teeth" and "second molar*"; "2nd molar*; "adjacent molar*"; "adjacent tooth"; "adjacent teeth" and "periodontitis"; "periodontal disease*"; "periodontal defects"; "periodontal destruction"; "periodontal pathology"; "periodontal inflammation"; "attachment loss"; "alveolar bone loss"; and "periodontal pockets".

Study selection

Two investigators (YY and YT) independently reviewed and screened the searched articles. The selection process involved reading the titles and abstracts, reading the full articles and assessing the inclusion/exclusion of potentially qualified articles. In the event of ambiguities, detailed information was obtained by contacting the authors. Any disagreements were resolved through discussion or through consultation with persisted, a third investigator (LJS) to make the final decision. The inclusion criteria used for the systemic review were as follows:

- cross-sectional studies that evaluated the periodontal status of M2s with neighbouring M3s, regardless of being symptomatic or asymptomatic;
- studies defining the periodontal pathology of A-M2s either through clinical or radiographic examination;
- studies providing explicit information for calculating the prevalence of periodontal pathology of A-M2s at the molar level.

Reviews, case reports, case series, articles with full texts unavailable, studies with a sample size < 200 at the molar level and controversial studies without responses from authors were excluded. Studies involving specific populations such as pregnant women and orthodontic patients were also excluded, as were studies that screened the periodontal status.

Data extraction

The following data were extracted: basic information (first author, year of publication, journal and country), sample characteristics (study design, source of sample, sample number, sample age and sex and periodontal condition of sample), methods (clinical and/or radiographic examination), outcomes (prevalence of periodontal pathology of A-M2s at the molar level) and quality evaluation. CAL, ABL and PD were the most commonly reported parameters for evaluating periodontal status; thus, relevant data at the molar level were

extracted to estimate the prevalence of periodontal pathology of A-M2s clinically and radiographically. Moreover, the prevalence of periodontology of A-M2s under different M3 locations, M3 impaction status, patient sex and patient age was further extracted and listed below the overall prevalence. If one study reported the prevalence of periodontal pathology with more than one parameter, the following priority sequence was followed for data extraction: CAL, ABL and PD. Only the preoperative data from studies that compared the clinical and radiological parameters before and after M3 surgery were extracted and used for statistical analysis. When the explicit prevalence of periodontal pathology was not reported directly, the prevalence was calculated by dividing the number of A-M2s with periodontal pathology by the total number of included A-M2s.

Assessment of study bias

We used the modified Newcastle-Ottawa scale (NOS), which was formulated for cross-sectional studies, to assess the bias of the included studies[21]. For cross-sectional studies, the NOS comprises sample selection, comparability among groups and outcome measurement, and there are detailed evaluation criteria for each item. Once the study met the evaluation criterion, it could be evaluated at one or two points depending on the evaluation standard. The maximum number of points was 10, and a study awarded a score higher than 7 was considered at low risk of bias. Bias was independently assessed by two investigators (YY and YT) and discussion was conducted to reach a consensus on the quality of the studies.

Data synthesis

For internal consistency and high efficiency in the meta-analysis, only studies that reported the prevalence of periodontal pathology for A-M2s with similar periodontal parameters were synthesised. CAL was defined as the distance from the cementoenamel junction to the base of the periodontal pockets greater than 3 mm[22,23], and ABL as the distance from the cementoenamel junction to the alveolar bone greater than 3 mm or 20% root length[24,25]. These general definitions were used to explain the threshold values selected in this meta-analysis (CAL ≥ 3 mm, ABL ≥ 3 mm or 20% root length) for the presence of early periodontal defects. Moreover, at least one site with PD ≥ 5 mm was used to define the deep periodontal pockets around A-M2s[10]. The relevant data were imported into specific software (metafor package, meta package, in R statistical language, version 4.0.2, R Core Team, Vienna, Austria) for meta-analysis. Forest plots were used to describe the estimated effect size and 95% confidence interval (95% CI) for meta-analysis. The heterogeneity of the data was reflected by the Q-statistic and the I^2 test. If heterogeneity was significant ($I^2 > 50\%$ or $P < 0.05$), a random-effects model was used to calculate pooled data. Moreover, subgroup analyses according to different characteristics of M3s (M3 locations and impaction status) and patients (overall periodontal health, sex and age) were conducted to explore possible reasons for heterogeneity. If a sufficient number of studies were included, publication bias and sensitivity were assessed.

Results

In total, 865 records were identified using the search strategies. After removal of duplicates and title/abstract screening, 212 records were included for full-text screening. Based on the inclusion criteria, 193 records were excluded. Consequently, 19 studies were included for qualitative synthesis[3,9-16,19,20,26-33], nine of which (14749 M3s) were used for meta-analysis (Fig 1)[3,10-12,14,15,29,30,33].

Qualitative synthesis

Table 1 presents the main characteristics of all the included studies for qualitative synthesis. Only four of them used the general population as samples[12-14,31]; the others included patients in the analysis. The periodontal status of M2s was confirmed through clinical or radiographic examinations in five prospective studies that recruited participants and conducted data collection at a single time point[3,10,13,30,31]. Fourteen studies retrospectively evaluated the prevalence of periodontal pathology of M2s by collecting radiographic records[9,11,12,14-16,19,20,26-29,32,33]. Only two studies evaluated the overall periodontal health of participants using case definitions from the US Centers for Disease Control and Prevention (CDC) and the American Academy of Pediatrics (AAP), and most of their participants had mild or moderate periodontitis[12,13]. The periodontal status of A-M2s was evaluated using different periodontal parameters in the included studies. Thirteen studies reported the prevalence of ABL of A-M2s[9,11,14-16,19,20,26-29,32,33] and eight described the specific degree of ABL, including ABL ≥ 1 mm[19], 3 mm[15,29,32], 5 mm[16,32] or 20% root length[11,14]. Five selected studies used PD as a parameter to evaluate the periodontal status of A-M2s[3,10,13,30,31], and in most cases, the measurement of at least one site of PD ≥ 5 mm around A-M2s was emloyed[3,10,30]. Only

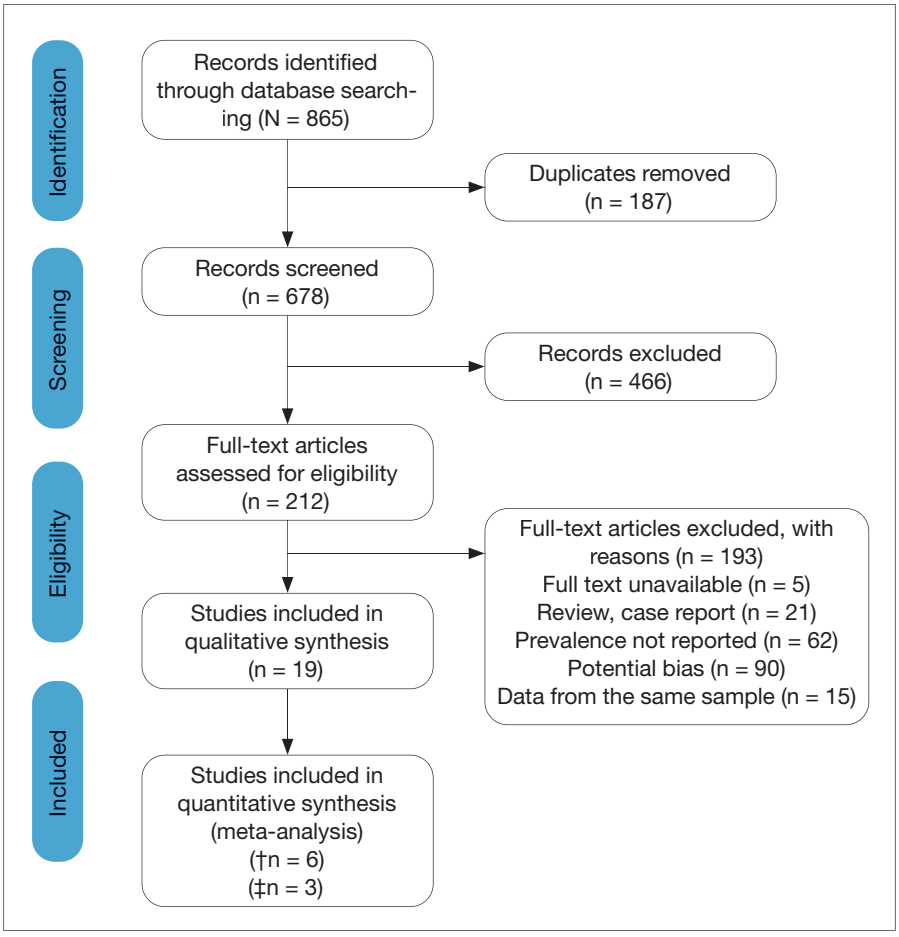

Fig 1 Flow diagram of the screening process. n, number of hits. †Analysis of early periodontal defects: CAL ≥ 3 mm, ABL ≥ 3 mm or ≥ 20% root length on distal sites of second molars with neighbouring third molars; ‡Analysis of deep periodontal pockets: at least one site with PD ≥ 5 mm around second molars with neighbouring third molars.

one study reported the prevalence of CAL on distal sites of A-M2s with depth ≥ 3 mm[12]. The NOS scores for the included studies ranged from 6 to 9, the mean score was 7.16 and the overall risk of bias was low (Appendix 2, provided on request). The main cause of bias was identified as comparability among groups.

Several studies have reported that various characteristics of M3s and patients affect the prevalence of periodontal pathology of A-M2s in different ways. Seven studies compared the difference in prevalence between mandibular and maxillary M3s[3,9-12,30,32], and only one of these found a higher prevalence with maxillary M3s than with mandibular M3s[32]. The impaction status of M3s was analysed in different ways. Four studies reported the difference in periodontal pathology among different angulations of I-M3s according to the Winter classification[9,13,15,19]. Even with different periodontal parameters, mesioangular and horizontal M3s were significantly associated with a higher risk of periodontal pathology than other angulations, and the risk for buccolingual and distal M3s was very low. Another four studies divided M3s into I-M3s (unerupted to the occlusal plane) and N-M3s (erupted to the occlusal plane) without explicit classifications of I-M3s[11,12,14,20], and three of them reported a higher prevalence of periodontal pathology with N-M3s[11,12,20]. Different impaction depths and covered tissues associated with I-M3s were analysed but indicated weak evidence with limited studies[13-15]. Additionally, four studies reported the prevalence of periodontal pathology between different age groups[13,16,28,32]. Older age was associated with a higher risk of periodontal pathology than younger age, especially ≥ 30 years; only one study came to the opposing conclusion[32]. Three studies reported a difference between sexes, but their results were completely different and showed no significant trend that sex influenced individuals' level of vulnerability to periodontal pathology of A-M2s[26,29,32].

Quantitative synthesis

Studies with similar periodontal parameters were included for the data synthesis. Six of those included in the qualitative synthesis evaluated the prevalence of early

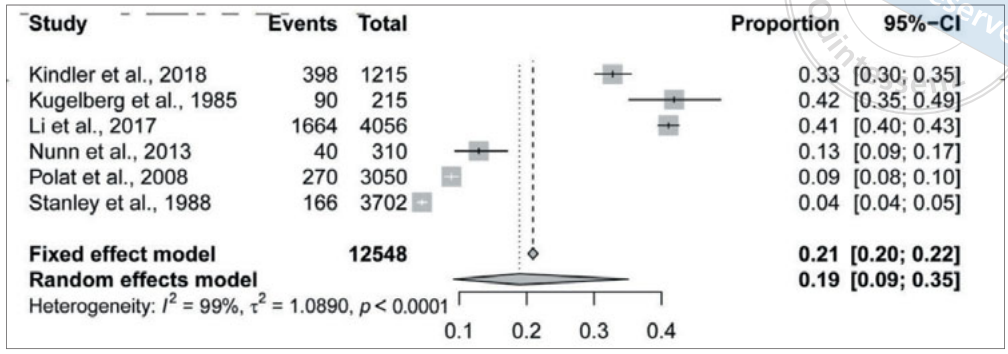

Fig 2 Forest plot of the prevalence of early periodontal defects on distal sites of second molars with neighbouring third molars.

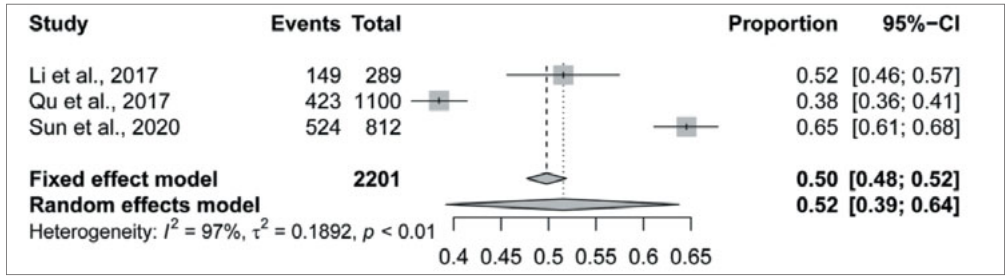

Fig 3 Forest plot of the prevalence of deep periodontal pockets around second molars with neighbouring third molars.

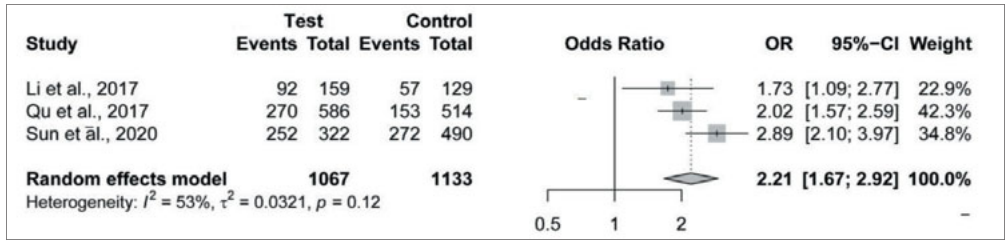

Fig 4 Forest plot of the odds ratio of deep periodontal pockets around second molars with neighbouring mandibular third molars versus maxillary third molars.

periodontal defects on distal sites of A-M2s with CAL ≥ 3 mm, ABL ≥ 3 mm or ≥ 20% root length[11,12,14,15,29,33], and three calculated the prevalence of deep periodontal pockets around A-M2s with at least one site with PD ≥ 5 mm[3,10,30], with subgroup analyses that were pooled and conducted separately. The data for other A-M2 sites and other periodontal parameters were not pooled due to the limited number of studies.

The results showed that the prevalence of early periodontal defects on distal sites of A-M2s was 19% (95% CI 9%–35%, I^2 100%, P < 0.0001) (Fig 2) and the prevalence of deep periodontal pockets around A-M2s was 52% (95% CI 39%–64%, I^2 97%, P < 0.01) with the random-effects method (Fig 3). Because the number of studies included in the meta-analysis was limited, we did not assess publication bias or conduct a sensitivity analysis.

Subgroup analyses on M3 locations

The prevalence of early periodontal defects on distal sites of A-M2s associated with mandibular M3s was 32% (95% CI 16%– 54%, I^2 99%, P < 0.01) (Appendix 3, provided on request). Meanwhile, a higher prevalence of deep periodontal pockets was recorded around A-M2s associated with mandibular M3s (62%, 95% CI 45%–76%, I^2 96%, P < 0.01) (Appendix 4, provided on request) than maxillary M3s (43%, 95% CI 31%–56%, I^2 94%, P < 0.01) (Appendix 5, provided on request), (odds ratio [OR] 2.21, 95% CI 1.67–2.92, I^2 53%, P = 0.12) (Fig 4).

Subgroup analyses on M3 impaction status

No significant difference was found in the prevalence of early periodontal defects on distal sites of A-M2s between I-M3s (19%, 95% CI 10%–35%, I^2 99%, P < 0.01) (Appendix 6, provided on request) and N-M3s (25%, 95% CI 12%–47%, I^2 99%, P < 0.01) (Appendix 7, provided on request) (OR 1.04, 95% CI 0.71–1.54, I^2 79%, P < 0.01) (Fig 5). Additionally, the prevalence of deep periodontal pockets around A-M2s with neighbouring N-M3s was 50% (95% CI 36%–64%, I^2 97%, P < 0.01) (Appendix 8, provided on request).

Table 1 Data extraction of the main characteristics of the included studies for final review (cross-sectional studies).

Study	Country	Journal	Study design	Source of sample	Number of participants	Sex	Number of molars	
Altan et al[19]	Turkey	J Dent Shiraz Univ Med Sci	Retrospective	Patients	954	NR	1598	
Akarslan and Kocabay[26]	Turkey	Oral Surg Oral Med Oral Pathol Oral Radiol	Retrospective	Patients	342	175 M, 167 F	400	
Blakey et al[13]	USA	J Oral Maxillofac Surg	Prospective	General population	329	159 M, 170 F	1289	
Chu et al[16]	China	Hong Kong Med J	Retrospective	Patients	2115	956 M, 1156 F	3178	
Gupta et al[27]	India	J Family Med Prim Care	Retrospective	Patients	400	240 M, 160 F	640	
Jung and Cho[9]	Korea	Imaging Sci Dent	Retrospective	Patients	2048	998 M, 1050 F	4455	
Kindler et al[12]	Germany	J Clin Periodontol	Retrospective	General population	1915	NR	1427	
Kim et al[28]	Korea	J Dent Sci	Retrospective	Patients	630	NR	748	
Kugelberg et al[29]	Sweden	Int J Oral Surg	Retrospective	Patients	144	NR	215	
Li et al[11]	China	J Periodontol	Retrospective	Patients	1958	774 M, 1184 F	4056	
Li et al[30]	China	J Oral Maxillofac Surg	Prospective	Patients	135	59 M, 76 F	289	
Nivedita et al[20]	India	Minerva Stomatol	Retrospective	Patients	749	490 M, 259 F	2342	
Nunn et al[14]	USA	J Dent Res	Retrospective	General population	416	NR	310	
Prahabkar et al[31]	India	Biomed & Phamacol J	Prospective	General population	200	NR	400	
Polat et al[15]	Turkey	Oral Surg Oral Med Oral Pathol Oral Radiol Endod	Retrospective	Patients	1914	828 M, 1086 F	3050	

	Age, y	Periodontitis by AAP/CDC case definition	Diagnostic criteria of periodontal pathology of A-M2s	Prevalence of periodontal pathology of A-M2s Under different M3 locations, M3 impaction status, age of patients and sex of patients (if reported)	Risk of bias
	Range 16–64, mean 26.42 ± 7.60	NR	DPT ABL > 1 mm on distal sites of A-M2s	4.9% Mesial 10.6%, horizontal 9%, vertical 0.2%, others 4.7%	7
	Range 20–25, mean 22.20 ± 1.80	NR	DPT ABL on distal sites of A-M2s	10.8% Male 9%, female 12.5%	7
	Range 14–45	AAP Class I–III	CE PD > 5 mm on distal sites of A-M2s	6.1% At/above OP 6%, below OP 6% Vertical/distal 9.3%, mesial/horizontal 10.2% < 25 y 2.9%, > 25 y 9.3%	8
	Range 17–89, mean 27.9	NR	DPT ABL > 5 mm on distal sites of A-M2s	8.9% < 30 y 5.7%, > 30 y 16.3%	7
	Mean 27 y	NR	DPT ABL on distal sites of A-M2s	39.1%	6
	Range 25–92, mean 50	NR	DPT ABL on distal sites of A-M2s	3.1% Mandibular 4.5%, maxillary 1.2% Mesial 13.5%, horizontal 13.9%, vertical 1.3%, distal 1.1%, inverted 16.1%, buccal 0.0%	7
	Mean 50	None or mild 48.8% Moderate 34.4% Sever 16.8%	Magnetic resonance imaging	32.8% Mandibular 43.5%, maxillary 24.2% I-M3s 27.9%, N-M3s 34.1%	7
	Range 13–74, mean 29.00 ± 10.20	NR	DPT ABL on distal sites of A-M2s	10.8% < 30 years < 3%, > 30 years > 97%	7
	Range 16–53, mean 27.20 ± 6.35	NR	DPT ABL > 3 mm on distal sites of A-M2s	41.9% Male 56.22%, female 26.2%	7
	≥ 19, mean 37.2	NR	DPT ABL ≥ 20% root length on distal sites of A-M2s	41.0% Mandibular 47.6%, maxillary 33.8% I-M3s 40.4%, N-M3s 41.5%	7
	Mean 40.60 ± 11.50	NR	CE PD > 5 mm around A-M2s	51.6% Mandibular 57.9%, maxillary 44.2%	8
	Range 18–83, mean 39.20 ± 12.80	NR	DPT ABL on distal and mesial sites of A-M2s	Distal sites 35.4% I-M3s 2.6%, N-M3s 38.9% Mesial sites 43.2% I-M3s 2.6%, N-M3s 47.6%	8
	Range 28.1–76.2, mean 45.80 ± 7.40	NR	DPT ABL ≥ 20% root length on distal sites of A-M2s	12.9% Soft tissue impaction 28%, bony impaction 16.9%, erupted 9.2%	7
	Range 21–25	NR	CE PD > 4 mm on distal sites of A-M2s	12.0%	7
	Range 18–60, mean 25.91 ± 6.34	NR	DPT ABL > 3 mm on distal sites of A-M2s	Mesial 18.5%, horizontal 16.8%, vertical 0.9%, distal 0.0%, inverted 0% Class A 10.1%, class B 8.8%, class C 3.7%	6

Study	Country	Journal	Study design	Source of sample	Number of participants	Sex	Number of molars	
Qu et al[3]	China	J Oral Maxillofac Surg	Prospective	Patients	572	339 M, 233 F	1100	
Sejfijia et al[28]	Kosovo	Acta Stomatologica Croatica	Retrospective	Patients	710	296 M, 414 F	1297	
Stanley et al[33]	USA	J Oral Pathol	Retrospective	Patients	1756	NR	3702	
Sun et al[10]	China	Oral Dis	Prospective	Patients	371	176 M, 195 F	812	

CE, clinical examination; DPT, dental panoramic tomogram; NR, not reported; OP, occlusal plane.

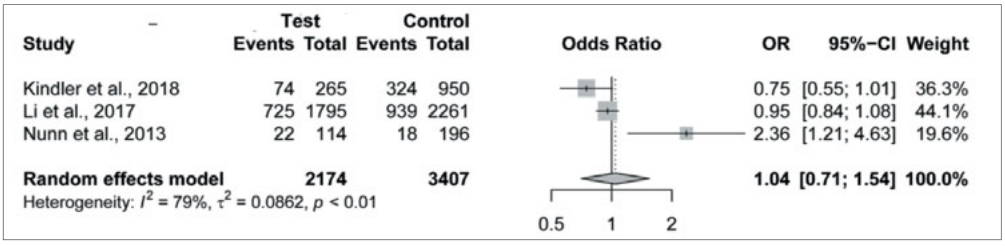

Fig 5 Forest plot of the odds ratio of early periodontal defects on distal sites of second molars with neighbouring impacted third molars versus nonimpacted third molars.

Patient characteristics such as M3 impaction classification, overall periodontal health, sex and age were not fully reported or were not reported with similar periodontal parameters that could be used to conduct a subgroup analysis.

Discussion

Recently, the periodontal impacts of M3s on A-M2s have attracted increasing attention due to great controversy regarding clinical decision making concerning M3s. There is a general consensus that M3s should undergo long-term observation and ultimately removal if symptoms of disease are significant[34,35]. On the other hand, it is not widely agreed that early treatment is necessary to prevent harm to A-M2s and avoid complications after removal in old age[36,37]; however, a wide range of prevalence estimates of periodontal pathology of M2s with neighbouring M3s has been reported across studies due to methodological variations and different sample characteristics, and therefore cannot provide reliable evidence for clinical practice. To better understand the periodontal risks associated with M3s, this systematic review and meta-analysis was conducted. To our knowledge, this is the first meta-analysis on the prevalence of periodontal pathology of A-M2s.

The present meta-analysis appears to indicate that the prevalence of early periodontal defects on distal sites of A-M2s at the molar level was 19%. Periodontal diseases include supporting connective tissue loss and alveolar bone loss[22]. Thus, the presence of early periodontal defects was reflected by a combination of the following parameters: CAL ≥ 3 mm, ABL ≥ 3 mm or ≥ 20% root length, which was a more comprehensive evaluation. M3s are located behind M2s, and periodontal defects distal to A-M2s provide direct evidence for the periodontal risks associated with the presence of M3s and reflect the cumulative effects of periodontal pathology. The high prevalence of deep periodontal pockets around A-M2s (52%) highlights the potential risk of active

	Age, y	Periodontitis by AAP/CDC case definition	Diagnostic criteria of periodontal pathology of A-M2s	Prevalence of periodontal pathology of A-M2s Under different M3 locations, M3 impaction status, age of patients and sex of patients (if reported)	Risk of bias
	Range 19–35, mean 36.80 ± 18.70	NR	CE PD > 5 mm around A-M2s	38.5% Mandibular 46.1%, maxillary 29.8% I-M3s 42.9%, N-M3s 33.9%	9
	Range 18–77, mean 29.30 ± 12.80	NR	DPT ABL > 5 mm on distal sites of A-M2s	5.5% Mandibular 4.9%, maxillary 6.5% < 30 y 6.9%, > 30 y 1.2% Male 4.8%, female 4.9%	7
	Range 20–83, mean 47	NR	DPT ABL > 3 mm on distal sites of A-M2s	4.5%	6
	Mean 35.10 ± 11.90	NR	CE PD > 5 mm around A-M2s	64.5% Mandibular 78.3%, maxillary 55.5%	8

periodontal pathology, and PD ≥ 5 mm has been confirmed to result in high levels of periodontal pathogens and inflammatory mediators in M3 regions[5,38].

In subgroup analyses, a higher prevalence of early periodontal defects was found to be associated with mandibular M3s (32%) than with M3s in general (19%), and the data on maxillary M3s were limited to be synthesised. However, both studies that analysed the difference between M3 locations reported a higher prevalence of early periodontal defects in mandibular than in maxillary molars[11,12]. Moreover, the prevalence of deep periodontal pockets around A-M2s associated with mandibular M3s was significantly greater than that with maxillary M3s (OR 2.21). The higher odds of M3 impaction in mandibular than in maxillary regions could partly explain this difference[1]. Furthermore, subgroup analyses were conducted on M3 impaction status. Intriguingly, a higher prevalence of early periodontal defects was found to be associated with N-M3s (25%) than I-M3s (19%), even with no significant difference (OR 1.04). In the subgroup analysis, two studies reported a higher prevalence of N-M3s without explicit classifications of I-M3s[11,12], while Nunn et al[14] reported that the prevalence of bony impacted and soft tissue impacted M3s was higher than that for N-M3s. The higher prevalence of N-M3s might be caused by the significant difference in the periodontal pathology between different impaction types[19], which affected the overall prevalence associated with I-M3s. In the analysis of deep periodontal pockets around A-M2s, only one study reported separate outcomes for I-M3s and N-M3s[3], which suggested a higher prevalence associated with I-M3s; however, the prevalence of deep periodontal pockets around A-M2s associated with N-M3s reached 50%, which reminds us that the presence of N-M3s is also an important periodontal risk factor for A-M2s. Additionally, some studies have reported other increased pathological parameters around A-M2s with N-M3s, such as Plaque Index and bleeding on probing[3,10].

Our meta-analysis indicated the periodontal risks associated with presence of M3s for A-M2s and highlighted which characteristics of M3s contributed to a higher prevalence of periodontal pathology of A-M2s. Considering the importance of M2s for masticatory function, clinicians need to examine the periodontal condition of A-M2s through clinical or radiographic assessment in regular oral examination, even in the absence of complaints about M3s and irrespective of the impaction status of M3s. The locations and impaction status of M3s should be taken into consideration to determine the best clinical decisions for individuals. It is worth noting that periodontal disease is always asymptomatic until the disease is severe[22], so it is difficult to find periodontal pathology in M3 regions in the early stages of periodontitis. A number of studies have confirmed that asymptomatic M3s are closely related to the periodontal pathology of A-M2s[13,17,30]. More importantly, even with mechanical debridement, it is difficult to reduce the periodontal pathology in M3

regions[4]. Several studies have verified that removal of M3s contributes to improving the periodontal status of A-M2s, regardless of I-M3s or N-M3s, but older age and preoperative deep periodontal pockets lead to an unfavourable prognosis[10,37,39,40].

Nevertheless, the early stages of the periodontal pathology of M2s were evaluated in the meta-analysis. Estimates of severe periodontal pathology are available in only a limited number of studies, making it difficult to provide a convincing clinical decision regarding M3s. The periodontal status of M2s is affected by not only the presence of M3s but also other systemic factors, such as the presence of periodontitis, smoking status and diabetes[22]. Considering the postoperative complications of M3 surgery, especially those involving chronic and irrecoverable symptoms such as paresthesia or temporomandibular joint disorder[41], removal of M3s should be conducted after comprehensive assessments, including of patients' age, general health and oral hygiene and willingness to undergo surgery. Only when the benefits of M3 surgery outweigh the risks to individuals is removal of M3s required.

The limitations of the meta-analysis were the small number of studies for data synthesis and the inconsistent definition of early periodontal defects. Some of the studies included in the meta-analysis involved patients with symptomatic M3s; thus, these participants did not effectively reflect the characteristics of the general population and resulted in a higher estimate. In studies using radiographic examination methods, it was difficult to randomly include samples because of ethical concerns, and selection bias may systematically increase the prevalence of periodontal defects; however, we tried to provide the best possible estimates of the prevalence of periodontal pathology of A-M2s through rigorous selection. Large-scale, population-based studies are needed to further demonstrate the adverse periodontal impact of M3s on A-M2s, and confounding factors at the patient level should be discussed. Furthermore, there is a critical need to determine which factors of N-M3s contribute to the periodontal pathology of A-M2s.

Conclusion

This systematic review and meta-analysis indicated that M3s are associated with early periodontal defects on distal sites of A-M2s in 19% of cases and associated with deep periodontal pockets around A-M2s in 52% of cases. In subgroup analyses, mandibular M3s and N-M3s showed a higher prevalence and were identified as risk factors for periodontal pathology of A-M2s. However, these results should be interpreted with caution because of high heterogeneity; thus, comprehensive assessments are imperative in M3 clinical decision making.

Acknowledgements

The authors would like to thank Dr Hari Petsos from Johann Wolfgang Goethe University, Germany, Dr Ahmet Altan from Gaziosmanpaşa University, Turkey, and Dr Martha Nunn from Creighton University School of Dentistry, USA, for providing more explicit data on their articles.

Conflicts of interest

The authors declare no conflicts of interest related to this study.

Author contribution

Dr Yang YANG acquired and interpreted the data and contributed to preparation of the manuscript; Drs Yi TIAN and Li Juan SUN contributed to the study design, data analysis and manuscript revision; Dr Hong Lei QU contributed to the study design.

(Received April 01, 2021; accepted Jun 23, 2021)

References

1. Carter K, Worthington S. Predictors of third molar impaction: A systematic review and meta-analysis. J Dent Res 2016;95:267–276.
2. Kruger E, Thomson WM, Konthasinghe P. Third molar outcomes from age 18 to 26: Findings from a population-based New Zealand longitudinal study. Oral Surg Oral Med Oral Pathol Oral Radiol Endod 2001;92:150–155.
3. Qu HL, Tian BM, Li K, Zhou LN, Li ZB, Chen FM. Effect of asymptomatic visible third molars on periodontal health of adjacent second molars: A cross-sectional study. J Oral Maxillofac Surg 2017;75:2048–2057.
4. Fisher EL, Blakey GH, Offenbacher S, Phillips C, White RP Jr. Mechanical debridement of subgingival biofilm in participants with asymptomatic third molars does not reduce deeper probing depths in the molar regions of the mouth. J Oral Maxillofac Surg 2013;71:467–474.
5. White RP Jr, Madianos PN, Offenbacher S, et al. Microbial complexes detected in the second/third molar region in patients with asymptomatic third molars. J Oral Maxillofac Surg 2002;60:1234–1240.
6. Mansfield JM, Campbell JH, Bhandari AR, Jesionowski AM, Vickerman MM. Molecular analysis of 16S rRNA genes identifies potentially periodontal pathogenic bacteria and archaea in the plaque of partially erupted third molars. J Oral Maxillofac Surg 2012;70:1507–1514.e1-6.
7. Blakey GH, Golden BA, White RP Jr, Offenbacher S, Phillips C, Haug RH. Changes over time in the periodontal status of young adults with no third molar periodontal pathology at enrollment. J Oral Maxillofac Surg 2009;67:2425–2430.

8. Ash MM, Costich ER, Hayward JR. A study of periodontal hazards of third molars. J Periodontol 1962;33:209–219.
9. Jung YH, Cho BH. Prevalence of missing and impacted third molars in adults aged 25 years and above. Imaging Sci Dent 2013;43: 219–225.
10. Sun LJ, Qu HL, Tian Y, Bi CS, Zhang SY, Chen FM. Impacts of non-impacted third molar removal on the periodontal condition of adjacent second molars. Oral Dis 2020;26:1010–1019.
11. Li ZB, Qu HL, Zhou LN, Tian BM, Chen FM. Influence of non-impacted third molars on pathologies of adjacent second molars: A retrospective study. J Periodontol 2017;88:450–456.
12. Kindler S, Holtfreter B, Koppe T, et al. Third molars and periodontal damage of second molars in the general population. J Clin Periodontol 2018;45:1365–1374.
13. Blakey GH, Marciani RD, Haug RH, et al. Periodontal pathology associated with asymptomatic third molars. J Oral Maxillofac Surg 2002;60:1227–1233.
14. Nunn ME, Fish MD, Garcia RI, et al. Retained asymptomatic third molars and risk for second molar pathology. J Dent Res 2013;92: 1095–1099.
15. Polat HB, Ozan F, Kara I, Ozdemir H, Ay S. Prevalence of commonly found pathoses associated with mandibular impacted third molars based on panoramic radiographs in Turkish population. Oral Surg Oral Med Oral Pathol Oral Radiol Endod 2008;105:e41–e47.
16. Chu FC, Li TK, Lui VK, Newsome PR, Chow RL, Cheung LK. Prevalence of impacted teeth and associated pathologies--A radiographic study of the Hong Kong Chinese population. Hong Kong Med J 2003;9:158–163.
17. Petsos H, Korte J, Eickholz P, Hoffmann T, Borchard R. Surgical removal of third molars and periodontal tissues of adjacent second molars. J Clin Periodontol 2016;43:453–460.
18. Petsos H, Korte J, Eickholz P, Hoffmann T, Borchard R. Effect of the surgeon's dominant hand on postoperative periodontal status of adjacent molars after removal of lower third molars. J Oral Maxillofac Surg 2019;77:912–919.
19. Altan A, Akbulut N. Does the angulation of an impacted mandibular third molar affect the prevalence of preoperative pathoses? J Dent (Shiraz) 2019;20:48–52.
20. Nivedita S, John ER, Acharya S, D'costa VG. Prophylactic extraction of non-impacted third molars: Is it necessary? Minerva Stomatol 2019;68:297–302.
21. Herzog R, Álvarez-Pasquin MJ, Díaz C, Del Barrio JL, Estrada JM, Gil Á. Are healthcare workers' intentions to vaccinate related to their knowledge, beliefs and attitudes? A systematic review. BMC Public Health 2013;13:154.
22. Pihlstrom BL, Michalowicz BS, Johnson NW. Periodontal diseases. Lancet 2005;366:1809–1820.
23. Page RC, Eke PI. Case definitions for use in population-based surveillance of periodontitis. J Periodontol 2007;78:1387–1399.
24. Haffajee AD, Socransky SS, Goodson JM, Lindhe J. Intraclass correlations of periodontal measurements. J Clin Periodontol 1985;12: 216–224.
25. Schei O, Waerhaug J, Lovdal A, Arno A. Alveolar bone loss as related to oral hygiene and age. J Periodontol 1959;30:7–16.
26. Akarslan ZZ, Kocabay C. Assessment of the associated symptoms, pathologies, positions and angulations of bilateral occurring mandibular third molars: Is there any similarity? Oral Surg Oral Med Oral Pathol Oral Radiol Endod 2009;108:e26–e32.
27. Gupta P, Naik SR, Ashok L, Khaitan T, Shukla AK. Prevalence of periodontitis and caries on the distal aspect of mandibular second molar adjacent to impacted mandibular third molar: A guide for oral health promotion. J Family Med Prim Care 2020;9:2370–2374.
28. Kim JY, Jee HG, Song HC, Kim SJ, Kim MR. Clinical and pathologic features related to the impacted third molars in patients of different ages: A retrospective study in the Korean population. J Dent Sci 2017;12:354–359.
29. Kugelberg CF, Ahlström U, Ericson S, Hugoson A. Periodontal healing after impacted lower third molar surgery. A retrospective study. Int J Oral Surg 1985;14:29–40.
30. Li ZB, Qu HL, Zhou LN, Tian BM, Gao LN, Chen FM. Nonimpacted third molars affect the periodontal status of adjacent teeth: A cross-sectional study. J Oral Maxillofac Surg 2017;75:1344–1350.
31. Prabhakar P, Bhuvaneshwarri J, Paddmanabhan P. Evaluation of the Impact of Impacted Mandibular Third Molars on Surrounding Structures: A Clinical and Radiographic Analysis in Students of Tagore Dental College and Hospital. Biomed Pharmacol J 2015;8SE: 241–243.
32. Sejfija Z, Koçani F, Macan D. Prevalence of pathologies associated with impacted third molars in Kosovar population: An orthopantomography study. Acta Stomatol Croat 2019;53:72–81.
33. Stanley HR, Alattar M, Collett WK, Stringfellow HR Jr, Spiegel EH. Pathological sequelae of "neglected" impacted third molars. J Oral Pathol 1988;17:113–117.
34. Hill CM. Removal of asymptomatic third molars: An opposing view. J Oral Maxillofac Surg 2006;64:1816–1820.
35. Dodson TB. The management of the asymptomatic, disease-free wisdom tooth: Removal versus retention. Atlas Oral Maxillofac Surg Clin North Am 2012;20:169–176.
36. Ventä I. How often do asymptomatic, disease-free third molars need to be removed? J Oral Maxillofac Surg 2012;70(9 suppl 1):S41–S47.
37. Petsos H, Fleige J, Korte J, Eickholz P, Hofmann T, Borchard R. Five-years periodontal outcomes of early removal of unerupted third molars referred for orthodontic purposes. J Oral Maxillofac Surg 2021;79:520–531.
38. White RP Jr, Offenbacher S, Phillips C, Haug RH, Blakey GH, Marciani RD. Inflammatory mediators and periodontitis in patients with asymptomatic third molars. J Oral Maxillofac Surg 2002;60: 1241–1245.
39. Passarelli PC, Lajolo C, Pasquantonio G, et al. Influence of mandibular third molar surgical extraction on the periodontal status of adjacent second molars. J Periodontol 2019;90:847–855.
40. Tian Y, Sun L, Qu H, Yang Y, Chen F. Removal of nonimpacted third molars alters the periodontal condition of their neighbors clinically, immunologically, and microbiologically. Int J Oral Sci 2021;13:5.
41. Huang GJ, Cunha-Cruz J, Rothen M, et al. A prospective study of clinical outcomes related to third molar removal or retention. Am J Public Health 2014;104:728–34.

COMPREHSENSIVE GUIDE TO GBR

NEW

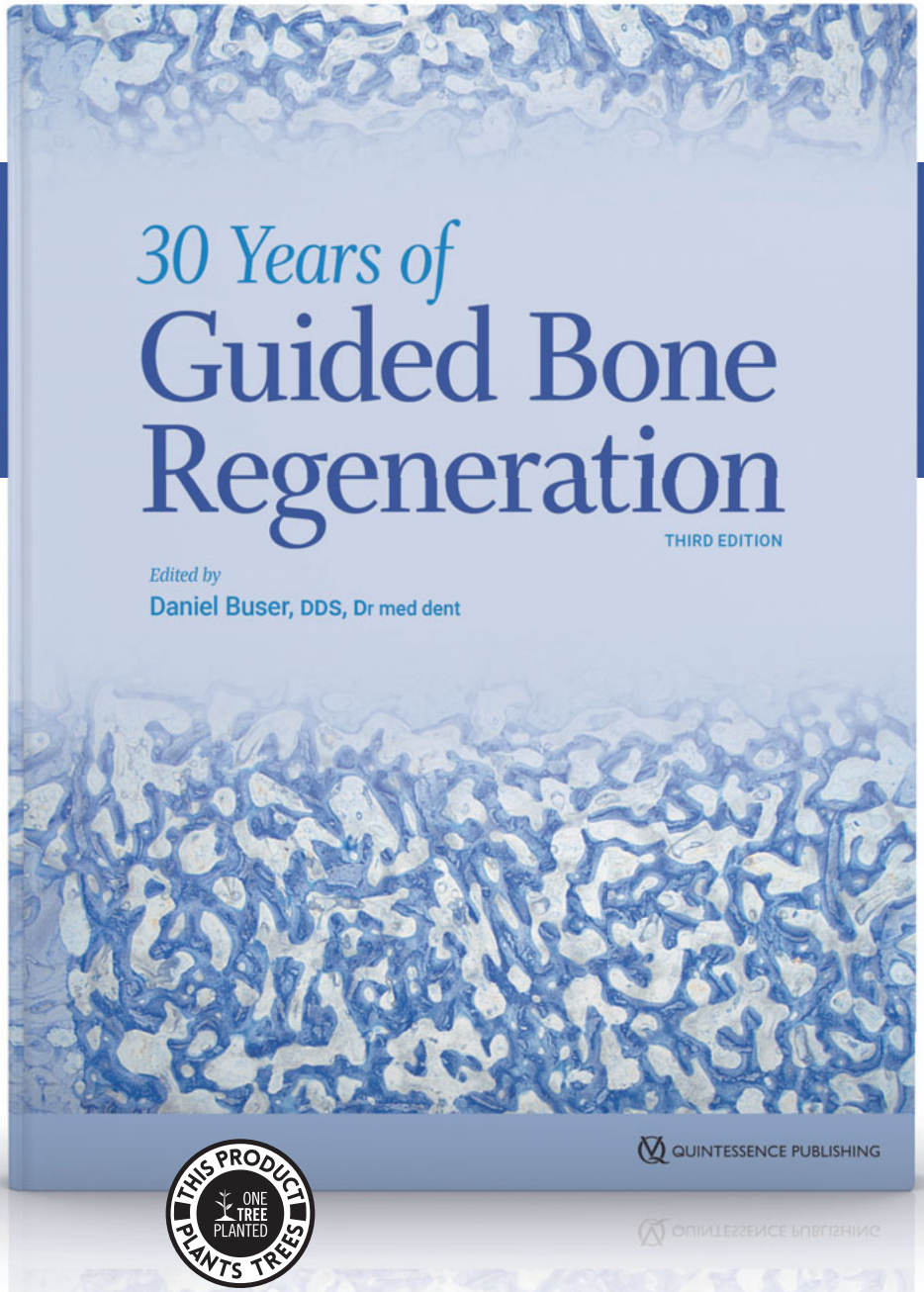

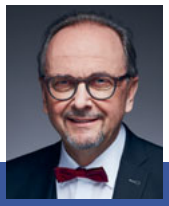

Daniel Buser

30 Years of Guided Bone Regeneration

3rd Edition, 344 pages, 1,040 illus.
ISBN 978-0-86715-803-8
€148

With each passing decade, more research is done on GBR, and more surgeons begin adopting this practice with incredible results. In this new edition, Prof Buser has assembled a team of the top names in implant surgery to put together a comprehensive guide on the materials, indications, techniques, timing, and results of GBR. The book begins with the science of bone regeneration before delving into the different methods and uses of GBR based on the presenting scenario. Case examples are presented with photos and radiographs documenting each patient's bone regeneration from start to finish. This book offers solutions for those who want to begin providing implants to a wider range of patients, for GBR veterans who want to refine their skills and practice more advanced techniques, and for implant surgeons who want to keep up to date with the most current research and technology in GBR.

www.quint.link/GBR
books@quintessenz.de
+49 (0)30 761 80 667

QUINTESSENCE PUBLISHING

Near Infrared Laser Photobiomodulation of Periodontal Ligament Stem Cells

Mohammd Ayyoub RIGI-LADEZ[1], Seyedeh Sareh HENDI[2], Alireza MIRZAEI[3], Leila GHOLAMI[4], Reza FEKRAZAD[5,6]

Objective: *To determine the effect of different energy densities of near infrared diode lasers with wavelengths of 810 or 940 nm on the proliferation and survival of periodontal ligament derived stem cells (PDLSCs).*

Methods: *After isolation and characterisation, PDLSCs were cultured in clear 96-well plates. Each well was irradiated by either 810 nm (L1) or 940 nm (L2) lasers, with energy densities of 0.5, 1.5 and 2.5 J/cm^2 and an output power of 100 mW. A non-irradiated well was used as a control. Cellular viability was measured 24 hours after irradiation using 3-(4,5-dimethylthiazol-2-yl)-2,5-diphenyl-2H-tetrazolium bromide (MTT) assay and proliferation was measured 24, 48 and 72 hours after irradiation using trypan blue staining and counting. Propidium iodide (PI) staining was used to identify any pyknotic nuclei or nuclear fragmentation 72 hours after irradiation*

Results: *An increase in viability was observed only in the group with the 940 nm laser irradiation at energy density of 2.5 J/cm^2 ($P < 0.001$). The proliferation of cells was significantly increased in the group with 940 nm laser irradiation at energy density of 2.5 J/cm^2 at all the time points examined in comparison to other groups ($P < 0.001$). PI staining showed no change in cell nuclei in any of the groups.*

Conclusion: *Irradiation of PDLSCs with a 940 nm laser at an energy density of 2.5 J/cm^2 could promote efficient cell proliferation.*

Key words: *periodontal ligament, photobiomodulation, stem cells*

Chin J Dent Res 2022;25(1):57–65; doi: 10.3290/j.cjdr.b2752657

1 Oral and Dental Research Centre, Department of Periodontology, Faculty of Dentistry, Zahedan University of Medical Sciences, Zahedan, Iran.
2 Department of Endodontics, Hamadan University of Medical Sciences, Hamadan, Iran.
3 Department of Laser in Dentistry, School of Dentistry, Islamic Azad University, Tehran, Iran.
4 Department of Periodontics, Dental Research Centre, Hamadan University of Medical Sciences, Hamadan, Iran.
5 Radiation Sciences Research Centre, Laser Research Centre in Medical Sciences, AJA University of Medical Sciences, Tehran, Iran.
6 International Network for Photo Medicine and Photo Dynamic Therapy (INPMPDT), Universal Scientific Education and Research Network (USERN), Tehran, Iran.

Corresponding author: Dr Leila GHOLAMI, Department of Periodontics, School of Dentistry, Hamadan University of Medical Sciences, Shahid Fahmideh Blvd Hamadan, Iran. Tel: +98 08138381062; Fax: 98-08138381085. Email: l.gholami@hotmail.com

This study was financially supported by Zahedan University of Medical Sciences (grant number 7348).

Treatment and control of the inflammatory process and regeneration of lost periodontal supporting structures, especially in severe cases, are among the challenges facing periodontists. Different surgical and nonsurgical methods have been proposed for periodontal regeneration, with varying success rates[1,2]. New regenerative therapies and tissue engineering methods to improve the clinical outcome using stem cells in regenerative tissue engineering of the periodontium have attracted attention in recent years[3,4].

The presence of stem cells in dental and periodontal tissues has created a new approach to repairing dental and periodontal defects[3,5]. In this approach, the differentiation capacity of these cells in oral lesions can be exploited by isolating and replicating them and transferring them to the lesion site. Periodontal ligament (PDL) derived stem cells (PDLSCs) have been reported to have osteogenesis, angiogenesis and cementogenesis properties and have also been shown

to successfully regenerate PDLs[4,6,7]. They also appear to have a better regenerative capability of differentiating into periodontal tissues compared with dental pulp stem cells (DPSCs) and periapical follicle stem cells (PAFSCs) and are considered the best candidates for stem cell–based regenerative treatments in periodontology[4]. These cells have appropriate tissue acceptance and have recorded effective results in the treatment of periodontal defects in in vitro and in vivo studies[4,8-11].

Laser technology has drawn a great deal of attention and found many applications in various areas of dentistry in recent years[12]. Low level laser (light) therapy (LLLT) employs visible (generally red) or near-infrared (NIR) light generated from a laser or light emitting diode (LED) system with low power and energy densities. This kind of irradiation with its non-thermal and non-invasive nature has been shown to be effective in treating diverse injuries or pathological conditions in medicine[13]. The process is now better known as photobiomodulation (PBM) and is characterised by the ability to induce photobiological responses at cellular levels[14].

The mechanism of PBM at the cellular level has been attributed to the absorption of monochromatic visible and NIR radiation by photoreceptors, most importantly the components of the cellular respiratory chain and changes in cellular adenosine triphosphate (ATP) levels[15,16].

Laser has been previously used in periodontology for its antibacterial and anti-inflammatory effects in the treatment of periodontal and peri-implant diseases[17-20]. PBM has also been found to be able to modulate the immune response and reduce chronic inflammation[19,21-23], and can therefore potentially facilitate periodontal tissue repair.

At a cellular level, several studies have shown the effects of phototherapy on different cells, indicating that PBM improves the proliferation of cells without causing cytotoxic effects[24-26]. Irradiation conditions and parameters such as wavelength, power and energy densities and even the tissue being irradiated can influence the clinical outcomes of PBM[13,27,28].

According to recent systematic reviews, great heterogeneity can be observed in the methods and parameters of light irradiation, and only a few studies on infrared irradiation and PDLSCs are available[29-31]. Further research is still needed to identify the optimal characteristics of the PBM setting on these cells as a basis for future translation of use of this wavelength into clinical practice[24].

In a study on this cell line, Wu et al[32] showed that low-power 660 nm, 70 mW red laser can enhance the proliferation and osteogenic differentiation of human PDL cells via cyclic AMP (cAMP) regulation. Soares et al[33] also studied the effect of 660 nm, 30 mW laser irradiation on the proliferation rate of human PDLSCs (hPDLSCs) and the cells were irradiated at 0 and 48 hours using two different energy densities (0.5 J/cm², 1.0 J/cm²). They found that PBM using 660 nm light and an energy density of 1.0 J/cm² has a positive stimulatory effect on the proliferation of hPDLSCs[32,33]. Yamauchi et al[34] also evaluated the effects of a high-power, red LED light device with a wavelength of 650 nm at a power density of 1100 mW/cm^2 and a total irradiance of 200 mW/cm^2 on hPDLSCs. They tested energy densities ranging from 0 to 10 J/cm^2 to determine the optimal dose and observed a significant increase in PDLSC proliferation and osteogenic differentiation through the activation of ERK1/2 with 8 J/cm^2[34].

Since previous studies have mostly focused on the red wavelength and considering the good penetration depth of infrared light in periodontal tissues, in the present study, we sought to evaluate the effect of two NIR diode lasers with wavelengths of 810 and 940 nm which are more routinely used in dental practice. The effect of different energy densities (fluence) on the proliferation and survival of PDLSCs was evaluated. The present study seeks to add to the existing evidence and prove useful in future cell-based regenerative periodontal therapies.

Materials and methods

Cell isolation and culture

The remaining PDL tissue was scraped from the middle third of the root surface of two fully erupted third molars extracted for orthodontic reasons in one patient. The obtained periodontal tissue was cultured in a microplate containing Dulbecco's Modified Eagle Medium (DMEM, Gibco, Waltham, MA, USA) and 15% foetal bovine serum (FBS, Gibco), then enzymatically digested for 1 hour at 37°C in a solution of 3 mg⁄ml collagenase type I (Sigma-Aldrich, St Louis, MO, USA) and 4 mg/ml dispase (Gibco).

Characterisation of PDL derived mesenchymal stem cells

The mesenchymal nature of cells was confirmed by evaluating surface markers of CD90, CD105 and CD45 using the flow cytometric method[35]. Positive CD90 and CD105 mesenchymal markers and a negative result for CD45, which is a haematopoietic marker, indicated that

Table 1 Laser irradiation parameters.

Parameter (unit)	Value	
Centre wavelength (nm)	L1: 810	L2: 940
Operating mode	Continuous wave	Continuous wave
Radiant power (mW)	100	100
Beam spot size diameter (cm)	0.8	0.8
Beam spot size at target (cm^2)	0.5	0.5
Irradiance at target (mW/cm^2)	200	200
Energy density((J/cm^2)	0.5, 1.5, 2.5	0.5, 1.5, 2.5
Exposure duration (s)	3, 8, 13	3, 8, 13

the separated cells were mesenchymal cells. After the third cell passage, the cells were detached from the base of the plates by adding trypsin. The cell suspension was counted and 10^5-10^6 cells were added to each vial. The vials were then filled with 1 ml of phosphate buffer solution-bovine saline albumin (PBS-BSA) 3% solution (Sigma-Aldrich) and the suspension was centrifuged at 2000 rpm for 5 minutes. For each marker, a test and control isotype vial were used. Antibodies (Abcam, Cambridge, MA, USA) were added; accordingly, CD45 with a concentration of 1:200 was incubated (Binder, Tuttlingen, Germany) for 30 minutes at room temperature, and CD90 and CD105 markers with a concentration of 1:50 were incubated for 45 minutes at 37°C. The Rabbit isotype control was incubated for 30 minutes at a concentration of 1:200 at room temperature, then PBS was added to each sample to reach a volume of 1 ml. The suspensions were then centrifuged at 2000 rpm for 5 minutes (Hettich, Tuttlingen, Germany). The secondary antibody was added with a concentration of 1:4 and incubated for 45 minutes at 37°C. A volume of 1 ml was then reached by adding PBS and centrifuged once more at 2000 rpm for 5 minutes. The cells were washed again with PBS and centrifuged. At the last stage, the cell sedimentation was turned into a suspension with 4% paraformaldehyde and stored at 2°C to 8°C until it was read under the flow cytometer (Becton Dickinson, Franklin Lakes, NJ, USA).

The differentiation ability of the isolated cells was also evaluated. For this purpose, the cells were cultured in osteogenic medium of DMEM containing 10% FBS (Gibco) and 100 nM dexamethasone, 10 mM beta-glycerol-phosphate and 50 µg/ml ascorbic acid (all Sigma Aldrich) and adipogenetic differentiation medium containing DMEM with 10% FBS (Gibco, Paisley, UK), 66 nM insulin, 0.2 mM indomethacin, 100 nM dexamethasone (all Sigma Aldrich) and 0.5 mM IBMX (Pepro Tech, Rocky Hill, NJ, USA) for 21 days. After this time, staining with Alizarin red and Oil red (Sigma Aldrich) showed their successful osteogenic and adipogenetic differentiation.

Photobiomodulation therapy

The laser probe was adjusted perpendicular to each plate and the cells were irradiated from underneath each well to completely cover the area of a single well with a diameter of 8 mm. The third passage cells were cultured in clear 96-well micro titre plates at a density of 5×10^3 cells. There was one empty well between the seeded wells to prevent unintentional dispersion of light between wells during irradiation. Three energy densities, namely 0.5, 1.5 and 2.5 J/cm^2, were applied using two different laser devices of 810 nm (Picasso, AMD Lasers, West Jordan, UT, USA) as L1, and 940 nm (Epic 10, Biolase, CA, USA) as L2, with 400-micron tips and a continuous wave output power of 100 mW. The wells were irradiated from a distance of 15 mm for 2.5, 7.5 and 12.5 seconds, respectively (Table 1). The output power was 100 mW and checked with a power meter (Ophir Nova II, Ophir Optronics Solutions, Jerusalem, Israel) before irradiation. A continuous wave mode was used and a single session of laser irradiation was performed. The laser groups were compared with a control group without any laser irradiation. All tests were performed in triplicate and repeated twice.

Viability assessment

The 5×10^3 cells were placed into 96-well plates and grown for 24 hours, then the extracts were added to cell cultures. MTT colorimetric assay using 3-(4,5-dimethylthiazol-2-yl)-2,5-diphenyl tetrazolium bromide (Sigma Aldrich) was used to evaluate cell viability, then 24 hours after laser irradiation, 10 ml MTT, 90% αMEM and 15% FBS were added to cells and incubated for 3 hours. At this time, formazan crystals could be seen under an inverted microscope. Viable cells with a normal functional mitochondrial enzyme of succinate dehydrogenase changed water-soluble MTT dye to insoluble

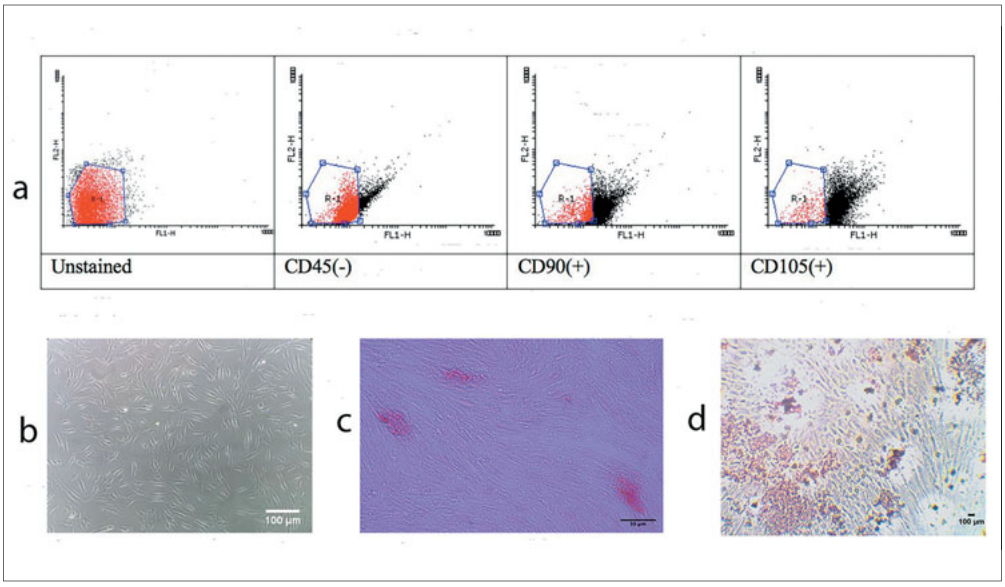

Fig 1 **(a)** Distribution of expression of CD45, CD90 and CD105 biomarkers. The black dots indicate the intensity of expression of the biomarkers and the red dots indicate the severity of the lack of biomarkers on the surface of the cells isolated from the periodontal ligament. **(b)** PDLSC with a spindle-shaped appearance. **(c)** Optical microscope photographs showing mineral deposition 21 days after culture in osteogenic medium and Alizarin red staining. **(d)** Oil red staining showing adipogenic differentiation of cells after 21 days.

purple formazan. After completion of incubation, the supernatant was removed and 100 ml dimethyl sulfide was pipetted to dissolve the crystals. An ELx808 microplate reader (BioTek, Bad Friedrichshall, Germany) was used to measure absorbance at 540 to 690 nm. The results were reported as percentages.

Proliferation rate assessment

To evaluate cell proliferation, cultured cells were stained with trypan blue 24, 48 and 72 hours after irradiation. They were counted using a neubauer chamber and their proportion to cell numbers at baseline were reported.

Effect of laser irradiation on cell nuclei

Cells were stained with propidium iodide (PI) to identify any pyknotic nuclei and nuclear fragmentation 72 hours after irradiation under a phase contrast microscope (BX51, Olympus, Tokyo, Japan).

Ethical considerations

The project was approved by the university's ethics committee (IR. ZUMS.94.5.11-7346). The teeth used for isolation of the cells were indicated to be removed for orthodontic reasons. The patient was informed about the study and signed an informed consent.

Statistical analysis

Data were analysed using a Student *t* test and three-way analysis of variance (ANOVA) with a Tukey post-hoc test and values were expressed as mean ± standard deviation (SD)/standard error (SE). All statistical analyses were performed at a significance level of 0.05 using R software, version 3.3.3 (R Core Team, Vienna, Austria) and SPSS version 16 (SPSS Statistics, IBM, Chicago, IL, USA).

Results

Characterisation of PDLSCs

The dot plot in Fig 1a displays the mesenchymal stem cell identifier markers. CD45 was at a minimum and negative and CD90, CD105 were positive, indicating the mesenchymal nature of isolated cells. PDLSCs were also differentiated into osteoblasts forming mineralised tissue after 21 days of culture in osteogenic medium and adipose tissue differentiation was also observed after 21 days by Oil red staining (Figs 1b and c).

PDLSC viability

A three-way ANOVA was used to compare the effects of laser, energy density and time on the MTT viability results based on percentages compared to controls.

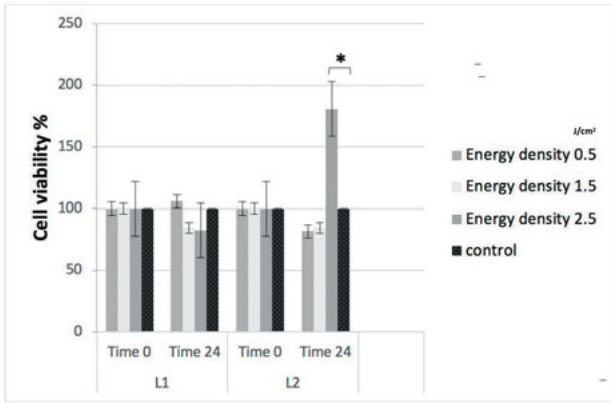

Fig 2 Effects of L1 810-nm and L2 940-nm laser irradiation on cell viability based on MTT assay after normalising to the control group.

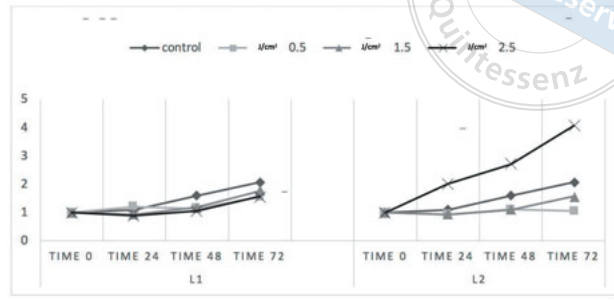

Fig 3 Effect of laser stimulation on PDLSC proliferation after 24, 48 and 72 hours based on trypan blue counting.

Table 2 Mean ± SD of proliferation in terms of time, energy density and type of laser.

		Control	L1			L2		
Energy density (J/cm^2)			0.5	2.5	1.5	0.5	1.5	2.5
Time point	T0	1.00 ± 0.00	1.00 ± 0.00	1.00 ± 0.00	1.00 ± 0.00	1.00 ± 0.00	1.00 ± 0.00	1.00 ± 0.00
	T24	2.02 ± 0.18	0.93 ± 0.06	0.92 ± 0.14	0.90 ± 0.06	0.93 ± 0.06	1.20 ± 0.14	1.09 ± 0.08
	T48	2.71 ± 0.34	1.09 ± 0.38	1.12 ± 0.17	1.05 ± 0.09	1.19 ± 0.15	1.14 ± 0.17	1.59 ± 0.24
	T72	4.07 ± 0.27	1.57 ± 0.18	1.05 ± 0.08	1.57 ± 0.06	1.76 ± 0.10	1.55 ± 0.09	2.08 ± 0.04

The results showed that laser and energy density affect survival rate ($P < 0.05$), and that the effect of laser is dependent on time and energy density ($P < 0.05$). After 24 hours, an increase in cellular viability was observed only with the 940 nm laser with an energy density of 2.5 J/cm^2. This increase was statistically significant compared to the other settings of L2 and L1 and the control group ($P < 0.001$). None of the other comparisons between different energy densities of the L1 group were significant at the 0.05 level (Fig 2).

PLDSC proliferation

The mean ± SD of proliferation in terms of time, density and lasers are shown in Table 2. The highest mean proliferation was seen in the L2 group and the energy density of 2.5 J/cm^2 (Fig 3).

The comparison of proliferation between different energy densities in the L1 group did not show any statistically significant results. In the L2 group, the energy density of 2.5 J/cm^2 showed higher proliferation, with statistically significant differences at 24, 48 and 72 hours compared to the other energy densities in this group ($P < 0.001$).

L2-0.5 and L2-1.5 showed a statistically significant increase at 72 hours ($P < 0.001$) but were still lower compared to the control group. When comparing proliferation in the same energy densities between the L1 and L2 group, the L2-2.5 J/cm^2 group also had statistically significant superior proliferative results compared to the L1-2.5 J/cm^2 group at all time points ($P < 0.001$). The 1.5 J/cm^2 energy density groups showed no statistically significant difference at any of the time points. The results of the comparison of the 0.5 J/cm^2 L1 and L2 groups showed a statistically significant difference only after 72 hours, when the L1 group had higher proliferative results (1.05 versus 1.55 folds compared to baseline [T0]), which were both lower compared to the amounts of cell proliferation in the control group (Table 2).

Effect of laser irradiation on cell nuclei

PI-stained cells were carefully evaluated. No pyknotic nuclei or nuclear fragmentation was observed in any of the groups (Fig 4).

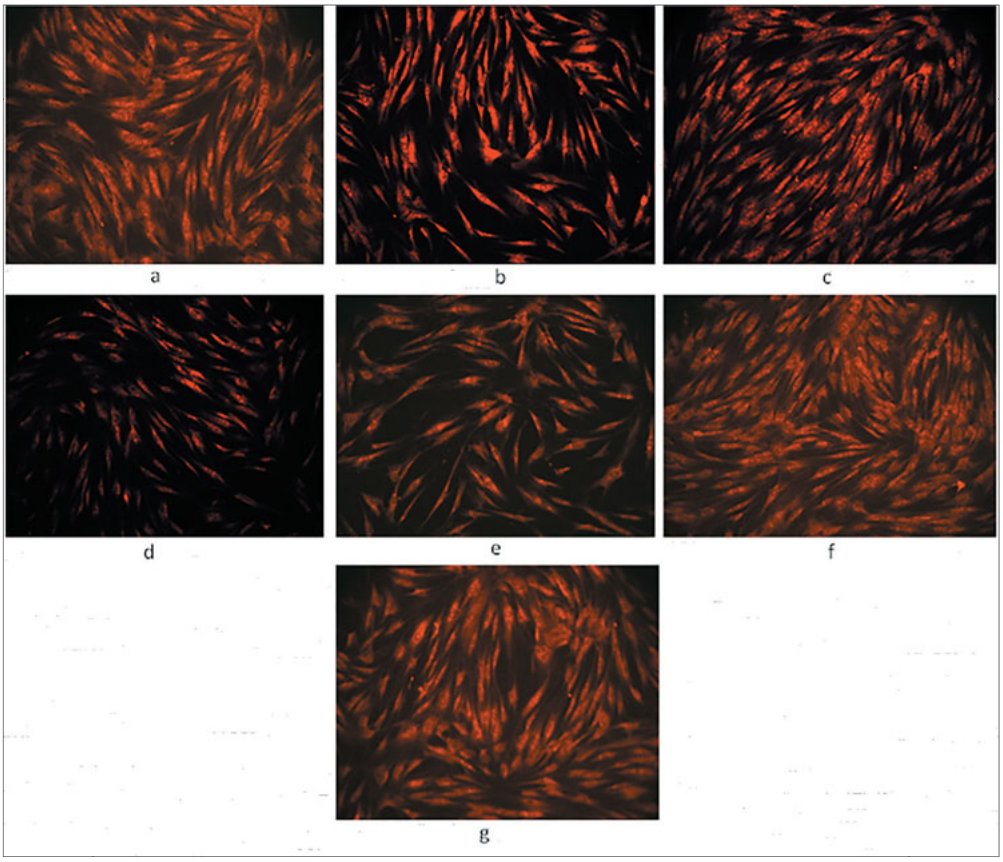

Fig 4 PI-stained cells from the different irradiation groups and nonirradiated control group observed under a phase contrast microscope. No pyknotic nuclei or nuclear fragmentation were observed. **(a)** 810 nm, 0.5 J/cm^2; **(b)** 810 nm, 1.5 J/cm^2; **(c)** 810 nm, 2.5 J/cm^2; **(d)** 940 nm, 0.5 J/cm^2; **(e)** 940 nm, 1.5 J/cm^2; **(f)** 940 nm, 2.5 J/cm^2; **(g)** Control (100x magnification).

Discussion

In the present study, the effect of different energy densities of two common NIR laser wavelengths in dentistry on the viability and proliferation of PDLSCs were comparatively evaluated. These wavelengths have a favourable penetration depth and the potential to be used as adjunctive tools in clinical practice. These wavelengths are much less studied and further investigation is needed to find an optimal setting for stimulating these cells using them.

According to our results, 940 nm laser with an energy density of 2.5 J/cm^2 (100 mW, CW) showed a better result compared to the control group, 810 nm laser with a 0.5 J/cm^2 setting also showed better results compared to its 1.5 and 2.5 J/cm^2 settings on PDLSC viability and proliferation. The results clearly demonstrate the sensitivity and importance of laser settings and wavelength. To our knowledge, this study is the first to compare diode lasers with these NIRs wavelengths on PDLSCs. Wavelengths in the 600 to 700 nm range are most often chosen to treat superficial tissue, and NIR is chosen for deeper seated tissues due to the longer optical penetration distances through tissue[14].

The most important law in photobiology is that photons of different wavelengths are absorbed by specific chromophores located inside cells or tissues. Lasers of 810 and 940 nm are well absorbed in tissue chromophores of haemoglobin and melanin. At a cellular level, Cytochrome C oxidase (CCO) has one absorption band in the red wavelength region around 660 nm and another in the NIR spectrum around 800 nm. The absorption bands of CCO are weaker for wavelengths greater than 900 nm. Other alternative chromophores such as water and ion channels have also been identified or proposed for these wavelengths and need to be elucidated further[14, 27].

In vitro studies on PBM have shown that the effect of lasers on cells is variable as it is dependent on many parameters[14,36]. The existence of a different 'window specificity' for every wavelength and energy dosage was postulated by Karu et al[37] in 1990. The results can be influenced by not only the wavelength but also the total dose of irradiation, application mode (pulsed or continuous), irradiation time and number and frequency of laser therapy sessions[13,27,28]. Since studies on PBM

do not have uniform methodological designs, it is complicated to compare the results with other wavelengths used in previous studies.

To our knowledge, only a few studies have been conducted into the 940 nm laser wavelength and its effect on proliferation and differentiation of mesenchymal stem cells. Jawad et al[38] studied the effect of different powers of 100, 200 and 300 mW with continuous wave mode of 940 nm diode LLLT on a human foetal osteoblast cell line cultured in 96-well plates and uniformly irradiated them for 3 and 6 minutes for a period of up to 7 days. The energy densities applied were much greater compared to the current study. The group exposed to 100 mW received 22.92 or 45.85 J/cm^2; the second group that was exposed to 200 mW received 45.85 or 91.79 J/cm^2; and the third group of 300 mW exposure received 68.78 or 137.57 J/cm^2 of energy. A significant increase in proliferation after 7 days was observed in all groups; however, at similar evaluation time points to those in the present study (1 and 3 days), no significant improvement in proliferation results was reported except for the group irradiated at 100 mW for 6 minutes which had the same output power as the one used in the present report. The researchers concluded that 300-mW irradiation significantly increased the amount of cell proliferation. By contrast, the 100 and 200 mW groups showed significantly better results only in cell differentiation[38].

The use of the lower laser powers and longer exposure time of LLLT was considered better than the higher power settings in improving osteogenic differentiation. Longer exposure times and repetition of irradiation might have also improved the effects observed with lower energy densities used in the present study.

A stimulatory effect of 940 nm laser was also reported in an animal study that investigated the radioprotective features of 940 nm laser on the lifespan and absolute counts of blood cells of gamma-irradiated mice[39]. Energy densities of 3, 12 or 18 J/cm^2 were tested at a fluence of 3 J/cm^2 and demonstrated interesting radioprotective features[39]. This setting significantly prolonged the lifespan of gamma-irradiated mice and the white blood cell, lymphocyte and neutrophil counts were higher in this group on day 12 after gamma irradiation[39]. The effective energy density recorded was quite similar to the results observed in the present study[39].

Only a few studies have been conducted into laser phototherapy of PDLSCs, and the previous studies were conducted using wavelengths different to those employed in the current study. As mentioned, Soares et al[33] studied the effect of laser therapy on PDLSCs with two sessions of 660 nm diode laser treatment in 48 hours at energy densities of 0.5 and 1.0 J/cm^2 for 16 and 33 seconds, respectively, and found that 1.0 J/cm^2 radiation recorded better results in terms of cell survival and proliferation compared to the 0.5 J/cm^2 laser and control groups at 48 and 72 hours[33]. In another study, Wu et al[32] provided PDLSCs with laser radiation from a 660-nm diode with energy densities of 1, 2 and 4 J/cm^2 for 66, 132 and 264 seconds, respectively, and evaluated them on days 1, 3 and 5, respectively. Irradiation of 2 J/cm^2 resulted in a significant increase in cell proliferation on days 3 and 5, and only two energy densities (2 and 4 J/cm^2) led to increased osteogenic differentiation of this group of cells[32]. These results demonstrate cell proliferation effects that are generally consistent with the findings of the present study, where a positive effect of a single session of laser irradiation was observed. Repetition of this single session of irradiation could result in an accumulative effect of laser energy and be useful in future in vivo studies.

In a recent study, Paschalidou et al[40] studied the effect of a similar single session of 940 nm laser irradiation with a 200-mW continuous mode on stem cells from the dental pulp of deciduous teeth (SHED) at energy fluences of 4, 8 and 16 J/cm^2. Their results indicated a statistically significant increase in proliferation based on MTT results after 48 and 72 hours in all energy densities of this wavelength; however, 8 J/cm^2 did not show a statistically significant increase at 24 hours and reported the lowest MTT results compared to the other two settings[40]. On the other hand, 8 J/cm^2 had the best effects on osteogenesis gene expression and biomineralisation[40]. This clearly shows how sensitive the results of PBM therapy can be and that even the same energy densities and laser parameters may influence proliferation and differentiation of cells in a different manner which needs to be investigated more thoroughly.

According to the results of the present study, the 810-nm laser with the energy densities and parameters used did not have a statistically significant positive effect on cell proliferation. Some studies have reported controversial findings regarding the effect of this wavelength on stem cells. Soleimani et al[41] evaluated 810-nm diode laser radiation on the proliferation of bone marrow mesenchymal stem cells and differentiated them into neuronal and bone cells. Radiation of 2, 3, 4 and 6 J/cm^2 was performed for 12, 18, 24 and 36 seconds respectively for three sessions at 1, 3 and 5 days after incubation, and MTT analysis for cell viability was performed on day 7[41]. The results showed that all of the above energies except 6 J/cm^2 resulted in a significant increase in cell viability[41]. Kreisler et al[42] also evalu-

ated the effect of low-level diode laser irradiation on human PDL fibroblasts with an 809-nm laser and three fluences of 1.96, 3.92 and 7.84 J/cm^2 were applied for 75, 150 and 300 seconds, respectively. The effect of one, two and three laser irradiation sessions at 24-hour intervals on cell proliferation was evaluated using Alamar Blue assay 24, 48 and 72 hours after irradiation, reported in relative fluorescence units (RFUs)[42]. Unlike in the present study, these researchers observed that at each energy level, these cells had a higher rate of proliferation than the non-irradiated cells for up to 72 hours[42]. When the laser treatments were repeated 24 and 48 hours after the first irradiation, the RFU values at days 1 and 2 were considerably higher, which the authors suggest may have been due to the repeated laser treatment or the longer incubation time prior to the first measurement[42]. We might have also recorded a better outcome with successive treatment sessions.

Wang et al[27] recently compared the laser irradiation of 810- and 980-nm diodes with adipose-derived stem cells. They found that the mechanisms of action of 810- and 980-nm lasers appear to have significant differences: 980 nm seems to rely on the activation of heat or light gated ion channels, whereas activation of CCO in mitochondria by 810 nm continues to be the most accepted mechanism[27]. The 980-nm laser with energy densities as low as 0.3 J/cm^2 resulted in ATP levels 40% higher than the control group but the 810-nm laser needed higher energy densities, with 3.0 J/cm^2 reporting the best results (20% higher than the control group)[27].

Based on this study and the present results, it seems that energy densities higher than those used in the present report are probably necessary to have biostimulatory effects with the 810-nm laser, and the effect of higher energy densities needs to be evaluated further in future studies. The differences in the results of the aforementioned studies and the present study and the difference observed between the two studied wavelengths are due to differences in irradiation conditions and characteristics of each wavelength that can influence the responses being measured. It must be noted that cell-based in vitro studies are highly technique sensitive. Further investigations are needed to elucidate the effect of different irradiation settings of these wavelengths on PDLSCs and the underlying molecular mechanisms. The differentiation of irradiated cells also needs to be investigated in future studies. Moreover, further clinical studies are needed for correct translation into clinical practice since it appears PBM can be considered an important future adjunctive tool in regenerative periodontal therapy and tissue engineering involving stem cells.

Conclusion

Based on the results of the present study, a 940-nm diode laser with an energy density of 2.5 J/cm^2 recorded better results compared to the same dose of 810-nm laser and controls and increased the viability and proliferation of PDLSCs.

Conflicts of interest

The authors declare no conflicts of interest related to this study.

Author contribution

Dr Mohammd Ayyoub RIGI-LADEZ contributed to the study design, data preparation and funding acquisition; Dr Seyedeh Sareh HENDI performed the data analysis and prepared the draft of the manuscript; Drs Alireza MIRZAEI and Reza FEKRAZAD contributed to the study design, supervision and editing of the final manuscript; Dr Leila GHOLAMI contributed to the study design and conducting of the study, data analysis and final revision.

(Received Oct 19, 2020; accepted Nov 20, 2021)

References

1. Genco RJ, Borgnakke WS. Risk factors for periodontal disease. Periodontol 2000 2013;62:59–94.
2. Heitz-Mayfield LJ, Lang NP. Surgical and nonsurgical periodontal therapy. Learned and unlearned concepts. Periodontol 2000 2013;62:218–231.
3. Mitsiadis TA, Orsini G, Jimenez-Rojo L. Stem cell-based approaches in dentistry. Eur Cell Mater 2015;30:248–257.
4. Park JY, Jeon SH, Choung PH. Efficacy of periodontal stem cell transplantation in the treatment of advanced periodontitis. Cell Transplant 2011;20:271–285.
5. Seo BM, Miura M, Gronthos S, et al. Investigation of multipotent postnatal stem cells from human periodontal ligament. Lancet 2004;364:149–155.
6. Kim SH, Kim KH, Seo BM, et al. Alveolar bone regeneration by transplantation of periodontal ligament stem cells and bone marrow stem cells in a canine peri-implant defect model: A pilot study. J Periodontol 2009;80:1815–1823.
7. Nagatomo K, Komaki M, Sekiya I, et al. Stem cell properties of human periodontal ligament cells. J Periodontal Res 2006;41:303–310.
8. Ding G, Liu Y, Wang W, et al. Allogeneic periodontal ligament stem cell therapy for periodontitis in swine. Stem Cells 2010;28:1829–1838.
9. Han J, Menicanin D, Marino V, et al. Assessment of the regenerative potential of allogeneic periodontal ligament stem cells in a rodent periodontal defect model. J Periodontal Res 2014;49:333–345.

10. Liu Y, Zheng Y, Ding G, et al. Periodontal ligament stem cell-mediated treatment for periodontitis in miniature swine. Stem Cells 2008;26:1065–1073.
11. Chen FM, Gao LN, Tian BM, et al. Treatment of periodontal intrabony defects using autologous periodontal ligament stem cells: A randomized clinical trial. Stem Cell Res Ther 2016;7:33.
12. Verma SK, Maheshwari S, Singh RK, Chaudhari PK. Laser in dentistry: An innovative tool in modern dental practice. Natl J Maxillofac Surg 2012;3:124–132.
13. Huang YY, Sharma SK, Carroll J, Hamblin MR. Biphasic dose response in low level light therapy–An update. Dose Response 2011;9:602–618.
14. Hamblin MR, Demidova TN. Mechanisms of low level light therapy. Proc SPIE-Int Soc Opt Eng 2006;6140:1–12.
15. de Freitas LF, Hamblin MR. Proposed mechanisms of photobiomodulation or low-level light therapy. IEEE J Sel Top Quantum Electron 2016;22:7000417.
16. Karu TI. Mitochondrial signaling in mammalian cells activated by red and near-IR radiation. Photochem Photobiol 2008;84:1091–1099.
17. Chondros P, Nikolidakis D, Christodoulides N, Rössler R, Gutknecht N, Sculean A. Photodynamic therapy as adjunct to non-surgical periodontal treatment in patients on periodontal maintenance: A randomized controlled clinical trial. Lasers Med Sci 2009;24:681–688.
18. Aykol G, Baser U, Maden I, et al. The effect of low-level laser therapy as an adjunct to non-surgical periodontal treatment. J Periodontol 2011;82:481–488.
19. Albertini R, Aimbire F, Villaverde AB, Silva JA Jr, Costa MS. COX-2 mRNA expression decreases in the subplantar muscle of rat paw subjected to carrageenan-induced inflammation after low level laser therapy. Inflamm Res 2007;56:228–229.
20. Gholami L, Asefi S, Hooshyarfard A, et al. Photobiomodulation in periodontology and implant dentistry: Part 2. Photobiomodul Photomed Laser Surg 2019;37:766–783.
21. Albertini R, Villaverde AB, Aimbire F, et al. Cytokine mRNA expression is decreased in the subplantar muscle of rat paw subjected to carrageenan-induced inflammation after low-level laser therapy. Photomed Laser Surg 2008;26:19–24.
22. de Jesus JF, Spadacci-Morena DD, dos Anjos Rabelo ND, Pinfildi CE, Fukuda TY, Plapler H. Low-level laser therapy in IL-1β, COX-2, and PGE2 modulation in partially injured Achilles tendon. Lasers Med Sci 2015;30:153–158.
23. Rizzi CF, Mauriz JL, Freitas Corrêa DS, et al. Effects of low-level laser therapy (LLLT) on the nuclear factor (NF)-kappaB signaling pathway in traumatized muscle. Lasers Surg Med 2006;38:704–713.
24. Borzabadi-Farahani A. Effect of low-level laser irradiation on proliferation of human dental mesenchymal stem cells; a systemic review. J Photochem Photobiol B 2016;162:577–582.
25. AlGhamdi KM, Kumar A, Moussa NA. Low-level laser therapy: A useful technique for enhancing the proliferation of various cultured cells. Lasers Med Sci 2012;27:237–249.
26. Ginani F, Soares DM, Barreto MP, Barboza CA. Effect of low-level laser therapy on mesenchymal stem cell proliferation: A systematic review. Lasers Med Sci 2015;30:2189–2194.
27. Wang Y, Huang YY, Wang Y, Lyu P, Hamblin MR. Photobiomodulation of human adipose-derived stem cells using 810nm and 980nm lasers operates via different mechanisms of action. Biochim Biophys Acta Gen Subj 2017;1861:441–449.
28. Huang YY, Chen AC, Carroll JD, Hamblin MR. Biphasic dose response in low level light therapy. Dose Response 2009;7:358–383.
29. Gholami L, Asefi S, Hooshyarfard A, et al. Photobiomodulation in periodontology and implant dentistry: Part 1. Photobiomodul Photomed Laser Surg 2019;37:739–765.
30. Marques MM, Diniz IM, de Cara SP, et al. Photobiomodulation of dental derived mesenchymal stem cells: A systematic review. Photomed Laser Surg 2016;34:500–508.
31. Fekrazad R, Asefi S, Allahdadi M, Kalhori KA. Effect of photobiomodulation on mesenchymal stem cells. Photomed Laser Surg 2016;34:533–542.
32. Wu JY, Chen CH, Yeh LY, Yeh ML, Ting CC, Wang YH. Low-power laser irradiation promotes the proliferation and osteogenic differentiation of human periodontal ligament cells via cyclic adenosine monophosphate. Int J Oral Sci 2013;5:85–91.
33. Soares DM, Ginani F, Henriques ÁG, Barboza CA. Effects of laser therapy on the proliferation of human periodontal ligament stem cells. Lasers Med Sci 2015;30:1171–1174.
34. Yamauchi N, Taguchi Y, Kato H, Umeda M. High-power, red-light-emitting diode irradiation enhances proliferation, osteogenic differentiation, and mineralization of human periodontal ligament stem cells via ERK signaling pathway. J Periodontol 2018;89:351–360.
35. Dominici M, Le Blanc K, Mueller I, et al. Minimal criteria for defining multipotent mesenchymal stromal cells. The International Society for Cellular Therapy position statement. Cytotherapy 2006;8:315–317.
36. Hawkins DH, Abrahamse H. Time-dependent responses of wounded human skin fibroblasts following phototherapy. J Photochem Photobiol B 2007;88:147–155.
37. Karu T, Tiphlova O, Samokhina M, Diamantopoulos C, Sarantsev VP, Shveikin V. Effects of near-infrared laser and superluminous diode irradiation on Escherichia coli division rate. IJQE 1990;26:2162–2165.
38. Jawad MM, Husein A, Azlina A, Alam MK, Hassan R, Shaari R. Effect of 940 nm low-level laser therapy on osteogenesis in vitro. J Biomed Opt 2013;18:128001.
39. Efremova Y, Sinkorova Z, Navratil L. Protective effect of 940 nm laser on gamma-irradiated mice. Photomed Laser Surg 2015;33:82–91.
40. Paschalidou M, Athanasiadou E, Arapostathis K, et al. Biological effects of low-level laser irradiation (LLLI) on stem cells from human exfoliated deciduous teeth (SHED). Clin Oral Investig 2020;24:167–180.
41. Soleimani M, Abbasnia E, Fathi M, Sahraei H, Fathi Y, Kaka G. The effects of low-level laser irradiation on differentiation and proliferation of human bone marrow mesenchymal stem cells into neurons and osteoblasts--An in vitro study. Lasers Med Sci 2012;27:423–430.
42. Kreisler M, Christoffers AB, Willershausen B, d'Hoedt B. Effect of low-level GaAlAs laser irradiation on the proliferation rate of human periodontal ligament fibroblasts: An in vitro study. J Clin Periodontol 2003;30:353–358.

TO DRAW IS TO SEE

NEW

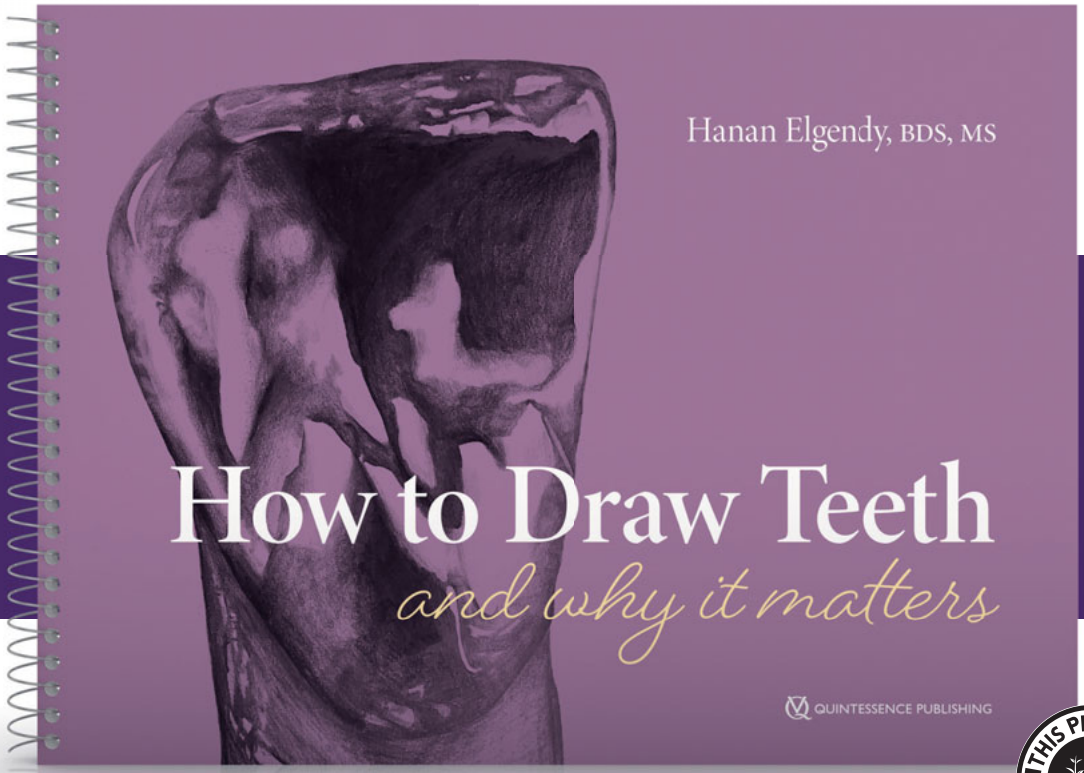

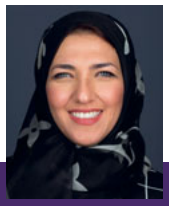

Hanan Elegendy

How to Draw Teeth and Why it Matters

120 pages, 160 illus.
ISBN 978-1-64724-044-8
€42

THIS PRODUCT ONE TREE PLANTED PLANTS TREES

Understanding tooth morphology and anatomical form is crucial to being a good dentist, to ensure both function and esthetics. Dr Elgendy contends that the ability to draw an accurate outline of a tooth is a good indication that a student has clearly seen and understood its external morphology. After all, learning to draw the fine details of the tooth is really learning to see them in the first place. For this reason, the author created this book to guide dental students to seeing and reproducing tooth morphology. The workbook begins with the basics of drawing and quickly shifts to the details of each tooth and how to tackle its morphology. Practice pages are included for each tooth, with extra pages at the end for further practice. Part art book and part workbook, this beautiful publication will inspire students and dentists alike to better see, and therefore capture what they see in their restorations.

www.quint.link/drawing
books@quintessenz.de
+49 (0)30 761 80 667
QUINTESSENCE PUBLISHING

Management of Separated Instruments Extruded into the Maxillary Sinus and Soft Tissue: a Case Series

Qian LIAO[1], Zi Meng HAN[1], Ru ZHANG[1], Ben Xiang HOU[1]

Extrusion of separated endodontic instruments is a frustrating complication that can occur during root canal treatment and is difficult to handle. This report aimed to introduce different methods to retrieve such separated instruments through three cases with different locations of fragments. Fragments extruded completely into the maxillary sinus, partially into the maxillary sinus and lying in the soft tissue were retrieved using a lateral window approach, ultrasonic method and minimally invasive surgery, respectively. These methods can be recommended for retrieving fragments in certain cases.

Key words: *lateral wall approach, maxillary sinus, separated instrument, soft tissue, ultrasonic technique*

Chin J Dent Res 2022;25(1):67–73; doi: 10.3290/j.cjdr.b2752707

One of the complications involved endodontic therapy is instrument separation within root canals, or worse, extruded out of the apical foramen[1]. Instruments may include dental burs, barbed broaches, Gates-Glidden drills, tips of hand instruments, lentulo paste fillers, files and reamers[2]. Instrument separation causes stress to clinicians and anxiety in patients[3]. It often occurs in the mandibular molars due to the poor access, small diameter and sharp curvature of the root canals[4]. The separation rate has been reported in the range of 0.25% to 6.00% for stainless steel instruments, and 1.30% to 10.00% for NiTi rotary instruments[1,5]. Instrument separation happens even to experienced clinicians and can frustrate both practitioners and patients.

Conventionally, several techniques have been attempted for removal of separated instruments, such as the use of chemical solvent, micro forceps, wire loops, hypodermic surgical needles, file braiding, Masserann extractors (Micro-Mega, Besancon, France), the Canal Finder system (FaSociete Endo Technique, Marseille, France), lasers, electrochemical procedures and ultrasonic techniques[6]. The success rate of retrieval of separated instruments ranges between 66.6% and 100.0%[7-9]. It depends on many factors, such as tooth location, the separated instrument, the patient and the technique used[1,10]. Unpredictable complications may occur during the retrieval of separated instruments[11].

Extrusion of separated instruments is a severe complication that is extremely difficult to handle, especially when fragments extrude into the maxillary sinus or soft tissue. Foreign bodies in the maxillary sinus can cause significant complications such as inflammatory reactions, sinusitis and fungal infections[12-15], and these complications tend to aggravate if the foreign bodies are not removed[12-14,16,17]. If the fragment migrates into the soft tissue, inflammation, infection and secondary trauma may occur. In general, prompt removal is necessary to avoid further damage to the surrounding tissues, particularly the vital nerves and blood vessels[18-21].

This report aimed to discuss the management of separated instruments extruded into the maxillary sinus cavity and soft tissue using different methods.

1 Department of Endodontics, School of Stomatology, Capital Medical University, Beijing, P.R. China.

Corresponding author: Dr Ben Xiang HOU, Department of Endodontics, School of Stomatology, Capital Medical University, No 4 Tian Tan XiLi, DongCheng District, Beijing 100050, P.R. China. Tel: 86-10-57099230. Email: Endohou@163.com

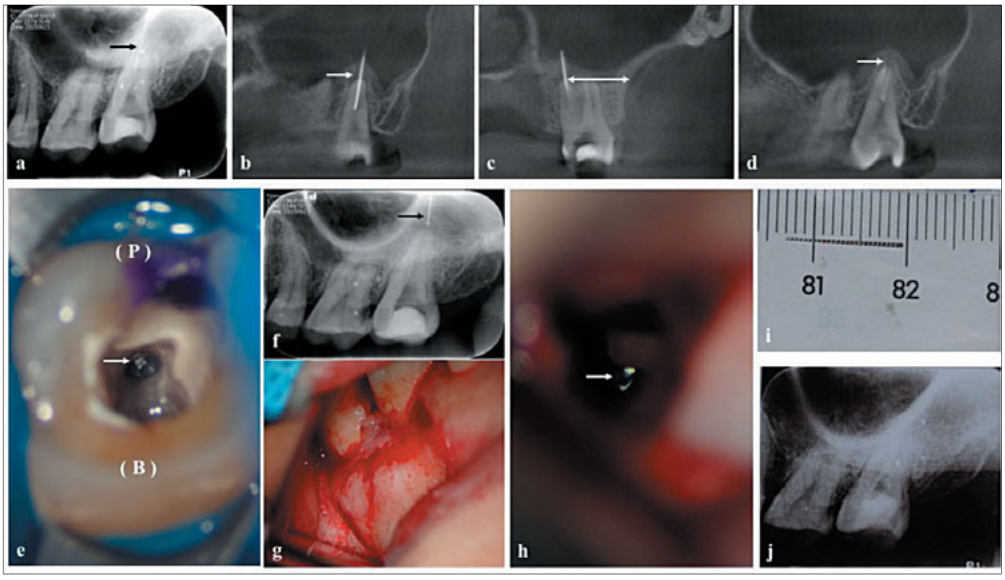

Fig 1 **(a)** A periapical radiograph revealed a fragment in the maxillary left second molar (black arrow). **(b)** Half of the fragment (approximately 6 mm) was extruded into the maxillary sinus (white arrow). **(c)** The distance between the root apex and the buccal cortex was 12.6 mm (white arrow). **(d)** Periapical periodontitis and fenestration of the maxillary floor could be observed (white arrow). **(e)** The fragment was located in the palatal canal (white arrow). **(f)** The fragment was extruded completely beyond the apex (black arrow). **(g)** The lateral wall of the maxillary sinus was exposed after flap elevation. **(h)** The fragment was located in the maxillary sinus (white arrow). **(i)** Removal of the fragment. **(j)** A postoperative periapical radiograph revealed complete removal of the fragment. B, buccal; P, palatal.

Case reports

Case 1

A 33-year-old woman was referred to the Department of Endodontics at Beijing Stomatological Hospital, Capital Medical University, for retrieval of a separated ultrasonic K15 file fragment. Her primary care dental practitioner had tried to retrieve the fragment but failed. Moreover, half of the fragment was extruded out of the apex (maxillary left second molar). The patient felt discomfort while chewing. Upon examination, the access cavity of the maxillary left second molar was filled with temporary material and was sensitive to percussion. The periapical radiograph and CBCT images revealed the presence of a fragment approximately 12.0 mm in size in the palatal canal, and half of it was in the maxillary sinus (Figs 1a and b). The measurement between the palatal root apex and the buccal cortex was approximately 12.6 mm (Fig 1c). Periapical periodontitis had resulted in bone loss between the palatal root apex and the maxillary sinus floor, and fenestration of the latter (Fig 1d).

The maxillary left second molar was isolated using rubber dam. After removal of the temporary filling, a straight-line access was modified so that the fragment could be seen through a dental operating microscope (Opmi 111, Carl Zeiss, Oberkochen, Germany) (Fig 1e). A staging platform was then prepared using a Satelec ET40 ultrasonic tip (Satelec Acteon, La Ciotat, France) until 2 to 3 mm of the fragment was exposed. An attempt to grasp the fragment using endodontic micro forceps (Broken Instrument Removal Kit, Zumax, Jiangsu, China) was unsuccessful, and moreover, the fragment moved forwards apically. The staging and exposure steps were repeated, and an ET25 ultrasonic tip (Satelec Acteon) was placed between the fragment and the surrounding root canal dentinal wall and circulated around the fragment in an anticlockwise motion. The vibration transmitted to the fragment was supposed to loosen it and make it jump out, but unfortunately, the fragment extruded beyond the apex completely, which was confirmed on the periapical radiograph (Fig 1f). Due to the location of the fragment, a lateral window approach was chosen instead of conventional apical surgery. Prior to surgery, the canals were irrigated using 2.5% sodium hypochlorite and dried with paper points. The palatal canal was obturated with mineral trioxide aggregate and the buccal canals were filled with calcium hydroxide. The cavity was filled with glass ionomer.

Surgery was performed under local anaesthesia (4% articaine with 1:100,000 adrenaline). Horizontal incision was made in the sulcus from the mesiobuccal margin of the maxillary left first molar to the distobuccal margin of the maxillary left second molar, and a releasing incision was made on the mesial aspect of the maxillary left first molar. The mucoperiosteal flap was elevated to expose the lateral wall of the sinus (Fig 1g). Piezoelectric instruments (Piezosurgery; Mectron, Genoa, Italy) and a steel fissure bur were used to create a 1.0 × 0.8 cm bony window, including the

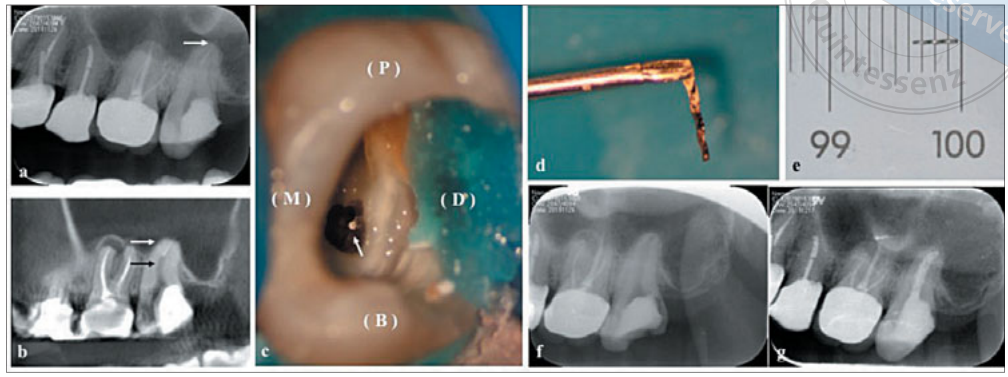

Fig 2 **(a)** A periapical radiograph revealed that there was a fragment in the maxillary left second molar, and it was extruded partly into the maxillary sinus (white arrow). **(b)** There was a curvature in the middle third of the buccal canal (black arrow) and the maxillary sinus floor was covered directly on the apical part of the maxillary left second molar (white arrow). **(c)** The fragment was against the distal wall of the buccal canal because of the curvature (black arrow). **(d and e)** Retrieval of the fragment. **(f)** A radiographic examination revealed complete removal of the fragment. **(g)** A periapical radiograph revealed obturation of the canals.

bony wall of the sinus and the underlying sinus membrane. The sinus cavity was directly under vision, and the fragment could be seen through a dental operating microscope (Fig 1h). The fragment was then removed using endodontic micro forceps (Fig 1i) and a radiograph was taken to confirm that removal had occurred (Fig 1j). The incision was closed with sutures, which were removed 1 week later. Oral antibiotics (250 mg Cefaclor, three times per day for 7 days) and analgesics (400 mg Ibuprofen sustained-release capsules, once a day if necessary) were prescribed postoperatively. After 2 weeks, the buccal canals were obturated with gutta percha, and full crown restoration was recommended.

Case 2

A 30-year-old woman with a separated file in the maxillary left second molar was referred to our department for retrieval of the fragment. It was a NiTi rotary file (25/0.06) that had fractured during a canal enlarging procedure. According to her dental history, the tooth was diagnosed as suffering from chronic pulpitis. The patient had no symptoms but felt anxious about future complications. The access of the tooth cavity was filled with temporary filling. The radiographic examination revealed a fragment in the apical part that was partially extruded into the maxillary sinus (Fig 2a). the CBCT images revealed a curvature in the middle third of the palatal canal, and the fragment was beneath the curvature (Fig 2b). There was no noticeable periapical periodontitis.

The ultrasonic method was chosen to retrieve the fragment. The tooth was isolated with rubber dam, the temporary filling was removed, and modification was performed to gain a straight-line access, as described in case 1. The end of the file was against the mesial wall of the buccal canal because of the curvature (Fig 2c). The dentine of the inner wall was partly removed to ensure that the end of the fragment could be free in the canal, then a staging platform was prepared using an ET40 ultrasonic tip until 2 to 3 mm of the coronal fragment was exposed. The fragment was vibrated using an ET25 ultrasonic tip as described in case 1 until it jumped out (Figs 2d and e). Radiographic examination confirmed retrieval of the fragment (Fig 2f). Irrigation was done with 2.5% NaOCl, and canal shaping, cleaning and obturation were performed 1 week later (Fig 2g). All the procedures were performed with the aid of a dental operating microscope.

Case 3

A 45-year-old woman with a separated barbed broach lying in the soft tissue was referred to our department to retrieve the fragment. Her dental history revealed that she had suffered from crown fractures of the maxillary central incisors, and root canal treatment had been completed on both teeth. Instrument separation occurred during root canal treatment of the maxillary right central incisor (Fig 3a). The fragment migrated into labial or palatal tissue of the maxillary left central incisor (Figs 3a and b). Both teeth had temporary filling material (Fig 3c), with negative reactions to percussion and palpation. A CBCT scan taken 2 weeks previously revealed that the fragment was 8.5 mm in length, 0.8 mm (cervical point) and 3.6 mm (apical point) labially to the convex surface of the labial cortical plate of the maxillary left central incisor, respectively; 2.9 mm (cervical point) and 4.3 mm (apical point) perpendicularly to the incisive canal, respectively; and 11.7 mm (cervical point) and 20.2 mm

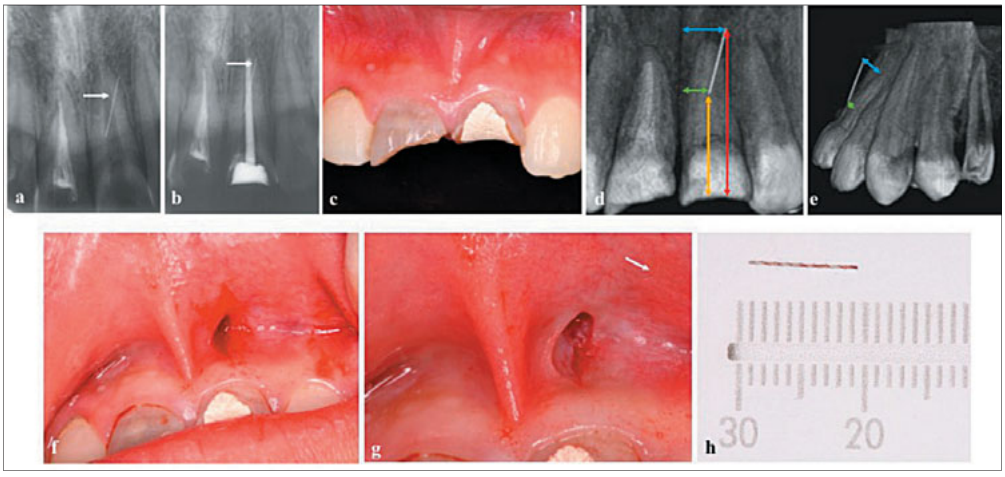

Fig 3 **(a)** A periapical radiograph revealed a fragment lying near the middle third of the root of the maxillary left central incisor (white arrow). **(b)** The fragment remained in the same position after root canal treatment on the maxillary left central incisor (white arrow). **(c)** The maxillary central incisors had crown fractures, and temporary filling material could be seen. **(d)** The measurements between the fragment and the incisive canal were 2.9 mm (green arrow) and 4.3 mm (blue arrow), and those between the fragment and the fractured margin were 11.7 mm (orange arrow) and 20.2 mm (red arrow). **(e)** The measurements between the fragment and the convex surface of the labial cortical plate of the maxillary left central incisor were 0.8 mm (green arrow) and 3.6 mm (blue arrow). **(f)** A small vertical incision was made based on the CBCT images. **(g)** The fragment was located in the mucosa (white arrow). **(h)** Retrieval of the fragment.

(apical point) perpendicularly to the fractured margin, respectively (Figs 3d and e).

After confirming the location on the CBCT scan, a minimally invasive approach was designed to expose the apical part of the fragment. After rinsing the patient's mouth with 0.2% chlorhexidine solution, local anaesthesia (4% articaine with 1:100,000 adrenaline) was administered. A small vertical incision was made, measuring approximately 10.0 mm from the buccal vestibule of the maxillary left central incisor to the upper lip (Fig 3f); however, the fragment could not be found with the aid of a dental operating microscope as it had migrated further. Thus, another CBCT examination to relocate it was considered. Suddenly, part of the fragment was seen in the mucosa of the upper lip (Fig 3g), and the fragment was clamped out (Fig 3h). Sutures were performed, and were removed 7 days postoperatively.

Discussion

No agreement has been reached with regard to whether separated instruments have an effect on prognosis, but they do compromise the effectiveness of cleaning, shaping and obturation procedures[1]. A study suggested that retained instruments do not affect the outcome of root canal treatment, but the presence of a preoperative periapical lesion reduces the rate of healing[22]. The presence of a separated instrument in the root canal makes patients anxious, and this can have a significant impact on treatment outcomes and lead to treatment failure[23]. A separated instrument lying in the soft tissue may migrate along with the muscle movement of the upper lip; this migration is particularly dangerous in the maxillofacial soft tissue. Thus, if periapical periodontitis exists, the patient is anxious or the separated instrument migrates into the soft tissue, it is advisable to remove the fragment.

There are various methods for retrieving separated instruments. Among them, the ultrasonic technique has been reported to be safe and successful[8,24,25]. This technique can be used to retrieve instruments both from within the canals and partly extruded in the apical region[26]. In case 1, the primary care dental practitioner had attempted to retrieve the fragment using the ultrasonic method; however, half of the fragment was extruded into the maxillary sinus. After clinical and CBCT examinations, we found that the palatal canal was large in diameter; thus, we tried using endodontic micro forceps and the ultrasonic method, but the separated file continued to move forwards into the sinus cavity. This may be due to the large diameter of the apical foramen and loss of the periapical bone.

The diameter of the palatal canal foramen of the maxillary left second molar has been reported to vary from 0.16 to 1.16 mm, with a mean diameter of 0.44 mm[27]. In this case, the palatal canal foramen had a large diameter, as visualised through a dental operating microscope. This may be because of development and enlargement by periapical periodontitis or previ-

ous canal enlarging and shaping procedures. Loss of periapical bone due to periapical periodontitis was confirmed on the CBCT images. The diameter of the ultrasonic K15 file was also much smaller than that of the apical foramen. A large apical foramen and loss of periapical bone provide little resistance to the fragment; thus, the fragment was pushed out easily using the ultrasonic method.

In case 2, the separated instrument was also extruded partially into the sinus cavity, but the ultrasonic method was a good management option in this case. The main reasons for this may have been as follows: the mean diameters of the mesiobuccal and distobuccal canal foramen are 0.24 and 0.26 mm, respectively[27], smaller than that of the palatal canal. According to the patient's dental history, the tooth was diagnosed as affected by chronic pulpitis, which means that no periapical lesion existed as shown by the CBCT images, and there was no inflammatory destruction of the root apex. The NiTi fragment (25/0.06) was larger in diameter than that in case 1. Thus, the foramen and periapical bone could prevent the fragment from continuing to slip out of the apex in ultrasonic retrieval procedures.

If separated files extruded into the maxillary sinus cavity cannot be retrieved using an orthograde approach or conventional apical surgery, other methods can be attempted. Many effective methods to retrieve foreign bodies from the maxillary sinus have been reported[17,28-30]. The Caldwell-Luc approach is the most commonly recommended method. It is a safe and fast procedure to open the canine fossa and gain access to the foreign body within the maxillary sinus[30,31]. The lateral window approach, commonly used to increase bone height in dental implant surgery, is also considered safe, although complications may arise during or after surgery[32]. In case 1, the location and the small diameter of the fragment made it impossible to be seen using a Caldwell-Lu approach; thus, the lateral window approach was chosen. In this case, osteotomy was performed using a piezoelectric saw. Piezoelectric osteotomy has many advantages such as speed, precision and minimal bone loss[33-35].

Endoscopy, also known as functional endoscopic surgery, is an important alternative to remove a foreign body from the maxillary sinus. There are two approaches for endoscopy: the nasal cavity approach[36] and the oral cavity approach[37-39]. The nasal cavity approach, by the middle nasal meatus or inferior nasal meatus, is minimally invasive, whereas the oral cavity approach requires a small incision in the canine fossa for the endoscope[28]. The excellent illumination and magnification of the monitoring system makes the surgical field clearly visible. Moreover, the technique offers the advantages of minimal surgical trauma, quick recovery and fewer complications[40-42]. Wang et al[43] reported the successful removal of a pulp needle extruded in the maxillary sinus using this technique. In practice, however, control of the surgical field might be limited, and foreign bodies displaced in the posterior and/or upper part of the maxillary sinus are not easily reachable[44].

To retrieve separated instruments, the first step is to locate the fragment. CBCT examination can provide an accurate assessment of tooth morphology[45-47] and locate fractured instruments[48,49]. In case 1, CBCT images revealed the location of the palatal root apex and the fragment and aided in choosing the lateral window approach to remove the fragment. In case 2, the CBCT images revealed the curvature of the canal and the location of the fragment; thus, complications such as perforation were avoided during the retrieval procedure. In case 3, CBCT images revealed the precise location of the fragment, which helped to make a minimally invasive incision to remove the fragment. Unexpectedly, the fragment could not be found through the incision, as it had migrated further after CBCT examination, probably during surgery for retraction of the upper lip. Any movement of the upper lip such as talking may also lead to migration. If the fragment cannot be located during surgery, another CBCT examination is necessary. During surgery, violent retraction should be avoided in case the separated fragment migrates to another place. Fortunately, in the present case, the fragment migrated to the mucosa of the upper lip and could be seen and removed easily.

Conclusion

When separated instruments are partially extruded into the maxillary sinus, the ultrasonic method can be used in cases where the apical foramen has a small diameter, the fragment has a large diameter, and periapical bone exists. Surgery is required when fragments have been extruded completely into the maxillary sinus. If conventional apical surgery is not possible, the lateral window approach is a management option. When separated files migrate into the soft tissue, minimally invasive surgery can be an option, to try to prevent the separated fragments from migrating to other places during surgery.

Conflicts of interest

The authors declare no conflicts of interest related to this study.

Author contribution

Drs Qian LIAO and Zi Meng HAN took part in the surgical procedures and drafted the manuscript; Dr Ru ZHANG revised the manuscript; Dr Ben Xiang HOU performed all the surgerical procedures and approved the final manuscript.

(Received Mar 26, 2021; accepted Sep 07, 2021)

References

1. Madarati AA, Hunter MJ, Dummer PM. Management of intracanal separated instruments. J Endod 2013;39:569–581.
2. McCoy T. Managing endodontic instrument separation. J Vet Dent 2015;32:262–265.
3. Pine J. What happens if you break a file during a root canal procedure? Oral Health 1996;86:29.
4. Yousuf W, Khan M, Mehdi H. Endodontic procedural errors: Frequency, type of error, and the most frequently treated tooth. Int J Dent 2015;2015:673914.
5. Cohen S, Hargreaves K (eds). Pathways of the pulp, ed 11. Kansas: Elsevier, 2016.
6. Pruthi PJ, Nawal RR, Talwar S, Verma M. Comparative evaluation of the effectiveness of ultrasonic tips versus the Terauchi file retrieval kit for the removal of separated endodontic instruments. Restor Dent Endod 2020;45:e14.
7. Gencoglu N, Helvacioglu D. Comparison of the different techniques to remove fractured endodontic instruments from root canal systems. Eur J Dent 2009;3:90–95.
8. Shahabinejad H, Ghassemi A, Pishbin L, Shahravan A. Success of ultrasonic technique in removing fractured rotary nickel-titanium endodontic instruments from root canals and its effect on the required force for root fracture. J Endod 2013;39:824–828.
9. Ward JR, Parashos P, Messer HH. Evaluation of an ultrasonic technique to remove fractured rotary nickel-titanium endodontic instruments from root canals: An experimental study. J Endod 2003;29:756–763.
10. Iqbal MK, Kohli MR, Kim JS. A retrospective clinical study of incidence of root canal instrument separation in an endodontics graduate program: A PennEndo database study. J Endod 2006;32:1048–1052.
11. Souter NJ, Messer HH. Complications associated with fractured file removal using an ultrasonic technique. J Endod 2005;31:450–452.
12. Burnham R, Bridle C. Aspergillosis of the maxillary sinus secondary to a foreign body (amalgam) in the maxillary antrum. Br J Oral Maxillofac Surg 2009;47:313–315.
13. Selmani Z, Ashammakhi N. Surgical treatment of amalgam fillings causing iatrogenic sinusitis. J Craniofac Surg 2006;17:363–365.
14. Macan D, Cabov T, Kobler P, Bumber Z. Inflammatory reaction to foreign body (amalgam) in the maxillary sinus misdiagnosed as an ethmoid tumor. Dentomaxillofac Radiol 2006;35:303–306.
15. Ueda M, Kaneda T. Maxillary sinusitis caused by dental implants: Report of two cases. J Oral Maxillofac Surg 1992;50:285–287.
16. Felisati G, Lozza P, Chiapasco M, Borloni R. Endoscopic removal of an unusual foreign body in the sphenoid sinus: An oral implant. Clin Oral Implants Res 2007;18:776–780.
17. Ucer TC. A modified transantral endoscopic technique for the removal of a displaced dental implant from the maxillary sinus followed by simultaneous sinus grafting. Int J Oral Maxillofac Implants 2009;24:947–951.
18. Callegari L, Leonardi A, Bini A, et al. Ultrasound-guided removal of foreign bodies: Personal experience. Eur Radiol 2009;19:1273–1279.
19. Lammers RL. Soft tissue foreign bodies. Ann Emerg Med 1988;17:1336–1347.
20. Lammers RL, Magill T. Detection and management of foreign bodies in soft tissue. Emerg Med Clin North Am 1992;10:767–781.
21. Yang XJ, Xing GF, Shi CW, Li W. Value of 3-dimensional CT virtual anatomy imaging in complex foreign body retrieval from soft tissues. Korean J Radiol 2013;14:269–277.
22. Spili P, Parashos P, Messer HH. The impact of instrument fracture on outcome of endodontic treatment. J Endod 2005;31:845–850.
23. Chatzopoulos GS, Koidou VP, Lunos S, Wolff LF. Implant and root canal treatment: Survival rates and factors associated with treatment outcome. J Dent 2018;71:61–66.
24. Fu M, Zhang Z, Hou B. Removal of broken files from root canals by using ultrasonic techniques combined with dental microscope: A retrospective analysis of treatment outcome. J Endod 2011;37:619–622.
25. Fu M, Huang X, Zhang K, Hou B. Effects of ultrasonic removal of fractured files from the middle third of root canals on the resistance to vertical root fracture. J Endod 2019;45:1365–1370.
26. Agrawal V, Kapoor S, Patel M. Ultrasonic technique to retrieve a rotary nickel-titanium file broken beyond the apex and a stainless steel file from the root canal of a mandibular molar: A case report. J Dent (Tehran) 2015;12:532–536.
27. Wolf TG, Paqué F, Sven Patyna M, Willershausen B, Briseño-Marroquín B. Three-dimensional analysis of the physiological foramen geometry of maxillary and mandibular molars by means of micro-CT. Int J Oral Sci 2017;9:151–157.
28. Hara Y, Shiratsuchi H, Tamagawa T, et al. A large-scale study of treatment methods for foreign bodies in the maxillary sinus. J Oral Sci 2018;60:321–328.
29. Kim SM. The removal of an implant beneath the optic canal by modified endoscopic-assisted sinus surgery. Eur Arch Otorhinolaryngol 2017;274:1167–1171.
30. Huang IY, Chen CM, Chuang FH. Caldwell-Luc procedure for retrieval of displaced root in the maxillary sinus. Oral Surg Oral Med Oral Pathol Oral Radiol Endod 2011;112:e59–e63.
31. Ong JC, De Silva RK, Tong DC. Retrieval of a root fragment from the maxillary sinus--An appreciation of the Caldwell-Luc procedure. N Z Dent J 2007;103:14–16.
32. Tükel HC, Tatli U. Risk factors and clinical outcomes of sinus membrane perforation during lateral window sinus lifting: Analysis of 120 patients. Int J Oral Maxillofac Surg 2018;47:1189–1194.
33. Sohn DS, Ahn MR, Lee WH, Yeo DS, Lim SY. Piezoelectric osteotomy for intraoral harvesting of bone blocks. Int J Periodontics Restorative Dent 2007;27:127–131.
34. Sohn DS. Color Atlas, Clinical Applications of Piezoelectric Bone Surgery. Seoul: Kunja Publishing Co, 2008.
35. Lee HJ, Ahn MR, Sohn DS. Piezoelectric distraction osteogenesis in the atrophic maxillary anterior area: A case report. Implant Dent 2007;16:227–234.
36. Kitamura A, Zeredo JL. Migrated maxillary implant removed via semilunar hiatus by transnasal endoscope. Implant Dent 2010;19:16–20.
37. Pagella F, Emanuelli E, Castelnuovo P. Endoscopic extraction of a metal foreign body from the maxillary sinus. Laryngoscope 1999;109:339–342.
38. Iida S, Tanaka N, Kogo M, Matsuya T. Migration of a dental implant into the maxillary sinus. A case report. Int J Oral Maxillofac Surg 2000;29:358–359.
39. Nogami S, Yamauchi K, Tanuma Y, et al. Removal of dental implant displaced into maxillary sinus by combination of endoscopically assisted and bone repositioning techniques: A case report. J Med Case Rep 2016;10:1.

40. Matti E, Emanuelli E, Pusateri A, Muniz CC, Pagella F. Transnasal endoscopic removal of dental implants from the maxillary sinus. Int J Oral Maxillofac Implants 2013;28:905–910.
41. Manfredi M, Fabbri C, Gessaroli M, Morolli F, Stacchini M. Surgical fenestrated approach to the maxillary sinus like alternative to Caldwell-Luc technique. Minerva Stomatol 2019;68:308–316.
42. Levin M, Sommer DD. Endoscopic removal of ectopic sinonasal teeth: A systematic review. J Otolaryngol Head Neck Surg 2019;48:30.
43. Wang Y, Zhu J, Ma Z. Two rare case report of maxillary sinus foreign body [in Chinese]. Lin Chung Er Bi Yan Hou Tou Jing Wai Ke Za Zhi 2015;29:2011–2012.
44. Biglioli F, Chiapasco M. An easy access to retrieve dental implants displaced into the maxillary sinus: The bony window technique. Clin Oral Implants Res 2014;25:1344–1351.
45. Patel S, Dawood A, Ford TP, Whaites E. The potential applications of cone beam computed tomography in the management of endodontic problems. Int Endod J 2007;40:818–830.
46. Patel S. New dimensions in endodontic imaging: Part 2. Cone beam computed tomography. Int Endod J 2009;42:463–475.
47. Venskutonis T, Plotino G, Juodzbalys G, Mickevičienė L. The importance of cone-beam computed tomography in the management of endodontic problems: A review of the literature. J Endod 2014;40:1895–1901.
48. Tyndall DA, Kohltfarber H. Application of cone beam volumetric tomography in endodontics. Aust Dent J 2012;57(suppl 1):72–81.
49. American Association of Endodontists, American Academy of Oral and Maxillofacial Radiology. Use of cone-beam computed tomography in endodontics Joint Position Statement of the American Association of Endodontists and the American Academy of Oral and Maxillofacial Radiology. Oral Surg Oral Med Oral Pathol Oral Radiol Endod 2011;111:234–237.

Chinese Journal of Dental Research

The Official Journal of the
Chinese Stomatological Association (CSA)

GUIDELINES FOR AUTHORS

Chinese Journal of Dental Research is a peer-reviewed general dental journal published in English by the Chinese Stomatological Association. The Journal publishes original articles, short communications, invited reviews, and case reports. Manuscripts are welcome from any part of the world. The Journal is currently published quarterly and distributed domestically by CSA and internationally by Quintessence Publishing Co Ltd.

All authors are asked to adhere to the following guidelines.

Manuscript submission

ScholarOne Manuscripts for *Chinese Journal of Dental Research* (CJDR) has been launched.
To submit your outstanding research results more quickly, please visit: http://mc03.manuscriptcentral.com/cjdr
Any questions, please contact:
4F, Tower C, Jia 18#, Zhongguancun South Avenue, HaiDian District, 100081, Beijing, P.R. China. E-mail: editor@cjdrcsa.com;
Tel: 86-10-82195785; Fax: 86-10-62173402.

Submitted manuscripts must be unpublished original papers that are not under consideration for publication elsewhere. Submissions that have been published with essentially the same content will not be considered. This restriction does not apply to results published as an abstract. The submission of a manuscript by the authors means that the authors automatically agree to assign exclusive licence to the copyright to CSA if and when the manuscript is accepted for publication.
Manuscripts must be accompanied by a letter from all authors or from one author on behalf of all the authors containing a statement that the manuscript has been read and approved by all the authors and the criteria for authorship have been met. It should also contain the following statement: "The attached (enclosed) paper entitled ... has not been published and is not being submitted for publication, in whole or in part, elsewhere".
Manuscripts that reveal a lack of proper ethical consideration for human subjects or experimental animals will not be accepted for publication. The Journal endorses the Recommendations from the Declaration of Helsinki.

Format of Papers

Preparation of manuscripts

The manuscript should be written clearly and concisely and be double-spaced on 21 x 29 cm white paper with at least 2.5 cm margin all around. All pages should be numbered, beginning from section of title page, and followed by abstract, introduction, materials and methods, results, discussion, acknowledgements, references, figure legends and figures/tables. Non-standard abbreviations should be defined when first used in the text. Use a standard font such as Times New Roman or Arial to avoid misrepresentation of your data on different computers that do not have the unusual or foreign language fonts. For units, the Journal recommends the use of the International System of Units (SI Units). For authors whose native language is not English, the Journal strongly recommends improving the English in the manuscript by consulting an English-speaking scientist before submission.

Title page should include: full title (a brief declarative statement of the major findings of the research), full names of authors, professional affiliations and complete postal address, telephone and fax number, and email address of the corresponding author. If the work was supported by a grant, indicate the name of the supporting organisation and the grant number.
Abstract and keywords: 250 words presented in a concise form and including the purpose, general methods, findings, and conclusions of the research described in the paper. A list of 5 keywords or short phrases (a few words per phrase) suitable for indexing should be typed at the bottom of the abstract page. Avoid vague or overly general terms. If necessary, the keywords will be adjusted to the standards of the Journal by the editors without consulting the authors.
Introduction: should begin with a brief introduction of background related to the research and should be as concise as possible. The rationale of the study should be stated.
Materials and Methods: should be described clearly and referenced in sufficient detail. Description should be such that the reader can judge the accuracy, reproducibility, reliability, etc. of the work.
Results: should present the experimental data in tables and figures with suitable descriptions and avoid extended discussions of its relative significance.
Discussion: should focus on the interpretation and significance of the findings with concise objective comments. Speculation is to be based on data only. The text should be written with a logical connection between the introduction and conclusions.
Acknowledgements: should only recognise individuals who provided assistance to the project.
References: should be cited in the text using superscript numbers and typed in numerical order following a style below:

1. Sorensen JA, Engleman MT, Torres TJ, Avera SP. Shear bond strength of composite resin to porcelain. Int J Prosthodont 1991;4:17-23.
2. Renner RP, Boucher LJ. Removable Particle Dentures. Chicago: Quintessence, 1987:24-30.
3. White GE, Johson A van Noort R, Northeast SE, Winstanley B. The quality of cast metal ceramic crowns made for the NHS [abstract 48]. J Dent Res 1990;69(special issue):960.
4. Jones DW. The strength and strengthening mechanisms of dental ceramics. In: McLean JW (ed). Dental ceramics: Proceedings of the First International Symposium on Ceramics. Chicago: Quintessence, 1983:83-41.
5. Rosenstiel S. The Marginal Reproduction of Two Elasto meric Impression Materials [Master's thesis]. Indianapolis: Indiana University, 1997.

Figures and Tables: should be numbered consecutively with Arabic numerals, with each one displayed on a separate page. Photographs should be of excellent quality with a width of 8 cm or 17 cm. All figures and tables should be cited in the text. Please refer to a current volume of this Journal for general guidance.
Legends for all figures, including charts and graphs, must be typed together on a separate page and should be understandable without reference to the text, including a title highlighting the key results and a key for any symbols or abbreviations used in the figure.
Case reports
Authors should describe one to three patients or a single family. The text is limited to no more than 2500 words, and up to 15 references.
Revised Manuscripts
All revisions must be accompanied by a cover letter to the Editor. The letter must detail on a point-by-point basis the contributors' disposition of each of the referees' comments, and certify that all contributors approve of the revised content.

100th ANNIVERSARY
of GC CORPORATION

Hybrid Event

THE 5TH INTERNATIONAL DENTAL SYMPOSIUM

2022.4.16 SAT ▸ 17 SUN

[Location] Tokyo International Forum
Some sessions will be broadcasted online
Changes might occur due
to COVID-19 pandemic

GC official website and app

GC Get Connected

GC

Smile for the World
Since 1921
100 years of Quality in Dental